NASA CR-176,772

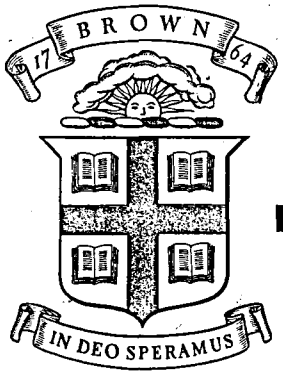

NASA-CR-176772
19860015461

Brown University
DIVISION OF ENGINEERING
PROVIDENCE, R.I. 02912

CONTRIBUTIONS TO THE UNDERSTANDING OF LARGE-SCALE COHERENT STRUCTURES IN DEVELOPING FREE TURBULENT SHEAR FLOWS

J. T . C. Liu
Division of Engineering
Brown University
Providence, Rhode Island 02912

CONTRIBUTIONS TO THE UNDERSTANDING OF LARGE-SCALE COHERENT STRUCTURES IN DEVELOPING FREE TURBULENT SHEAR FLOWS

J. T . C. Liu
Division of Engineering
Brown University
Providence, Rhode Island 02912

NASA Langley Research Center Grant NAG1-379
NASA Lewis Research Center Grant NAG3-673
NSF Fluid Dynamics and Hydraulics Program Grant MSM83-20307
NSF U.S.-China Cooperative Research Program Grant INT85-14196
NATO Research Grant 343/85

April 1986

CONTRIBUTIONS TO THE UNDERSTANDING OF LARGE-SCALE COHERENT STRUCTURES IN DEVELOPING FREE TURBULENT SHEAR FLOWS

J. T. C. Liu
The Division of Engineering
Brown University
Providence, Rhode Island 02912

Advances in Applied Mechanics, Vol. 26 (J. W. Hutchinson and T. Y. Wu, eds.) 1986. Academic Press, New York

TABLE OF CONTENTS

I. INTRODUCTION

In his article on recent advances in the mechanics of boundary layer flow, published in Volume I of this series, Dryden (1948) recalls that at the Fifth International Congress for Applied Mechanics von Kármán (1938) pointed out the difficulties in reconciling a scalar mixing length with turbulence measurements done in a channel by Wattendorf and by Reichardt. In the discussions that followed, which were not precisely recorded in the 1938 Proceedings, Dryden (1948) pointed out that both Tollmien and Prandtl suggested that the measured fluctuations include both random and non-random elements and that the correctness of these ideas are borne out by later turbulence measurements in the boundary layer at the National Bureau of Standards discussed by Dryden (1948). It is important to note that Dryden (1948) emphasized that "... it is necessary to separate the random processes from the non-random processes", but concluded that "... as yet there is no known procedure either experimental or theoretical for separating them". In the early fifties, Liepmann (1952) surveyed aspects of the turbulence problem and pointed out the importance of the presence of a secondary, large-scale structure superimposed upon turbulent shear flows, citing as examples measurements of Corrsin (1943) and Townsend (1947) in free turbulent flows, Pai (1939, 1943) and MacPhail (1941, 1946) in the flow between rotating cylinders and Roshko (1952; see also 1954, 1961) in the far turbulent wake behind a cylinder. Liepmann (1952) concluded that although the details of the large-scale structure may be in doubt, but that such structures cannot

be ignored in many of the technological problems such as in aerodynamic sound, combustion and in general, mixing controlled problems.

More quantitative discussions of the large-scale structure in free turbulent flows were initiated by Townsend (1956, §6.5) in the first edition of his monograph on the structure of turbulent shear flows. He considered the total flow to consist of a mean motion and fluctuations consisting of a large-scale disturbance and the balance of the motion to be fine-scaled fluctuations. The scales are taken to be nonoverlapping so that the spatial, volume integral of the products of the disparate-sized fluctuations vanish. The resulting global energy balance of the large-scale structure (Townsend 1956) gave the essence of the physical interpretation that the large-scale structure gains energy from the mean flow and exchanges energy with the fine-grained turbulence by the rate of working of the large-scale motion against the excess Reynolds stress owing to its presence. Townsend (1956) hypothesized certain kinematical details of the large-scale motion but ruled out motions of the hydrodynamical instability type. The splitting of fluctuations into large-scale structures and fine-grained turbulence was further underscored by Liepmann (1962) in his discussion of free turbulent flows. He advanced the idea that the large-scale motion could be attributable to the hydrodynamic instability of the prevailing mean flow. It was still not clear then as to how the large-scale motions could be sorted out, either experimentally or theoretically, from the total fluctuations. Liepmann (1962) emphasized, however, that the large-scale structures in turbulent shear flows ought to be studies in a well-controlled manner, similar to the studies of the

Tollmien-Schlichting waves leading to transition in a laminar flow (Schubauer & Skramsted 1948).

The well-controlled experiments suggested by Liepmann (1962) in terms of perturbing or enhancing the periodicity in a turbulent shear flow, when the usual Reynolds (1895) average is accompanied by a form of conditional averaging (Kovasznay et al. 1970), now widely known as the phase average geared to the periodicity, allows fluctuations measured at a point to be split into coherent and random parts. This, in principle, takes the jittering out of the phases of otherwise coherent fluctuations (e.g., Thomas and Brown 1977). This is similar to the Schubauer and Skramsted (1948) experiments that place the Tollmien-Schlichting wave where it is desired. The pioneering experiments leading to the recognition of coherent oscillations in turbulent shear flows were associated with Bradshaw (1966), Bradshaw, et al (1964), Davis, et al (1963) and Mollo-Christensen (1967). Experiments on **well-controlled** coherent oscillations in turbulent free flows began with Crow and Champagne (1971) and Binder and Favre-Marinet (1973) for the round jet, Hussain and Reynolds (1970a) for turbulent channel flow and with Kendall (1970) for a wavy wall perturbation beneath a turbulent boundary. The primary advantage of the phase-averaging procedure (Binder and Favre-Marinet 1973, Hussain and Reynolds 1970a), from a theoretical point of view, is that it allows the systematic derivation of the coupled fundamental equations for the mean flow, the large-scale coherent fluctuations with a dominant periodicity and the fine-grained turbulence. The presentation of these equations for a homogeneous, incompressible fluid may be found

in Hussain and Reynolds (1970b), Elswick (1971), Reynolds and Hussain (1972) and Favre-Marinet (1975). The description of the perturbed turbulent shear flow problem is entirely similar to the limited-time (or space) averaging procedure for educing naturally occurring coherent features in turbulent shear flows (Blackwelder and Kaplan 1972, 1976) and the fundamental equations from this point of view are given at the 1970 von Kármán Lecture by Mollo-Christensen (1971) who discussed many facets of interactions between disparate scales of motion in the turbulent boundary layer problem.

Lumley (1967) developed a more formal definition of the large-scale motions and obtained their dynamical equations, using "conventional" (as compared to "conditional") averaging methods. As in Townsend (1956), it is suggested that the effect of the motion of smaller scales in the dynamical equations for the large-scale motion be represented by a constitutive relation. In the lowest order approximation the large-scale motion satisfy the Orr-Sommerfeld equation for small disturbances. Lumley (1967) further suggested that the mean velocity profile could be neutrally stable corresponding to the minimum Reynolds number maintained by an eddy-viscosity. This is reminiscent of the marginal stability ideas for wall-bounded turbulent shear flows put forth by Malkus (1956) in which the turbulent velocity fluctuations are represented by a collection of neutral wave solutions of the Orr-Sommerfeld equation. This idea was extended by Landahl (1967) to the superposition of wave solutions satisfying a non-homogeneous Orr-Sommerfeld equation; the nonlinearities are assumed weak and prescribed. However, free-wave

disturbances corresponding to the standard turbulent eddy viscosity in wall-bounded turbulent shear flows are strongly decaying. Thus the presence of these waves is attributed to a continuous driving mechanism arising from variations of the turbulent Reynolds stresses. In general, this class of theoretical problems are linear and some are associated with the eddy viscosity representations of the effect of the background turbulence. Further discussions of the role of wavelike representations in turbulent shear flows are given by Moffatt (1967, 1969), Lighthill (1969), Phillips (1967, 1969), and Kovasznay (1970). Hussain and Reynolds' (1970a) experiments on imposed monochromatic disturbances in turbulent channel flow indicate that such disturbances propagate like Tollmein-Schlichting waves but that they decay strongly downstream as would be expected from theoretical considerations (Reynolds and Tiederman 1967). As we now appreciate, the coherent large-scale motions in wall-bounded turbulent shear flows are much more involved than free turbulent shear flows (see, for instance, the review by Cantwell 1981). However, some of the theoretical ideas that evolved in the above discussions are more relevant to the **free shear flow** problem, which is the main subject of this article.

For free turbulent shear flows it is not necessary to conjecture that the local fine-grained turbulence rearranges itself to give bursts of white noise in order to maintain the hydrodynamically "unstable" waves as for wall-bounded shear flows, **nor** does there appear to be experimental evidence indicating such a mechanism. It is easily seen that the existence of large-scale coherent motions in free turbulent shear flows would be a manifestation of hydrodynamic instability associated with local inflectional

mean velocity profiles. This would account for the observed pronounced large-scale and, what appears now, wavelike structures in this class of flows (Corrsin 1943, Townsend 1947, Roshko 1954, 1961, Grant 1958, Bradshaw et al 1964, Mollo-Christensen 1967, Brown and Roshko 1974, Papailiou and Lykoudis 1974). The present impetus about the existence and importance of large-scale coherent structures in free turbulent shear flows is essentially brought about by optical observations of such flows (e.g., Brown and Roshko 1971, 1972, 1974) where such structures having been almost obscured by previous correlation measurements. Prior to the more recent recognition of the role of coherent structures in turbulent free shear flows, it was widely thought that such flows were independent of initial and environmental conditions (Townsend 1956, Laufer 1975). The experiments of Crow and Champagne (1971) and Binder and Favre-Marinet (1973) pointed out the distinct possibilities of controlling the downstream development of the jet flow oscillations via the upstream forcing of the large-scale coherent structure. This has an enormous implication with regard to technological applications, such as jet noise supression (Bishop et al 1971, Liu 1974a, Mankbadi and Liu 1981, 1984), mixing and instabilities in combustion chambers and chemical lasers (Carrier et al 1975, Marble and Broadwell 1977, Broadwell and Breindenthal 1982) to mention a few. Thus the study of large-scale coherent structures in free turbulent shear flows is of technological interest not only because such structures directly and indirectly affect the local mixing but that they render the downstream flow controllable.

The present article is intended to address the physical problem of large-scale

coherent structures in real, developing free turbulent shear flows from point of view of a broader minded interpretation of the nonlinear aspects of hydrodynamic stability. This, indeed, has to be the case in view of the presence of fine-grained turbulence in the problem and, even in its absence, there exists the distinct lack of a small parameter. We shall present the discussion on the basis of conservation principles and thus on the dynamics of the problem. It is directed towards extracting the most physical information with the minimal necessary computations and thus must necessarily involve approximations. As such, the discussions presented here are seen to supplement other works using methods such as numerical simulation or straightforward inviscid linearized stability theory and other kinematical interpretations.

II. FUNDAMENTAL EQUATIONS AND THEIR INTERPRETATION

A. GENERAL DESCRIPTION AND AVERAGING PROCEDURES

Both visual observations and unconditioned quantitative measurements of turbulent flows sample the total flow quantities. Flows that occur naturally or in the laboratory do so without regard to the artificial separation into mean and fluctuating quantities. On the other hand for purposes of understanding and, particularly, for possible flow control the Reynolds (1895) type splitting of the flow into mean flow and fluctuations is helpful. This has been particularly useful in problems of hydrodynamic stability (Lin 1955). Flow instabilities are efficient extractors of energy from the mean motion under certain conditions and it is thus not overly simplistic to say that instabilities can thus be controlled via appropriate alterations of the mean motion. It would be most difficult to gain insights into the problem if viewed on an overall basis without regard to such Reynolds splitting. With the present widespread recognition of the important role of large-scale coherent structures in turbulent shear flows, the usual Reynolds splitting has become inadequate in that it blends the coherent structures and the "real" fine-grained turbulence. While the latter is most likely to be "universal" the former definitely is not. Particularly if it is argued (Liu 1981) that the large-scale coherent structures in turbulent shear flows are a manifestation of hydrodynamical instabilities. Such instabilities are attributable to different specific mechanisms such as dynamical or inertial instabilities associated with inflexional mean flows, centrifugal instability in the Taylor vortex problem, viscous instabilities in wall bounded shear flows and so on. Thus

it is not at all surprising that in Reynolds stress modelling for turbulent shear flows that include all fluctuations as "turbulence", the closure constants are by no means universal but that they are dependent upon the problem concerned. Of course, one would generally not entertain ideas of using such closure methods for nonlinear hydrodynamical stability problems. This should also be the case for the coherent structure problem in turbulent shear flows.

The suggestion of Liepmann (1962) that perhaps the properties of large-scale structures could best be studied by well-controlled forcing, similar to the experimental study of Tollmien-Schlichting waves, leads us to the natural synthesis of numerous theoretical ideas. With the fixing of the phase of the large-scale motions, appropriate conservation and transport equations could be derived for the large-scale coherent motions, the modulated fine-grained turbulent stresses and the mean motion problem. The relevant description of the devleopment of the large-scale motion is inherently nonlinear, for which a broader interpretation of ideas from nonlinear hydrodynamic stability theory (Stuart 1958, 1960, 1962a, b, 1971a) will naturally follow. This would be coupled with the fine-grained turbulence problem through the modulated- and Reynolds-mean stresses for which the large-scale coherent motions have already been separated out. In this case Reynolds-stress closure (see, for instance Lumley 1978) ideas applied to the fine-grained turbulence could be judiciously drawn. This was somewhat anticipated by Lumley earlier (1967, 1970). The formalism leading to the derivation of the conservation and transport equations for the monochromatic perturbation problem, originally intended for the study of imposed

Tollmien-Schlichting waves in a turbulent channel flow (Hussain and Reynolds 1970a; Reynolds and Hussain 1972) is more relevant as the starting point for the study of large-scale coherent motions in **free-turbulent shear flows** (Elswick 1971). In the subsequent exploration of the consequences of the basic equations, we shall make use of the richness of ideas from nonlinear hydrodynamic stability, particularly in the interpretation of observations.

The study of a monochromatic large-scale disturbance in a turbulent shear flow is of considerable difficulty in itself, since any such study relevant to observations must necessarily take into account its interaction with the fine-grained turbulence as well as the mean motion (Liu and Merkine 1976, Alper and Liu 1978, Gatski and Liu 1980, Mankbadi and Liu 1981, Liu 1981). We shall, however, present the derivation of the more general fundamental equations with multiple large-scale mode interactions in mind. To this end, the idea (Stuart 1962a) of splitting the coherent modes into odd modes and even modes is used. Originally Stuart (1962a) used this framework to illustrate the energy transfer mechanism between the fundamental disturbance and its harmonic. For the subharmonic problem one can in turn reinterpret that the previous first harmonic mode is now the fundamental component and that the previous fundamental mode as the present subharmonic component. In mixing regions and jets it is now well known that spatially occurring subharmonics take place (see, for instance, Freymuth 1966, Miksad 1972, 1973, Winant and Browand 1974, Ho and Huang 1982, Hussain 1983).

Accordingly, we shall consider that any flow quantity q can be split into

$$q = Q + (\tilde{q}+\hat{q}) + q', \tag{2.1}$$

where Q denotes the mean flow quantity obtained by Reynolds averaging, $\tilde{q}$ the odd modes, $\hat{q}$ the even modes and q' the fine-grained turbulence. In the usual Reynolds' framework $(\tilde{q}+\hat{q}+q')$ would be considered as turbulence.

The form of the Reynolds averaging procedure would be attached to the type of periodicity associated with $(\tilde{q}+\hat{q})$. In the hydrodynamic stability sense the **spatial problem**, as is usually found in laboratory wind tunnels or water channels, is where the mean flow develops and spreads spatially and the amplitudes of coherent modes (or wave envelopes) grow and decay in the streamwise direction; the periodicities are in time. Consequently, the time average, denoted by an overbar, over at least the longest period T (of frequency β) would be the appropriate Reynolds average

$$\overline{q} = Q = \frac{1}{T}\int_0^T q\, dt. \tag{2.2}$$

In this case we denote the special conditional average, which here is the phase average geared to the frequency β, by $\langle\ \rangle$

$$\langle q \rangle = \frac{1}{T}\sum_{n=0}^{N} q(x_i, t + \frac{n}{\beta}), \tag{2.3}$$

where x_i is the spatial coordinate, t is the time. A "layman's" interpretation of this can best be visualized by considering that hot wire signals, taken at a given spatial location,

are recorded as a continuous function of time on tape. The average is performed by adding the signals at N number of the interval T (or β^{-1}) and then dividing by N. This is somewhat related to the limited-time-averaging procedure used in turbulent boundary layers where the phase is not fixed by forcing (see, for instance, Blackwelder & Kaplan 1972). The average (2.3) will pick up all the coherent mode contributions from frequencies $m\beta$, where m is an integer. The phase average of linearly occurring fine-grained turbulence signals is zero, $\langle q' \rangle = 0$, while $\langle Q \rangle = Q$. Thus

$$\langle q \rangle = Q + \tilde{q} + \hat{q}. \tag{2.4}$$

The sum of odd and even modes is obtained from

$$\langle q \rangle - \overline{q} = \tilde{q} + \hat{q}. \tag{2.5}$$

We denote further a similar phase average tied in with frequency 2β by $\langle\langle\ \rangle\rangle$ so that, with $\langle\langle \tilde{q} \rangle\rangle = 0$, the even modes are obtained from

$$\langle\langle \tilde{q}+\hat{q} \rangle\rangle = \hat{q}. \tag{2.6}$$

The 2β-phase average picks up all the $m(2\beta)$ contributions, with m being an integer. The odd modes are then explicitly obtained by subtracting (2.6) from (2.5). For linearly occurring flow quantities, (2.6) is equivalent to the procedure in directly performing the 2β-phase average upon the total signal $\langle\langle q \rangle\rangle - Q = \hat{q}$. However, for nonlinear quantities this latter procedure would give rise to the introduction of the Reynolds average of partially-modulated fine-grained turbulence stresses which are to be necessarily

augmented by their corresponding transport equations, thereby unnecessarily complicating the issue further. To anticipate the more straightforward procedure indicated by (2.6), the corresponding modulated turbulent stress, $\tilde{r}_{ij}$ and $\hat{r}_{ij}$ are obtained from the products of fine-grained turbulence velocity fluctuations through

$$\langle u_i' u_j' \rangle - \overline{u_i' u_j'} = \tilde{r}_{ij} + \hat{r}_{ij}, \tag{2.7}$$

and, applying the 2-β phase average to both sides of (2.7), we obtain

$$\langle\langle(\langle u_i' u_j' \rangle - \overline{u'u'})\rangle\rangle = \hat{r}_{ij}. \tag{2.8}$$

In this case, only the appropriate Reynolds stresses

$$\overline{\langle u_i' u_j' \rangle} = \overline{u_i' u_j'}$$

would occur in the nonlinear equations. (In the undesirable procedure, $\langle\langle u_j' u_j' \rangle\rangle$, which is not equivalent to $u_i' u_j'$, would be introduced).

The **temporal problem** is illustrated by the tilting tube experiment, where a lighter liquid is placed on top of a heavier one (e.g., Thorpe 1971); a slight tilt sets up a mean shear layer that is homogeneous in the "horizontal" direction which then spreads vertically as a function of time. In this case, the coherent modes are spatially periodic and the amplitudes or wave envelopes develop in time. The appropriate

Reynolds average would be the horizontal average over the longest spatial wavelength λ

$$\bar{q} = \frac{1}{\lambda}\int_0^{\lambda} q \, dx.$$

The appropriate $\langle\ \rangle$-phase average in this case is

$$\langle q \rangle = \frac{1}{N} \sum_{n=0}^{'} q(x+n\lambda,y,z,t).$$

The subharmonic in this case would have wavelength 2λ. The $\langle\langle\ \rangle\rangle$-phase average in obtaining the even modes is entirely similar to the spatial problem.

The temporal problem is similar to the prevailing numerical simulation techniques in that the Reynolds average is taken with respect to the spatial direction and the Reynolds mean flow grows or decays in time. In the laboratory situation, the Reynolds averaging procedure is with respect to time. The contrasting situations have been referred to as the "temporal" and "spatial" problems, respectively, in the hydrodynamic stability literature. The transformations between the two cases are given significant discussions (Gaster 1962, 1965, 1968) for linearized problems. For nonlinear problems the transformation between the two situations is achievable only on a "mimicking" basis with the use of some convection velocity. There is, however, no suitable velocity available to achieve physical identicalness between the temporal and spatial problems, particularly for the large scales.

In cases where "three-dimensional" coherent modes are important, such as the

spanwise periodicities in the plane shear layer (Huang 1985, Corcos and Lin 1984, Jimenz 1983) or the helical modes in the round jet (Mankabadi and Liu 1981, 1984), the averages already discussed would have to be supplemented by those pertaining to the spatial periodicities of the "three dimensonality" problem. For instance, as part of the Reynolds average these would introduce spanwise averaging pertaining to the spanwise periodicities in an otherwise basic two-dimensional flow or circumferential averaging pertaining to helical coherent modes in an otherwise round jet.

B. EQUATIONS OF MOTION

We begin with the continuity and Navier-Stokes equations for an incompressible homogeneous fluid

$$\frac{\partial u_i}{\partial x_i} = 0 \tag{2.9}$$

$$\frac{\partial u_i}{\partial t} + u_j \frac{\partial u_i}{\partial x_j} = - \frac{\partial p}{\partial x_i} + \nu \frac{\partial^2 u_i}{\partial x_j^2}, \tag{2.10}$$

where ν is the kinematic viscosity; the density has been absorbed into the pressure p. If we substitute the splitting of flow quantities (2.1) into (2.9) and (2.10), the Reynolds average of the total flow produces the mean flow problem

$$\frac{\partial U_i}{\partial x_i} = 0 \tag{2.11}$$

$$\frac{\bar{D}U_i}{Dt} = -\frac{\partial P}{\partial x_i} + \nu \frac{\partial^2 U_i}{\partial x_j^2} - \frac{\partial}{\partial x_j}\left(\overline{\tilde{u}_i\tilde{u}_j} + \overline{\hat{u}_i\hat{u}_j} + \overline{u_i'u_j'}\right), \tag{2.12}$$

where $\bar{D}/Dt = \partial/\partial t + U_j\partial/\partial x_j$. If we deal with the **spatial** problem, the mean flow is steady then $\bar{D}/Dt = U_j\partial/\partial x_j$. For the **temporal** problem then $\bar{D}/Dt = \partial/\partial t$ according to the discussions of Section II.A. In the subsequent section we will retain such usage and interpretation of $\bar{D}/Dt$. After the $\langle\ \rangle$-phase averaging of the total flow and subtracting out the mean flow, the overall large-scale motion is given by

$$\frac{\partial(\tilde{u}_i+\hat{u}_i)}{\partial x_i} = 0. \tag{2.13}$$

$$\frac{\bar{D}}{Dt}(\tilde{u}_i+\hat{u}_i) + (\tilde{u}_j+\hat{u}_j)\frac{\partial U_i}{\partial x_j} = -\frac{\partial(\tilde{p}+\hat{p})}{\partial x_i} + \nu\frac{\partial^2(\tilde{u}_i+\hat{u}_i)}{\partial x_j^2}$$

$$-\frac{\partial}{\partial x_j}\left[(\tilde{u}_i+\hat{u}_i)(\tilde{u}_j+\hat{u}_j) - \overline{(\tilde{u}_i+\hat{u}_i)(\tilde{u}_j+\hat{u}_j)}\right]$$

$$-\frac{\partial}{\partial x_j}(\tilde{r}_{ij}+\hat{r}_{ij}), \tag{2.14}$$

where the modulated fine-grained turbulent stresses are already defined in (2.7). In obtaining (2.14) the property that the coherent motions and the turbulent fluctuations

are uncorrelated is used. Equations (2.13) and (2.14) for the overall large-scale motion ($\tilde{u}_i+\hat{u}_i$) appear in the same form as that for a monochromatic disturbance (e.g., Hussain and Reynolds 1970b).

Following the procedure indicated by (2.6) and (2.8), we perform the $\langle\langle\ \rangle\rangle$-phase average on (2.13) and (2.14) to obtain the conservation equations for the even modes

$$\frac{\partial \hat{u}_i}{\partial x_i} = 0. \tag{2.15}$$

$$\frac{\bar{D}}{Dt}\hat{u}_i + \hat{u}_j\frac{\partial U_i}{\partial x_j} = -\frac{\partial \hat{p}}{\partial x_i} + \nu\frac{\partial^2 \hat{u}_i}{\partial x_j^2} - \frac{\partial}{\partial x_j}(\hat{u}_i\hat{u}_j - \overline{\hat{u}_i\hat{u}_j}) - \frac{\partial}{\partial x_j}(\tilde{u}_i\tilde{u}_j - \overline{\tilde{u}_i\tilde{u}_j}) - \frac{\partial \hat{r}_{ij}}{\partial x_j}. \tag{2.16}$$

We note that the products of odd modes, such as $\tilde{u}_i\tilde{u}_j$, contribute to the even modes and thus $\langle\langle\tilde{u}_i\tilde{u}_j\rangle\rangle$ reproduces itself, $\tilde{u}_i\tilde{u}_j$. The nonlinear effects of even-mode self-interaction, $\hat{u}_i\hat{u}_j$, produces even modes as well. If we subtract (2.15) and (2.16) from (2.13) and (2.14), respectively, the conservation equations for the odd modes are obtained

$$\frac{\partial \tilde{u}_i}{\partial x_i} = 0. \tag{2.17}$$

$$\frac{\bar{D}}{Dt}\tilde{u}_i + \tilde{u}_j\frac{\partial U_i}{\partial x_j} = -\frac{\partial \tilde{p}}{\partial x_i} + \nu\frac{\partial^2 \tilde{u}_i}{\partial x_j^2} - \frac{\partial}{\partial x_j}(\hat{u}_i\tilde{u}_j + \tilde{u}_i\hat{u}_j) - \frac{\partial \tilde{r}_{ij}}{\partial x_j}. \tag{2.18}$$

It is noted here that nonlinear effects formed by the products of even modes with

that of odd modes, $\hat{u}_i\tilde{u}_j$ and $\tilde{u}_i\hat{u}_j$, give rise to odd mode contributions. The system (2.15) through (2.18) forms the starting point for studying nonlinear interactions between coherent modes themselves and between coherent modes and fine-grained turbulence. The second term on the left of (2.16) and (2.18) is the advection of mean flow momentum by the coherent motion and forms the basic mechanism of shear flow hydrodynamic instabilities (Lin 1955). The mechanism of viscous diffusion of momentum is augmented by the modulated stresses of the fine-grained turbulence. The transport equation for these stresses will be obtained in the sections to follow. The nonlinear effects, which are appropriately split into even- and odd-mode contributions in (2.16) and (2.18), respectively, contribute to coherent-mode amplitude limiting mechanisms as ideas from nonlinear hydrodynamic stability would indicate (Stuart 1958, 1960, 1971). The momentum equation for the mean motion (2.12) indicates that finite-coherent mode disturbances, as would the fine-grained turbulence, affect the mean motion through their respective Reynolds stresses. We also note that the effect of the fine-grained turbulence on the mean motion and on the coherent motion occur in the form of stresses, through the Reynolds average and the phase average, respectively. The detailed, instantaneous fine-grained turbulence motions are thus not directly involved. However, for purposes of obtaining the Reynolds stresses and modulated stresses, the conservation equations for the instantaneous turbulent fluctions are stated here, which are obtained from the continuity and Navier-Stokes equations for the total flow quantity by subtraction of the contributions from the mean flow and coherent modes,

$$\frac{\partial u_i'}{\partial x_i} = 0. \tag{2.19}$$

$$\frac{\bar{D}}{Dt} u_i' + u_j' \frac{\partial U_i}{\partial x_j} + (\tilde{u}_j+\hat{u}_j) \frac{\partial u_i'}{\partial x_j} + u_j' \frac{\partial}{\partial x_j} (\tilde{u}_i+\hat{u}_i) = - \frac{\partial p'}{\partial x_i} + \nu \frac{\partial^2 u_i'}{\partial x_j^2}$$

$$- \frac{\partial}{\partial x_j} (u_i'u_j' - \langle u_i'u_j' \rangle). \tag{2.20}$$

C. KINETIC ENERGY BALANCE

The physical mechanisms underlying the coupling between different scales of motion indicated by the momentum equations can be better illustrated by energy considerations. Although the fluctuation kinetic energy equation can be obtained from its Reynolds stress equation by equating indices, we prefer to deal with the Reynolds stresses and the modulated stresses separately in the subsequent section. Here, we shall obtain the kinetic energy equations directly for the various scales of motion by multiplying the relevant i^{th}-component momentum equation by the corresponding i^{th}-component velocity and summing.

The mean flow energy equation is obtained by multiplying (2.12) by U_i,

$$\frac{\tilde{D}}{Dt} U_i^2/2 = - \frac{\partial}{\partial x_j} \left[P U_j + \underbrace{\left(\overline{\tilde{u}_i\tilde{u}_j} + \overline{\hat{u}_i\hat{u}_j} + \overline{u_i'u_j'} \right)}_{\text{transport}} U_i \right] - \underbrace{\left(\overline{-\tilde{u}_i\tilde{u}_j} - \overline{\hat{u}_i\hat{u}_j} - \overline{u_i'u_j'} \right)}_{\text{exchange}} \frac{\partial U_i}{\partial x_j}$$

$$+ \nu \frac{\partial^2 U_i^2/2}{\partial x_j^2} - \nu \left(\frac{\partial U_i}{\partial x_j} \right)^2. \tag{2.21}$$

A comment about the viscous terms in (2.21) is warranted. These are common to similar terms in the energy equations for the other components of the flow. The form in (2.21) is written for convenience, the first viscous term being interpretable as the viscous diffusion of kinetic energy. The second viscous term, though the negative of positive-definite quantity, is not the actual viscous dissipation rate. The less convenient but physically meaningful form of the viscous effects is as follows. The rate of viscous dissipation is of the form

$$\frac{1}{2}\nu\left[\frac{\partial U_i}{\partial x_j}+\frac{\partial U_j}{\partial x_i}\right]^2, \tag{2.22}$$

and is combined with the "viscous diffusion" term in the form

$$\nu\frac{\partial}{\partial x_j}\left[U_j\left[\frac{\partial U_i}{\partial x_j}+\frac{\partial U_j}{\partial x_i}\right]\right]=\nu\left[\frac{\partial^2 U_i^2/2}{\partial x_j^2}+\frac{\partial^2 U_i U_j}{\partial x_i \partial x_j}\right] \tag{2.23}$$

where, through the use of continuity

$$\frac{\partial^2 U_i U_j}{\partial x_i \partial x_j}=\frac{\partial U_i}{\partial x_j}\frac{\partial U_j}{\partial x_i}$$

(see, for instance, Townsend (1976)). The form appearing in (2.21) will be used throughout, with the physical interpretation through (2.22) and (2.23) kept in mind. The first group of terms on the right of (2.21) include the pressure work and the

transport of mean flow energy by the Reynolds stresses of the even- and odd-coherent modes and the fine-grained turbulence. The second group of terms is the energy exchange mechanism between the mean flow and the fluctuations consisting of the coherent modes and the turbulence. If

$$(-\overline{\tilde{u}_i\tilde{u}_j}-\overline{\hat{u}_i\hat{u}_j}-\overline{u_i'u_j'})\frac{\partial U_i}{\partial x_j} > 0$$

then there is a net energy transfer from the mean flow to the overall fluctuations; the opposite is true if the sign is negative. Of course, this interpretation holds for the individual components of the fluctuations as well.

The energy equation for the odd modes is obtained from (2.18) by multiplying by $\tilde{u}_i$ and then performing the Reynolds average,

$$\frac{\bar{D}}{Dt}\overline{\tilde{u}_i^2/2} = -\frac{\partial}{\partial x_j}\left[\overline{\tilde{p}\tilde{u}_j}+\overline{\hat{u}_j\tilde{u}_i^2/2}+\overline{\tilde{u}_i\tilde{r}_{ij}}\right] + \left[\overline{-\tilde{u}_i\tilde{u}_j}\frac{\partial U_i}{\partial x_j} - \left[\overline{-\tilde{r}_{ij}\frac{\partial\tilde{u}_i}{\partial x_j}}\right] - \overline{\tilde{u}_i\tilde{u}_j\frac{\partial\hat{u}_i}{\partial x_j}}\right]$$

transport exchange

$$+\nu\frac{\partial^2\overline{\tilde{u}_i^2/2}}{\partial x_j^2} - \nu\overline{\left[\frac{\partial\tilde{u}_i}{\partial x_j}\right]^2} \quad . \qquad (2.24)$$

The contributions within the first group of terms on the right represent, respectively, the pressure work, transport of odd-mode energy by the even modes and by the modulated fine-grained turbulence. The second group of terms include the

mechanism of energy exchange between the odd modes and the mean flow, fine-grained turbulence and the even modes, respectively. If

$$-\overline{\tilde{u}_i\tilde{u}_j}\,\frac{\partial U_i}{\partial x_j} > 0,$$

energy is transferred from the mean flow to the odd modes and this term has the opposite sign as that occurring in the mean flow energy equation (2.21). If

$$-\overline{\tilde{r}_{ij}\,\frac{\partial \tilde{u}_i}{\partial x_j}} > 0,$$

energy is transferred from the odd modes to the fine-grained turbulence via the work done by the modulated stresses $\tilde{r}_{ij}$ against the odd-mode rates of strain $\partial\tilde{u}_i/\partial x_j$. If

$$-\overline{\tilde{u}_i\tilde{u}_j\,\frac{\partial \hat{u}_i}{\partial x_j}} > 0,$$

then energy is transferred from the odd modes to the even modes. The viscous terms are similar to those occurring in the mean flow equations and have the similar interpretations already discussed.

The energy equation for the even modes is similarly obtained from (2.16),

$$\frac{\bar{D}}{Dt}\,\overline{\hat{u}_i^2}/2 = -\frac{\partial}{\partial x_j}\left[\overline{\hat{p}\hat{u}_j}+\overline{\hat{u}_j\hat{u}_i^2}/2+\overline{\tilde{u}_j\tilde{u}_i\hat{u}_i}+\overline{\hat{u}_i\hat{r}_{ij}}\right] +$$

transport

$$+\left[\overline{-\hat{u}_i\hat{u}_j}\frac{\partial U_i}{\partial x_j}-\left[\overline{-\hat{r}_{ij}\frac{\partial \hat{u}_i}{\partial x_j}}\right]-\left[\overline{-\tilde{u}_i\tilde{u}_j\frac{\partial \hat{u}_i}{\partial x_j}}\right]\right]+\nu\frac{\partial^2\overline{\hat{u}_i^2/2}}{\partial x_j^2}\times\nu\overline{\left[\frac{\partial \hat{u}_i}{\partial x_j}\right]^2}\,. \qquad (2.25)$$

exchange

Again, the first group of terms on the right of (2.25) represent pressure work, transport of even-mode energy by itself, by the odd modes and by the modulated fine-grained turbulence. The second group represents energy exchanges between the even modes and the mean flow, fine-grained turbulence and the odd modes. The first and third of these have opposite signs to similar terms in (2.21) and (2.24), respectively. The viscous terms need no further comment.

The kinetic energy equation of the fine-grained turbulence is obtained from (2.20) by multiplying by u_i', first $\langle\ \rangle$-phase averaging and then Reynolds averaging,

$$\frac{\bar{D}}{Dt}\overline{u_i'^2/2}=-\frac{\partial}{\partial x_j}\left[\overline{p'u_j'}+\overline{u_j'u_i'^2/2}+(\overline{\tilde{u}_j\sum_i\tilde{r}_{ii}}+\overline{\hat{u}_j\sum_i\hat{r}_{ii}})/2\right]$$

transport

$$+\left[\overline{-u_i'u_j'}\frac{\partial U_i}{\partial x_j}+\left[\overline{-\tilde{r}_{ij}\frac{\partial \tilde{u}_i}{\partial x_j}}\right]+\left[\overline{-\hat{r}_{ij}\frac{\partial \hat{u}_i}{\partial x_j}}\right]\right]$$

exchange

$$+\nu\frac{\partial^2\overline{u'^2}/2}{\partial x_j^2}-\nu\overline{\left[\frac{\partial u_j'}{\partial x_j}\right]^2}\,. \qquad (2.26)$$

The first group of terms include the usual pressure work and self-transport and the transport of fine-grained turbulence energy by the coherent fluctuations. The first term in the second group of terms, commonly known as the turbulence production mechanism, has the sign opposite that of the similar mechanism in the mean flow energy equation (2.21), the second and third terms are the energy exchange mechanisms involving the odd and even modes, respectively. They have opposite signs to their counterparts in (2.24) and (2.25), respectively. The combined viscous effects include, again, "diffusion" and rate of viscous dissipation previously interpreted.

We note here that the advective mechanism in the momentum equations provide in the kinetic energy equations mechanisms of transport and of energy exchanges among the various scales of motion. From the structure of the latter mechanism occurring in the same form but of opposite sign in a "binary" interaction, we have emphasized energy exchanges rather than "production". The latter perhaps implying too often the regulation of the directon of energy transfer in terms of a (positive) eddy-viscosity effect. For instance, from hydrodynamic stability it is well-known that energy could return from fluctuating motions to the mean flow (a "dampled" disturbance in the inviscid sense). In the next section we shall consider the consequences of vorticity considerations. One would expect vorticity-magnitude exchanges among the different scales of motion to arise from advective effects but that no such exchanges would result from the vorticity-stretching and tilting effects in three-dimensional motions.

D. VORTICITY CONSIDERATIONS

There is an extensive discussion of the role of mean and fluctuating vorticity, within the context of the Reynolds splitting procedure in turbulent flows, in Tennekes and Lumley (1972). Some aspects of the role of coherent-mode vorticity in turbulent shear flows and the resulting interactions between different scales is given attention in Mollo-Christensen (1971). The vorticity equation, which is obtained by taking the curl of the momentum equation (2.10), is in a way simpler in form for the description of fluid motion in that it is devoid of the presence of the pressure. Let us define the overall vorticity in the "shorthand" notation,

$$\omega_i = \epsilon_{ikm} \frac{\partial u_m}{\partial x_k},$$

where ϵ_{ikm} is the alternating tensor. It has the property that $\epsilon_{ikm} = 0$ if any two of ikm are the same; if all ikm are different and in cyclic order then $\epsilon_{ikm} = 1$, but is equal to -1 if the cyclic order is disrupted by the interchange of any two numbers. The overall vorticity equation, obtained by taking the curl of (2.10) is

$$\frac{\partial \omega_i}{\partial t} + u_j \frac{\partial \omega_i}{\partial x_j} = \omega_j \frac{\partial u_i}{\partial x_j} + \frac{\partial^2 \omega_i}{\partial x_j^2} . \tag{2.27}$$

In addition to the continuity condition $\partial u_j/\partial x_j = 0$, we shall also make use of the condition $\partial \omega_j/\partial x_j = 0$ in the splitting procedure to follow. The nonlinear advective term

on the left of (2.27) will anticipate the transport of vorticity and vorticity exchanges among the different scales of motion, similar to the interpretations of the kinetic energy balances. However, the vorticity stretching (i = j) and tilting (i ≠ j) mechanism on the right of (2.27) will anticipate net intensification of vorticity: while the mechanism of vorticity exchanges are present even for plane (coherent) motions, the net intensification mechanism is necessarily a three-dimensional phenomenon.

Similar to the overall velocity splitting, we let

$$\omega_i = \Omega_i + \tilde{\omega}_i + \hat{\omega}_i + \omega_i',$$

where Ω_i, $\tilde{\omega}_i$, $\hat{\omega}_i'$ and ω_i' are the mean vorticity, odd- and even-mode vorticity and turbulent vorticity, respectively. The procedure in obtaining the individual vorticity equations is similar to that for the momentum equations. At this stage it is helpful to introduce the symmetrical, rate of strain tensor

$$s_{ij} = \frac{1}{2}\left[\frac{\partial u_i}{\partial x_j} + \frac{\partial u_j}{\partial x_i}\right]$$

specifically for use in the vorticity stretching/tilting mechanism. Thus

$$\omega_j \frac{\partial u_i}{\partial x_j} = \omega_j s_{ij},$$

to which the antisymmetrical, rotational part of $\partial u_i/\partial x_j$, make no contribution. The

occurrence of s_{ij} in the present context then readily identifies the stretching/tilting mechanism, whereas the occurrence of u_j identifies the advective role of the fluid velocity. In what follows the stretching/tilting mechanism will be referred as "stretching" for simplicity. The splitting of s_{ij} into appropriate flow components readily follows.

The mean flow vorticity equation is then

$$\frac{\bar{D}}{Dt}\,\Omega_i = -\frac{\partial}{\partial x_j}\left[\overline{\tilde{u}_j\tilde{\omega}_i}+\overline{\hat{u}_j\hat{\omega}_i}+\overline{u_j'\omega_i'}\right] + \left[\Omega_j S_{ij} + \left(\overline{\tilde{\omega}_j\tilde{s}_{ij}}+\overline{\hat{\omega}_j\hat{s}_{ij}}+\overline{\omega_j' s_{ij}'}\right)\right] + \nu\frac{\partial^2\Omega_i}{\partial x_j^2}\,. \qquad (2.28)$$

transport stretching

The first group of terms on the right of (2.28) is the transport of vorticity by the fluctuating motions, the second group includes the net intensification of mean vorticity by the rates of strain of the mean flow and that of the fluctuations. Equation (2.28) differs from the vorticity equation in a laminar viscous flow, which would have the same form as (2.27), through the fluctuation contributions to vorticity transport and stretching in the mean.

The vorticity equations for the odd- and even-modes are, respectively,

$$\frac{\bar{D}}{Dt}\,\tilde{\omega}_i = -\frac{\partial}{\partial x_j}\left[\tilde{u}_j\Omega_i+\tilde{u}_j\hat{\omega}_i+\hat{u}_j\tilde{\omega}_i+\tilde{m}_{ji}\right] + \left[\Omega_j\tilde{s}_{ij}+\tilde{\omega}_j S_{ij}+\tilde{\omega}_j\hat{s}_{ij}+\hat{\omega}_j\tilde{s}_{ij}+\tilde{c}_i\right] + \nu\frac{\partial^2\tilde{\omega}_i}{\partial x_j^2}, \qquad (2.29)$$

transport stretching

$$\frac{\bar{D}}{Dt}\hat{\omega}_i = -\frac{\partial}{\partial x_j}\Big[\hat{u}_j\Omega_i + (\tilde{u}_j\tilde{\omega}_i - \overline{\tilde{u}_j\tilde{\omega}_i}) + (\hat{u}_j\hat{\omega}_i - \overline{\hat{u}_j\hat{\omega}_i}) + \hat{m}_{ji}\Big]$$

transport

$$+\Big[\Omega_j\hat{s}_{ij} + \hat{\omega}_j S_{ij} + (\tilde{\omega}_j\tilde{s}_{ij} - \overline{\tilde{\omega}_j\tilde{s}_{ij}}) + (\hat{\omega}_j\hat{s}_{ij} - \overline{\hat{\omega}_j\hat{s}_{ij}}) + \hat{c}_i\Big] + \nu\frac{\partial^2\hat{\omega}_i}{\partial x_j^2}. \qquad (2.30)$$

stretching

Similar to the introduction of the modulated fine-grained turbulence stresses $\tilde{r}_{ij}$ and $\hat{r}_{ij}$, we have defined and used the modulated fine-grained turbulence-produced transport and stretching effects, respectively

$$\langle u_j'\omega_i'\rangle - \overline{u_j'\omega_i'} = \tilde{m}_{ji} + \hat{m}_{ji},$$

$$\langle \omega_j' s_{ij}'\rangle - \overline{\omega_j' s_{ij}'} = \tilde{c}_i + \hat{c}_i.$$

The vorticity transport effects, reflected by the first group of terms on the right of (2.29) and (2.30), are due to interactions with the mean flow, mode interactions and that due to the fine-grained turbulence. The second group of terms in (2.29) and (2.30) are due to vorticity stretching and tilting. In the odd-mode vorticity equation (2.29), the effects of $(\Omega_j+\hat{\omega}_j)\tilde{s}_{ij}$ is due to the stretching of the mean and the even-mode vorticity by the odd-mode rates of strain, while $\tilde{\omega}_j(S_{ij}+\hat{s}_{ij})$ is the stretching

of odd-mode vorticity by the rates of strain of the mean flow and of the odd modes; $\tilde{c}_i$ is contribution from modulated-stretching effects due to the fine-grained turbulence. Similar interpretations hold for $\Omega_j\hat{s}_{ij}$ and $\hat{\omega}_j S_{ij}$ found in (2.30). However, the nonlinear effects of odd-mode vorticity stretching by the odd-mode rates of strain $(\tilde{\omega}_i\tilde{s}_{ij}-\overline{\tilde{\omega}_j\tilde{s}_{ij}})$ give rise to even-mode contributions, similar to the nonlinear effects present in the even-mode momentum equation (2.16). The vorticity stretching due self-straining effects of the even-mode $(\hat{\omega}_i\hat{s}_{ij}-\overline{\hat{\omega}_j\hat{s}_{ij}})$ give rise to even contributions. Similar odd-mode and even-mode self-interactions give rise to the nonlinear transport effects in (2.30). These two nonlinear self-interaction effects are peculiar to the even-mode vorticity only, whereas similar stretching and transport effects for the odd- mode vorticity come from even-odd mode interactions only. In (2.30), $\hat{c}_i$ is again the even part of the modulated fine-grained turbulence vorticity stretching effects. Finally, the diffusion of vorticity by viscosity are the last terms (2.29) and (2.30).

In the description of the evolution of the vorticies of the mean flow and of the odd and even modes, the fine-grained turbulence enters into the problem through Reynolds averaged quantities, $\overline{u_j'\omega_i'}$ and $\overline{\omega' s_{ij}'}$ in (2.28) and through the modulated quantities $\tilde{m}_{ji},\tilde{c}_i$ and $\hat{m}_{ji},\hat{c}_i$ in (2.29) and (2.30), respectively. The transport equations for such quantities could be readily obtained, if desired, through the instantaneous equation for ω_i' in conjunction with that of u_i' given by (2.20). The equation for ω_i' will be stated here, which will subsequently be used to obtain the magnitude $\overline{\omega_i'^2}/2$. The fine-grained turbulence vorticity equation is obtained in a similar way as that

for u_i',

$$\frac{\bar{D}}{Dt}\omega_i' = -\frac{\partial}{\partial x_j}\underbrace{\left[u_j'(\Omega_i+\tilde{\omega}_i+\hat{\omega}_i) + (\tilde{u}_j+\hat{u}_j)\omega_i' + u_j'\omega_i' - \langle u_j'\omega_i'\rangle\right]}_{\text{transport}}$$

$$+ \underbrace{\left[(\Omega_j+\tilde{\omega}_j+\hat{\omega}_j)s_{ij}' + \omega_j'(S_{ij}+\tilde{s}_{ij}+\hat{s}_{ij}) + \omega_j's_{ij}' - \langle\omega_j's_{ij}'\rangle\right]}_{\text{stretching}} + \nu\frac{\partial^2\omega_i'}{\partial x_j^2}. \qquad (2.31)$$

The transport effects are immediately obvious, that due to turbulent transport of the total coherent vorticity present, the transport of turbulent vorticity by the coherent fluctuations (transport by the mean flow is already accounted in the left side of (2.31)), and effects of self-transport. The turbulent vorticity stretching is contributed by the presence of total coherent vorticity in the rate of strain field of the turbulence, and the presence of turbulent vorticity in the total coherent rate of strain field and the self-stretching effects indicated by $\omega_i's_{ij}' - \langle\omega_i's_{ij}'\rangle$. The viscous diffusion of turbulent vorticity being obvious.

While the physical understanding of the interactions among the various scales of motion was provided by the energy considerations in Section II.C, similarly, understanding of interactions between the mean and the various scales of fluctuating vorticities would be provided by the "magnitude" of vorticities $\Omega_i^2, \overline{\tilde{\omega}_i^2}, \overline{\hat{\omega}_i^2}$ and $\overline{\omega_i'^2}$, known as the enstrophy (e.g., Pedlosky 1979). The derivation of transport equations for such quantities is similar to that of the energy equations. The mean flow

problem is obtained from (2.28) by multiplying by Ω_i, with some rearrangements,

$$\frac{\bar{D}}{Dt}\,\Omega_i^2/2 = -\frac{\partial}{\partial x_j}\left[\Omega_i\left(\overline{\tilde{u}_j\tilde{\omega}_i}+\hat{u}_j\hat{\omega}_i+\overline{u'_j\omega'_i}\right)\right] + \left(\overline{\tilde{u}_j\tilde{\omega}_i}+\hat{u}_j\hat{\omega}_i+\overline{u'_j\omega'_i}\right)\frac{\partial\Omega_i}{\partial x_j}$$

transport exchange

$$+\left[\Omega_i\left(\overline{\tilde{\omega}_j\tilde{s}_{ij}}+\hat{\omega}_j\hat{s}_{ij}+\overline{\omega'_j s'_{ij}}\right) + \Omega_i\Omega_j S_{ij}\right] + \frac{\partial^2}{\partial x_j^2}\,\Omega_i^2/2 - \nu\left(\frac{\partial\Omega_i}{\partial x_j}\right)^2 . \qquad (2.32)$$

(shared) (self)

stretching

The transport of $\Omega_i^2/2$ by the fluctuations, indicated by the first group of terms on the right, is entirely analogous to that for the mean kinetic energy. The exchange of vorticity with the fluctuations is indicated by the second group of terms on the right and these are analogous to the similar exchange mechanisms for the kinetic energy. As we have emphasized already, the mechanisms of transport and exchange of the square of vorticity is affected by the advection mechanism in the momentum equation. The third group of terms on the right of (2.32) is the intensification of $\Omega_i^2/2$ due to the effect of stretching of fluctuation vorticity by the rates of strain of the fluctuations and the stretching of mean vorticity by the mean rates of strain. The viscosity effects, indicated by the sum of the fourth and fifth terms on the right include the viscous diffusion of $\Omega_i^2/2$ and its rate of viscous dissipation. If the mean flow is two-dimensional then the self-stretching mechanism $\Omega_i\Omega_j S_{ij}$ vanishes. If the coherent modes are also

two-dimensional the intensification of $\Omega_i^2/2$ due to stretching of the coherent-mode vorticity $\Omega_i(\overline{\tilde{\omega}_j\tilde{s}_{ij}}+\overline{\hat{\omega}_i\hat{s}_{ij}})$ by the coherent mode rates of strain would also vanish, leaving the only stretching mechanism due to the turbulent fluctuations $\overline{\Omega_i\omega_j's_{ij}'}$ (where i = 3 and the motion is in the 1-2 plane, say).

The equations for the square of the odd- and even-mode vorticities are, respectively

$$\frac{\bar{D}}{Dt}\overline{\tilde{\omega}_i^2}/2 = -\frac{\partial}{\partial x_j}\left[\overline{\hat{u}_j\tilde{\omega}_i}/2 + \overline{\tilde{\omega}_i\tilde{m}_{ji}}\right] - \left[\overline{\tilde{u}_j\tilde{\omega}_i\frac{\partial\Omega_i}{\partial x_j}} + \overline{\tilde{u}_j\tilde{\omega}_i\frac{\partial\hat{\omega}_i}{\partial x_j}} - \overline{\tilde{m}_{ji}\frac{\partial\tilde{\omega}_i}{\partial x_j}}\right]$$

transport — exchange

$$+\left[\left(\Omega_j\overline{\tilde{\omega}_i\tilde{s}_{ij}}+\overline{\tilde{\omega}_i\tilde{c}_i}\right) + \left(\overline{\tilde{\omega}_i\tilde{\omega}_j\hat{s}_{ij}}+\overline{\tilde{\omega}_i\hat{\omega}_j\tilde{s}_{ij}}\right) + \overline{\tilde{\omega}_i\tilde{\omega}_j}S_{ij}\right] + \nu\frac{\partial^2}{\partial x_j^2}\overline{\tilde{\omega}_i^2}/2 - \nu\overline{\left(\frac{\partial\tilde{\omega}_i}{\partial x_j}\right)^2} \quad . \qquad (2.33)$$

(shared) (self) (other)

stretching

$$\frac{\bar{D}}{Dt}\overline{\hat{\omega}_i^2}/2 = -\frac{\partial}{\partial x_j}\left[\overline{\hat{u}_j\hat{\omega}_i^2}/2 + \overline{\hat{\omega}_i\tilde{u}_j\tilde{\omega}_i} + \overline{\hat{\omega}_i\hat{m}_{ji}}\right] - \left[\overline{\hat{u}_j\hat{\omega}_i\frac{\partial\Omega_i}{\partial x_j}} - \overline{\tilde{u}_j\tilde{\omega}_i\frac{\partial\hat{\omega}_i}{\partial x_j}} - \overline{\hat{m}_{ji}\frac{\partial\hat{\omega}_i}{\partial x_j}}\right]$$

transport — exchange

$$+\left[\left(\Omega_j\overline{\hat{\omega}_i\hat{s}_{ij}}+\overline{\hat{\omega}_i\hat{c}_i}\right) + \left(\overline{\hat{\omega}_i\tilde{\omega}_j\tilde{s}_{ij}}+\overline{\hat{\omega}_i\hat{\omega}_j\hat{s}_{ij}}\right) + \overline{\hat{\omega}_i\hat{\omega}_j}S_{ij}\right] + \nu\frac{\partial^2}{\partial x_j^2}\overline{\hat{\omega}_i^2}/2 - \nu\overline{\left(\frac{\partial\hat{\omega}_i}{\partial x_j}\right)^2} \quad . \qquad (2.34)$$

(shared) (self) (other)

stretching

In the above two equations, (2.33) and (2.34), the first group on terms in the right represents the transport of the mean square coherent-vorticity fluctuations by the coherent-mode fluctuations and by the modulated turbulent fluctuations. The latter is associated with the modulated turbulent vorticity transport $\tilde{m}_{ji}$ and $\hat{m}_{ji}$. These transport effects are similar to those for the transport of coherent-mode kinetic energies. The second group of terms on the right side include the exchange of coherent-mode mean square vorticities with the square of the mean flow vorticity associated with $\partial\Omega_i/\partial x_j$. The signs of these effects in (2.33) and (2.34) are opposite to those in (2.32). Similar exchanges exist between odd- and even-mode mean square vorticies as indicated by the opposite signs of $\overline{\tilde{u}_j\tilde{\omega}_i\partial\hat{\omega}_i/\partial x_j}$ in (2.33) and (2.34). The exchange mechanisms with the fine-grained turbulence, as will be anticipated in the transport equation for $\overline{\omega_i'^2}/2$ to follow, are given by $\overline{\tilde{m}_{ji}\partial\tilde{\omega}_i/\partial x_j}$ and $\overline{\hat{m}_{ji}\partial\hat{\omega}_i/\partial x_j}$. The form of these exchange mechanisms have in common the product between the vorticity flux of one component of flow and the vorticity gradient of another. These are analogous to the kinetic energy exchange mechanisms due to the product of a stress and a velocity gradient or rate of strain. The third group of terms on the right side of (2.33) and (2.34) is the effect of intensification of $\overline{\tilde{\omega}_i^2}/2$ and $\overline{\hat{\omega}_i^2}/2$, respectively, due to vorticity stretching. The effect due to interaction between the mean vorticity and fluctuating rates of strain of the coherent mode, $\overline{\Omega_j\tilde{\omega}_i\tilde{s}_{ij}}$ and $\overline{\Omega_j\hat{\omega}_i\hat{s}_{ij}}$, give rise to an overall intensification rate of $\overline{\tilde{\omega}_i^2}/2$ and $\overline{\hat{\omega}_i^2}/2$, respectively, that is the same as that for $\Omega_i^2/2$ in (2.32), which is $\Omega_i(\overline{\tilde{\omega}_j\tilde{s}_{ij}}+\overline{\hat{\omega}_j\hat{s}_{ij}})$. Both $\overline{\tilde{\omega}_i\tilde{c}_i}$ and $\overline{\hat{\omega}_i\hat{c}_i}$ are due to the modulated turbulent vorticity and rates of strain fluctuations. As

will be apparent subsequently, the sum of these rates of intensification are the same as that for $\overline{\omega_i'^2}/2$. The stretching effects due to the mean flow rates of strain, $\overline{\bar{\omega}_i\bar{\omega}_j}S_{ij}$ and $\overline{\hat{\omega}_i\hat{\omega}_j}S_{ij}$, are not "shared". Finally, the middle group of terms in stretching group are due to coherent-mode rates of strain fluctuations themselves. Except for $\hat{\omega}_i\hat{\omega}_j\hat{s}_{ij}$, the other three self-stretching effects are due to odd-even mode interactions. The sum of the last two terms in (2.33) and (2.34) are again due to the viscous diffusion and dissipation.

Finally, the evolution equation for $\overline{\omega_i'^2}/2$ is

$$\frac{\bar{D}}{Dt}\overline{\omega_i'^2}/2 = -\frac{\partial}{\partial x_j}\left[\overline{u_j'\omega_i'^2}/2 + \overline{(\bar{u}_j\Sigma_i\tilde{\zeta}_{ii}+\hat{u}_j\Sigma_i\hat{\zeta}_{ii})/2}\right] - \left[\overline{u_j'\omega_i'}\frac{\partial\Omega_i}{\partial x_j} + \overline{\tilde{m}_{ji}\frac{\partial\bar{\omega}_i}{\partial x_j}} + \overline{\hat{m}_{ji}\frac{\partial\hat{\omega}_i}{\partial x_j}}\right]$$

transport exchange

$$+\left[\left\{\Omega_j\overline{\omega_i's_{ij}'}+\overline{\bar{\omega}_i\tilde{c}_i}+\overline{\hat{\omega}_i\hat{c}_i}\right\} + \overline{\omega_i'\omega_j's_{ij}'} + \overline{\omega_i'\omega_j'}S_{ij} + (\overline{\tilde{\zeta}_{ij}\tilde{s}_{ij}}+\overline{\hat{\zeta}_{ij}\hat{s}_{ij}})\right]$$

(shared) (self) (other)

stretching

$$+\nu\frac{\partial^2\overline{\omega_i'^2}/2}{\partial x_j^2} - \nu\overline{\left(\frac{\partial\omega_i'}{\partial x_j}\right)^2}\,. \qquad (2.35)$$

We have defined $\langle\omega_i'\omega_j'\rangle$ in terms of the sum of its Reynolds mean and modulated parts

$$\langle \omega_i' \omega_j' \rangle = \overline{\omega_i' \omega_j'} + \tilde{\zeta}_{ij} + \hat{\zeta}_{ij}.$$

Both terms describing the transport of $\overline{\omega_i'^2}/2$ on the right side of (2.35) are analogous to that for the turbulent kinetic energy (2.26); they are due to the turbulent fluctuations and the coherent-mode fluctuations. The first term in the vorticity energy exchange mechanism reflects an exchange of $\overline{\omega_i'^2}/2$ with $\Omega_i^2/2$, with the same term having opposite signs in (2.35) and (2.32); the second and third terms in this group are the vorticity exchange mechanisms between $\overline{\omega_i'^2}/2$ and that of the odd and even modes, $\overline{\tilde{\omega}_i^2}/2$ and $\overline{\hat{\omega}_i^2}/2$, respectively. Again, these terms have opposite signs terms in (2.33) and (2.34). The intensification of $\overline{\omega_i'^2}/2$ due to vorticity stretching is again grouped into three effects. The first is that the total rate of intensification which is shared by other components of flow and are due to fluctuations of the turbulent rates of strain $\Omega_j \overline{\omega_i' s_{ij}'}$, which is in common with that for $\Omega_i^2/2$; and to the modulated fluctuations of the turbulent rates of strain $(\overline{\tilde{\omega}_i \tilde{c}_i} + \overline{\hat{\omega}_i \hat{c}_i})$ which is in common with the same stretching mechanism for the overall coherent-mode vorticity intensities. The second effect in this group in the stretching mechanism is due to self-stretching. The last effect in this group consist of the stretching mechanism of rates of strain of the mean flow and of the coherent modes. The last two terms are the familiar viscous effects. If the coherent fluctuations are predominantly two-dimensional in a two-dimensional mean flow, the only coherent-mode vorticity intensification from stretching effects are due to the modulated-stretching effects of

the turbulence, $\overline{\tilde{\omega}_i \tilde{c}_i}$ and $\overline{\hat{\omega}_i \hat{c}_i}$. Such two-dimensional coherent motions, however, fully participates in the transport of vorticity and, particularly, in the exchanges of vorticity with other scales of motions as is evident in (2.33) and (2.34).

E. THE PRESSURE FIELD

Mollo-Christensen (1973) emphasized that the pressure fluctuations associated with one scale of velocity fluctuations may in fact have scales larger than the scale of such velocities. The pressure depends on the entire flow field since it is given by an equation of Poisson's type (Townsend 1956) in terms of the double spatial derivatives of the "stress tensor", $u_i u_j$ (a special case of Lighthill's stress tensor T_{ij} for the sound pressure generated by fluid motions, (Lighthill 1952; 1962)). The question that naturally arises is what is the role of the pressure field in the light of the splitting procedure for flow quantities that we already used. We begin with the momentum and continuity equations. Taking the divergence of (2.10) and using (2.9), the equation satisfied by the pressure is

$$\frac{\partial^2 p}{\partial x_i^2} = - \frac{\partial^2 u_i u_j}{\partial x_i \partial x_j} . \tag{2.36}$$

Following similar splitting and averaging procedures in obtaining the momentum equations, we obtain the components of the pressure corresponding to that of the mean flow, coherent and turbulent fluctuations. The mean flow pressure field is

given by

$$\frac{\partial^2 P}{\partial x_i^2} = - \frac{\partial^2}{\partial x_i \partial x_j}\left[U_i U_j + \overline{\tilde{u}_i \tilde{u}_j} + \overline{\hat{u}_i \hat{u}_j} + \overline{u_i' u_j'}\right], \tag{2.37}$$

that of the odd-coherent modes by

$$\frac{\partial^2 \tilde{p}}{\partial x_i^2} = - \frac{\partial^2}{\partial x_i \partial x_j}\left[(U_i + \hat{u}_i)\tilde{u}_j + (U_j + \hat{u}_j)\tilde{u}_i + \tilde{r}_{ij}\right] \tag{2.38}$$

and that of the even modes by

$$\frac{\partial^2 \hat{p}}{\partial x_i^2} = - \frac{\partial^2}{\partial x_i \partial x_j}\left[U_i \hat{u}_j + U_j \hat{u}_i + (\tilde{u}_i \tilde{u}_j - \overline{\tilde{u}_i \tilde{u}_j}) + (\hat{u}_i \hat{u}_j - \overline{\hat{u}_i \hat{u}_j}) + \hat{r}_{ij}\right]. \tag{2.39}$$

The instantaneous turbulent pressure fluctuations are given by

$$\frac{\partial^2 p'}{\partial x_i^2} = - \frac{\partial^2}{\partial x_i \partial x_j}\left[(U_i + \tilde{u}_i + \hat{u}_i)u_j' + (U_j + \tilde{u}_j + \hat{u}_j)u_i' + (u_i' u_j' - \overline{u_i' u_j'})\right]. \tag{2.40}$$

The above individual "Poisson's equation" could also have been obtained from their respective original momentum equations by taking the divergence and then using the continuity relation. The individual Poisson's equation has solution of the form

$$p(\underline{x}) = - \frac{1}{4\pi} \int \frac{\partial^2}{\partial x_i' \partial x_j'} [\tau_{ij}] \frac{1}{|\underline{x}' - \underline{x}|} \, dR(\underline{x}'), \tag{2.41}$$

where p represent any of the pressures above in (2.37) - (2.40) and $[\tau_{ij}]$ is the

corresponding "stress tensor" on the right side of the appropriate Poisson's equation, the pressure takes the field coordinates at $\underline{x}$ whereas $[\tau_{ij}]$ takes the same coordinates at $\underline{x}'$ and $dR(\underline{x}')$ is a volume element occupied by the "sources". This illustrates that the pressure, though could be consistently split into mean, coherent and turbulent contributions, is a field quantity that depends on the appropriate overall flow field. In the present context one is tempted to argue that even if $U_i, \tilde{u}_i$ and $\hat{u}_j$ flow fields were absent, $\tilde{p}$ and $\hat{p}$ will be different from zero because of, respectively, the modulated fine-grained turbulence stresses $\tilde{r}_{ij}$ and $\hat{r}_{ij}$. However, the modulated stresses are set up by the flow fields of the coherent modes, $\tilde{u}_i$ and $\hat{u}_i$. The contributions of large-scale structures to the far pressure field, or aerodynamic sound (Lighthill 1952, 1962), was recently addressed by Mankbadi and Liu (1984), supplementing earlier works on contributions from eddies of relatively low correlation radius.

F. THE REYNOLDS AND MODULATED STRESSES

The importance of Reynolds stresses is illustrated in Section II.B through the transport of mean flow momentum by the sum of all the Reynolds stresses of the fluctuations, much in the same way as the modulated stresses transport the coherent-mode momentum. In the energy considerations of Section II.C, the Reynolds stresses of all the fluctuations do work against the rates of strain of the mean flow, thereby effecting energy exchanges between the mean flow and the fluctuations. In a

similar manner, the modulated stresses do work against the rates of strain of the coherent modes, resulting in the energy exchange between coherent motions and the turbulence. The interactions between the coherent modes and the mean flow and between the coherent modes themselves involve coherent-mode stresses and these are taken into account in principle by the explicit consideration of the coherent-mode motions.

In this section we shall obtain and interpret the transport equations of the Reynolds stresses and the modulated stresses of the fine-grained turbulence. We begin with the momentum equation for the instantaneous turbulent fluctuations u_i' given by (2.20) and multiply by u_j' then add to a similar equation through exchanging indicies i and j, first $\langle\ \rangle$-phase averaging and then Reynolds averaging, we obtain

$$\frac{\bar{D}}{Dt}\overline{u_i'u_j'} = -\frac{\partial}{\partial x_k}\left[\overline{u_k'u_i'u_j'} + (\overline{\tilde{u}_k\tilde{r}_{ij}} + \overline{\hat{u}_k\hat{r}_{ij}})\right]$$

transport

$$-\overline{u_j'u_k'}\frac{\partial U_i}{\partial x_k} - \overline{u_i'u_k'}\frac{\partial U_j}{\partial x_k} - \left[\overline{\tilde{r}_{jk}\frac{\partial \tilde{u}_i}{\partial x_k}} + \overline{\hat{r}_{jk}\frac{\partial \hat{u}_i}{\partial x_k}}\right] - \left[\overline{\tilde{r}_{ik}\frac{\partial \tilde{u}_j}{\partial x_k}} + \overline{\hat{r}_{ik}\frac{\partial \hat{u}_j}{\partial x_k}}\right]$$

"Production" from mean — "Production" from coherent modes

$$-\left[\overline{u_j'\frac{\partial p'}{\partial x_i}} + \overline{u_i'\frac{\partial p'}{\partial x_j}}\right] + \nu\frac{\overline{\partial^2 u_i'u_j'}}{\partial x_k^2} - 2\nu\overline{\frac{\partial u_i'}{\partial x_k}\frac{\partial u_j'}{\partial x_k}}. \qquad (2.42)$$

action of pressure gradients — viscous effects

The kinetic energy equation (2.26), which is a contraction of (2.42), yield similar

interpretations for (2.42). Thus the development of Reynolds stresses is dictated by the balance on the right side of (2.42) between transport, "production" from the mean flow and from the coherent motions, the action of pressure gradients and viscous effects.

The transport equation of the total modulated stresses $(\bar{r}_{ij}+\hat{r}_{ij})$ is obtained from that of $\langle u_i' u_j' \rangle$ by subtracting out the Reynolds mean $\overline{u_i' u_j'}$. It has the same form as that obtained by Hussain and Reynolds (1970b) for their monochromatic modulated stresses,

$$\frac{\bar{D}}{Dt}(\bar{r}_{ij}+\hat{r}_{ij}) =$$

$$- \frac{\partial}{\partial x_k} \left\{ \left[\langle u_k' u_i' u_j' \rangle - \overline{u_k' u_i' u_j'} \right] + \left[(\bar{u}_k+\hat{u}_k)(\bar{r}_{ij}+\hat{r}_{ij}) - \overline{(\bar{u}_k+\hat{u}_k)(\bar{r}_{ij}+\hat{r}_{ij})} \right] + (\bar{u}_k+\hat{u}_k)\overline{u_i' u_j'} \right\}$$

(nonlinear) Transport (linear)

$$- \left[(\bar{r}_{jk}+\hat{r}_{jk}) \frac{\partial U_i}{\partial x_k} + (\bar{r}_{ik}+\hat{r}_{ik}) \frac{\partial U_j}{\partial x_k} \right] - \left[\overline{u_j' u_k'} \frac{\partial}{\partial x_k}(\bar{u}_i+\hat{u}_i) + \overline{u_i' u_k'} \frac{\partial}{\partial x_k}(\bar{u}_j+\hat{u}_j) \right]$$

"Production" from mean flow

Work done by mean stresses against coherent rates of strain

$$- \left\{ \left[(\bar{r}_{jk}+\hat{r}_{jk}) \frac{\partial}{\partial x_k}(\bar{u}_i+\hat{u}_i) + (\bar{r}_{ik}+\hat{r}_{ik}) \frac{\partial}{\partial x_k}(\bar{u}_j+\hat{u}_j) \right] \right.$$

$$\left. - \left[\overline{(\bar{r}_{jk}+\hat{r}_{jk}) \frac{\partial}{\partial x_k}(\bar{u}_i+\hat{u}_i)} + \overline{(\bar{r}_{ik}+\hat{r}_{ik}) \frac{\partial}{\partial x_k}(\bar{u}_i+\hat{u}_j)} \right] \right\}$$

(nonlinear) Work done by modulated stress against coherent rates of strain

$$- \left[\left\langle u_j' \frac{\partial p'}{\partial x_i} \right\rangle + \left\langle u_i' \frac{\partial p'}{\partial x_j} \right\rangle - \left[\overline{u_j' \frac{\partial p'}{\partial x_i}} + \overline{u_i' \frac{\partial p'}{\partial x_j}} \right] \right] +$$

Action of pressure gradients

$$- \nu \frac{\partial^2}{\partial x_k^2} (\tilde{r}_{ij} + \hat{r}_{ij}) - 2\nu \left[\left\langle \frac{\partial u_i'}{\partial x_k} \frac{\partial u_j'}{\partial x_k} \right\rangle - \overline{\frac{\partial u_i'}{\partial x_k} \frac{\partial u_j'}{\partial x_k}} \right]. \qquad (2.43)$$

Viscous effects

The physical interpretation of (2.43) is similar to that of (2.42). The right side of (2.43) indicate that the transport of the modulated stresses is due to that by the turbulent fluctuations in terms of the triple correlations and that by the coherent velocity fluctuations comprising the nonlinear contributions. The linear contribution to transport is due to the advection of the mean stresses by the coherent velocity fluctuations. The "production" of the modulated stresses is due to the work done by the modulated stresses against the mean flow rates of strain and that by the mean stresses against the coherent rates of strain; these two mechanisms are linear effects. The third "production" mechanism is the nonlinear effect of work done by the modulated stresses against the coherent rates of strain. The remainder in the balance include the action of the pressure gradients and viscous effects.

Upon << >>-phase averaging, the transport equation for $(\tilde{r}_{ij}+\hat{r}_{ij})$ would yield that for $\hat{r}_{ij}$. Upon subtraction of the latter from the former the transport equation for $\tilde{r}_{ij}$ would be obtained. Before stating the individual transport equations for $\tilde{r}_{ij}$ and

$\hat{r}_{ij}$, we shall define certain symbols for ease of presentation. Following similar splitting of $\langle u_i' u_j' \rangle - \overline{u_j' u_j'}$ into $\tilde{r}_{ij}$ and $\hat{r}_{ij}$, we define the simplifying symbolic representations for the triple correlations

$$\langle u_k' u_i' u_j' \rangle - \overline{u_k' u_i' u_j'} = \tilde{q}_{kij} + \hat{q}_{kij}, \tag{2.44}$$

for the action of the pressure gradients

$$\left\langle u_j' \frac{\partial p'}{\partial x_i} \right\rangle - \overline{u_j' \frac{\partial p'}{\partial x_i}} = \tilde{p}_{ji} + \hat{p}_{ji} \tag{2.45}$$

$$\left\langle u_i' \frac{\partial p'}{\partial x_j} \right\rangle - \overline{u_i' \frac{\partial p'}{\partial x_j}} = \tilde{p}_{ij} + \hat{p}_{ij} \tag{2.46}$$

and for the viscous "dissipation"

$$\left\langle \frac{\partial u_i'}{\partial x_k} \frac{\partial u_j'}{\partial x_k} \right\rangle - \overline{\frac{\partial u_i'}{\partial x_k} \frac{\partial u_j'}{\partial x_k}} = \tilde{\phi}_{ij} + \hat{\phi}_{ij}. \tag{2.47}$$

The transport equations for the odd-mode $\tilde{r}_{ij}$ and the even-mode $\hat{r}_{ij}$ are, respectively

$$\frac{\bar{D}}{Dt} \tilde{r}_{ij} = - \frac{\partial}{\partial x_k} \left[\tilde{q}_{kij} + \tilde{u}_k \hat{r}_{ij} + \hat{u}_k \tilde{r}_{ij} + \tilde{u}_k \overline{u_i' u_j'} \right]$$

Transport

$$- \left[\tilde{r}_{jk} \frac{\partial U_i}{\partial x_k} + \tilde{r}_{ik} \frac{\partial U_j}{\partial x_k} \right] - \left[\overline{u_j' u_k'} \frac{\partial \tilde{u}_i}{\partial x_k} + \overline{u_i' u_k'} \frac{\partial \tilde{u}_j}{\partial x_k} \right]$$

"Production" from mean

Work done by mean stresses against coherent rates of strain

$$- \left[\tilde{r}_{jk} \frac{\partial \hat{u}_i}{\partial x_k} + \hat{r}_{jk} \frac{\partial \tilde{u}_i}{\partial x_k} \right] - \left[\tilde{r}_{ik} \frac{\partial \hat{u}_j}{\partial x_k} + \hat{r}_{ik} \frac{\partial \tilde{u}_j}{\partial x_k} \right]$$

Work done by modulated stresses against coherent rates of strain

$$- (\tilde{p}_{ji} + \tilde{p}_{ij}) + \nu \frac{\partial^2}{\partial x_k^2} \tilde{r}_{ij} - 2\nu \tilde{\phi}_{ij}, \qquad (2.48)$$

action of pressure gradients — viscous effects

and

$$\frac{\bar{D}}{Dt} \hat{r}_{ij} = - \frac{\partial}{\partial x_k} \left[\hat{q}_{kij} + (\tilde{u}_k \tilde{r}_{ij} - \overline{\tilde{u}_k \tilde{r}_{ij}}) + (\hat{u}_k \hat{r}_{ij} - \overline{\hat{u}_k \hat{r}_{ij}}) + \hat{u}_k \overline{u_i' u_j'} \right]$$

Transport

$$- \left[\hat{r}_{jk} \frac{\partial U_i}{\partial x_k} + \hat{r}_{ik} \frac{\partial U_j}{\partial x_k} \right] - \left[\overline{u_j' u_k'} \frac{\partial \hat{u}_i}{\partial x_k} + \overline{u_i' u_k'} \frac{\partial \hat{u}_j}{\partial x_k} \right]$$

"Production" from mean — Work done by mean stresses against coherent rates of strain

$$- \left[\left[\tilde{r}_{jk} \frac{\partial \tilde{u}_i}{\partial x_k} + \tilde{r}_{ik} \frac{\partial \tilde{u}_j}{\partial x_k} \right] - \left[\overline{\tilde{r}_{jk} \frac{\partial \tilde{u}_i}{\partial x_k}} + \overline{\tilde{r}_{ik} \frac{\partial \tilde{u}_j}{\partial x_k}} \right] \right]$$

Work done by modulated stresses against coherent rates of strain

$$- \left[\left[\hat{r}_{jk} \frac{\partial \hat{u}_i}{\partial x_k} + \hat{r}_{ik} \frac{\partial \hat{u}_j}{\partial x_k} \right] - \left[\overline{\hat{r}_{jk} \frac{\partial \hat{u}_i}{\partial x_k}} + \overline{\hat{r}_{ik} \frac{\partial \hat{u}_j}{\partial x_k}} \right] \right]$$

Work done by modulated stresses against coherent rates of strain

$$- \left[\hat{p}_{ij}+\hat{p}_{ji}\right] + \nu \frac{\partial^2}{\partial x_k^2} \hat{r}_{ij} - 2\nu\hat{\phi}_{ij}. \qquad (2.49)$$

actions of pressure gradients — viscous effects

Their interpretations are similar to that for (2.43). We note again that the products between even modes and between odd modes give rise to odd modes whereas the product between even and odd modes give rise to odd modes. This accounts for the nonlinear transport effects as well as the nonlinear production effects in (2.48) and (2.49). The self-interaction of odd modes produce effects upon the even modes and the mixed products of odd/even modes produce effects upon the odd modes. These mode-interaction mechanisms are already noticed in the energy considerations.

III. SOME ASPECTS OF QUANTITATIVE OBSERVATIONS

In order to set the stage for using certain of the conservation principles of Section II to describe the large-scale structures in sections following Section IV we shall discuss some of the features of quantitative results from experiments that would be susceptible to interpretation, either qualitative or quantitative, from a dynamical point of view. This would certainly supplement, if not preferable to, the purely kinetic interpretations and artistic descriptions of the observations. The present section is not intended to be a complete survey of experimental results. Complimentary to this incompleteness would be the more recent surveys of observations by Roshko (1976), Browand (1980), Cantwell (1981), Hussain (1983) and Wygnanski and Petersen (1985).

We shall place emphasis on the **development** of the large-scale coherent structures in free turbulent flows as they evolve through interactions with the mean flow, among themselves and with fine-grained turbulence. The coherent-mode amplitudes would evolve in the streamwise direction for the spatial problem, such as in the mixing region established in a wind tunnel or water channel. In this case, the coherent-mode periodicities are in terms of frequencies and the mean flow spreads along in the streamwise direction. This would correspond to that of most technological applications. Mimicking this situation is the temporal problem, such as the tilting-tube experiment or numerical simulations, where the periodicities are in the streamwise direction, the mean flow spreading rate is time dependent as is the

evolution of the coherent-mode amplitudes. The nonlinear temporal problem yield theoretical and computational conveniences but we have already emphasized that there is no one-to-one transformation to the spatial problem.

The emphasis on develoment and evolution is mainly because of the strong initial condition dependence on part of the coherent modes in turbulent shear flows, recognized theoretically sometime ago (Liu 1971b, 1974a) and for which experimental evidence is now omni present. In the spatial problem, the coherent-mode amplitudes have spectrally-dependent fixed streamwise distributions. The amplitudes (or wave envelopes) grow and decay, with the lower-frequency components peaking further downstream and higher-frequency modes peaking closer to the initiation of the free turbulent flow for a given initial energy level (e.g., Liu 1974a). Under the spatially fixed amplitude or wave envelope, the propagating coherent modes enter from its region of initiation and exits downstream, if at all. The nature of such modes and the spatial distribution of their envelope depend on a number of factors in addition to their own spectral content and initial amplitudes, such as the fine-grained turbulence level and the initial mean flow distribution and the length scale in forming the initial Strouhal number. As such, the description of the local structure of coherent motions would be meaningful only if it is placed in an overall context in order to fix the identity of their otherwise apparent nonuniversalities.

In order to illustrate the coherent-mode amplitude development, we show in Figure 1 the results from Favre-Marinet and Binder (1979). They forced a turbulent jet at rather large initial coherent-mode amplitudes. The open circles indicate the

root mean square of measured streamwise velocity of the coherent-mode, obtained via phase averaging, at the Strouhal number $St = fd/U_c$ of 0.18, where f is the forcing frequency, d the jet diameter and U_c the mean velocity at the nozzle exit centerline. The signals were measured on the jet axis. The evolution in terms of x/d, where x is the streamwise distance from the nozzle exit, show that the signal, which is indicative of the coherent mode amplitude behavior, amplifies and then decays. The turbulence signal, again on the jet axis, is characterized by the root mean square of the turbulent streamwise velocity is shown as blackend circles for the case without forcing, and as open triangles with forcing. There is an indication that the turbulence is enhanced, the jet spreading rate and centerline mean flow decay are also enhanced. On the basis of the theoretical discussions in Section II, the questions that naturally arise is what is the role of the coherent mode in the enhancement of the turbulence and mean flow spreading rate, what are the meachanisms leading to the amplification and decay of the coherent mode.

To illustrate the coherent mode energy production (and destruction) mechanism through its interaction with the mean flow, we show in Figure 2 the measurements of Fiedler, et al (1981) of this mechanism along the line of most intense mean velocity gradient in a controlled, one-sided turbulent mixing layer. Here w is the vertical velocity and z the vertical coordinate, U_∞ is the free stream velocity. However, the coherent signal was obtained by filtering at the controlled frequency rather than via phase averaging. One can argue that if the monchromatic coherent signal is as energetic as the overall broadband turbulence, then the energy content of

the turbulence at the coherent signal frequency could conceivably be relatively weak. Filtering would then produce the similar result as that from phase averaging.

Fiedler et al (1981) compared the measured coherent structure production mechanism, as shown in Figure 2, with that of the total fluctuation production mechanism along the line of maximum mean shear. While the random fluctuation production remained positive, that of the coherent structure increased, reflecting the energy extraction process, and then decreased below the axis indicating the negative production or return of kinetic energy to the mean shear flow. This typifies similar negative production mechanism observed by Hussain and Zaman (1980), Oster and Wygnanski (1982), Weisbrot (1984) (see also Hussain 1983). Such observations are not entirely surprising from the perspective of ideas from hydrodynamic stability for developing shear flows. The development of this energy exchange mechanism between the mean flow and coherent structure is very similar to that in a laminar free shear flow (Ko, Kubota and Lees 1970, Liu 1971b) except that the rate of this development is significantly modified in the more rapidly spreading turbulent shear flow. Not only the "negative production" mechanism itself, but the observed evolution of the coherent mode as in Figure 2, is entirely explected from theoretical considerations (e.g., Liu 1971b, Gatski and Liu 1980, Mankbadi and Liu 1981). This negative production mechanism is only partially responsible for the decay of the coherent mode.

Fiedler, et al (1981) also showed that the shear layer spreading rate is altered by the enhanced coherent mode. However, we shall ilustrate the similar observed effect

of coherent-mode development through the use of results from Ho and Huang (1982). Although the shear layer in Ho and Huang (1982) is one undergoing transition, it is used here to illustrate the role of fluctuations on the mean flow spreading rate. (A collection of spreading rates from various laboratories, though not exhaustive, appear in Ho and Huerre 1984, Figure 24). Ho and Huang's (1982) measured mean shear flow thickness developing as a function of the streamwise distance is shown in Figure 3; the conditions correspond to their "Mode II", in which the subharmonic component (2.15 Hz) is forced at a streamwise velocity (route mean square) of about 0.10% of the averaged upper and lower free streams and at an R parameter (ratio of the upper and lower stream velocity difference to the sum) value of 0.31. The steplike structure of the mean flow thickness is fairly obvious. The thickness of disturbed turbulent shear layers also exhibit such steplike behaviors (Fiedler, et al 1981, Weisbrot 1984, Fiedler and Mensing 1985; see also Wygnanski and Petersen 1985). The coresponding coherent-mode energy measured by Ho and Huang (1982) is shown in Figure 4, where E(f) is the kinetic energy due to the streamwise velocity fluctuation associated with each of the frequencies, integrated across the shear layer. As we shall see later, such a quantity, but including all the contributions to the coherent-mode kinetic energy integral, is related to the amplitude or wave envelope of each mode. Figure 4 indicates that the peak of the fundamental component (4.30 Hz) energy is associated with the first plateau of the shear layer thickness in Figure 3, the peak of the subharmonic energy is associated with the second plateau in the shear layer thickness further downstream. The linear growth far downstream is

attributable to turbulence dominating the rate of spread. As will be shown more formally in the next section, it is not difficult to show that the shear layer spreading rate $d\delta/dx$ can be obtained from the mean flow kinetic energy equation, integrated across the shear layer (see, for instance, Liu and Merkine 1976, Alper and Liu 1978), with a change in sign and retaining only the dominant energy exchange mechanisms,

$$\frac{d\delta}{dx} \sim \int_{-\infty}^{\infty} \left[-\overline{\hat{u}\hat{w}}-\overline{\bar{u}\bar{w}}-\overline{u'w'}\right]\frac{\partial U}{\partial z}\,dz + \nu \int_{-\infty}^{\infty} \left[\frac{\partial U}{\partial z}\right]^2 dz. \tag{3.1}$$

In a purely laminar viscous flow, the shear layer will spread as long as kinetic energy is removed from the mean flow via viscous dissipation. In a transitional shear flow, this viscous spreading rate would be augmented by the emergence of finite amplitude coherent disturbances. In a turbulent shear flow, a highly enhanced coherent mode would similarly augment the turbulent spreading rates. If we denote the fundamental disturbance-mode Reynolds stress contribution by $-\overline{\hat{u}\hat{w}}$, the magnitude of the energy exchange mechanism $-\overline{\hat{u}\hat{w}}\ \partial U/\partial Z$ very nearly follows the development of the wave envelope as appearing in Figure 4. Its value along the line of most intense mean shear, illustrated by Fiedler, et al's (1981) measurement, very nearly represent the entire sectional integral of this quantity. Thus the first peak of $d\delta/dx$ is associated with the vigorous transfer of energy from the mean flow to the fundamental. The shear layer thickness itself, which is a running streamwise integral of the energy exchange mechanism, reaches a plateau after the streamwise peak of of the fundamental

component. The second, distinct plateau follows similar reasoning for the subharmonic-mode energy transfer mechanism $-\overline{\tilde{u}\tilde{w}}\ \partial U/\partial Z$. It seems that after the coherent modes have subsided relative to the turbulence, the linear growth is attributable to $-\overline{u'w'}\ \partial U/\partial Z$. The development of the negative production mechanism on part of the coherent mode discussed earlier, which corresponds to "damped disturbances" in the hydrodynamic stability sense for dynamically unstable flows, would make a negative contribution to $d\delta/dx$, thus contributing to a decrease in δ. This decrease in δ would be obviously observable if the negative production rate were the dominant energy exchange mechanism within a streamwise region (see Weisbrot 1984, Fiedler and Mensing 1985).

Although not decoupled from the direct interactions between coherent modes and fine-grained turbulence, the production of the fine-grained turbulence by the mean motion appear both experimentally (e.g., Fiedler, et al 1981) and theoretically (e.g., Liu and Merkine 1976, Alper and Liu 1978, Mankbadi and Liu 1981) to be devoid of the large-scale amplification and negative production as was found for the coherent modes. Consequently, the turbulence energy, excluding the coherent-mode contributions, appears to be developing, if at all, monotonically even in the nonequilibrium region of coherent mode/turbulence/mean flow interactions. The contribution of $-\overline{u'w'}\ \partial U/\partial Z$ to the shear layer spreading rate eventually becomes very nearly constant along the streamwise direction rendering the linear spread of the shear layer due to this mechanism. For the transition problem (e.g., Ho and Huang 1982) or the forced turbulent shear layer (e.g., Weisbrot 1984, Fiedler and Mensing 1985), the initial steep step-like development of the shear layer is thus conclusively

reasoned from the above discussion to be due to vigorous energy transfer to the coherent modes. The arrest of this steep development is due to the decay of the coherent disturbance in the downstream region where production becomes small or negative. The existence of the plateau region between steep increases of $\delta(x)$ indicate that the production mechanism of the first mode has subsided prior to the rise in production of the subsequent mode (or fine-grained turbulence). The downstream persistent linear growth of the shear layer, again from our present discussions, indicate that the coherent mode activities have subsided and that fine-grained turbulence is now responsible for the shear layer spreading rate. This spreading rate is not necessarily universal in that it has an upstream dependence on what nonlinear coherent mode interactions have taken place (e.g., Alper and Liu 1978, Mankbadi and Liu 1981). This lack of universality in the measured turbulent shear layer spreading rate, summarized, for instance, by Brown and Roshko (1974) and by Ho and Huerre 1984, is thus not surprising but expected.

The basic two-dimensional free shear flow appears to support dominantly two-dimensional coherent modes, with its vorticity axis perpendicular to the mean motion. In the following sections, our theoretical discussions will interpret the role of such observed dominant modes as well as the three-dimensional coherent modes in terms of observed spanwise standing waves (e.g., Konrad 1977, Bernal 1981, Breidenthal 1982, Jimenez 1983, Browand and Troutt 1980, 1984). An issue to be addressed with the three-dimensional modes is that the spanwise wavelengths appear to increase downstream, somewhat similar to the formation of longer, streamwise wavelength of frequency subharmonics.

IV. VARIATIONS ON THE AMSDEN AND HARLOW PROBLEM - THE TEMPORAL MIXING LAYER

A. INTRODUCTORY COMMENTS

Amsden and Harlow (1964) considered the "temporal" mixing layer formed by parallel opposite streams. The disturbance is two-dimensional and is periodic horizontally. The growth in amplitude and the spreading of the Reynolds mean motion is in time. However, they considered the entire flow velocity as a single dependent variable, encompassing the Reynolds mean and the disturbance, and solved the unsteady Navier Stokes equations with horizontal periodic boundary conditions. The study of mean flow and disturbance interactions can always be obtained from the numerical result by performing the Reynolds average, which is the horizontal average in this case. The utility of the idea in using the total flow quantity as the dependent-dynamical variable is particularly suitable for the simple temporal mixing layer problem. This has been fully exploited by Patnaik, et al (1976) in the case of stratified flow. The two-dimensional problem (Amsden and Harlow 1964) for a homogeneous fluid, including the consideration of passive scalar advection and diffusion, was given greater detailed consideration by Corcos and Sherman (1984). The secondary instabilities in the form of spanwise periodicities, solved on the basis of linearizing about the two-dimensional motion, was considered by Corcos and Lin (1984) and Lin and Corcos (1984). These are still relatively low Reynolds number problems and the participation of fine-grained turbulence was not intended.

The dominant two-dimensional coherent mode problems in turbulent shear layers have been studied by Knight (1979) and Gatski and Liu (1977, 1980) using different closure models for the fine-grained turbulence; the coherent mode agglomeration problem was studied by Murrary (1980) and Knight and Murray (1981) with an eddy-vsicosity model. The basic aim of the present section, through Reynolds averaged diagnostics obtained from results recovered from the numerical solutions, is to motivate the subsequent approximate considerations directed towards spatially developing turbulent free shear flows. This will naturally lead to the discussion of the role of linear theory in the Section V, bridging that of the Section VI on the spatially devleoping free shear flows.

B. THE "TURBULENT" AMSDEN-HARLOW PROBLEM

The problem of presence of a coherent structure in a **turbulent** mixing layer considered by Gatski and Liu (1980), in the "spirit" of Amsden and Harlow (1964), shall be given some attention because of the physical information that can be extracted out of the results. In the present context the coherent flow variable to be solved would be

$$\begin{aligned} U_i &\equiv U_i + (\tilde{u}_i + \hat{u}_i), \\ P &\equiv P + (\tilde{p} + \hat{p}). \end{aligned} \tag{4.1}$$

Their governing equations are obtainable from the continuity and Navier Stokes equations, (2.9) and (2.10), by substituting

$$u_i = U_i + u_i'$$
$$p = P + p' \tag{4.2}$$

and taking only the phase average < >; the Reynolds average is not performed at the outset. The resulting equation for U_i would be coupled to the phase-averaged, total stresses

$$R_{ij} = \langle u_i' u_j' \rangle = \overline{u_i' u_j'} + (\tilde{r}_{ij} + \hat{r}_{ij}). \tag{4.3}$$

The system U_i, P, R_{ij}, which involves no explicit Reynolds stresses, $\overline{u_i' u_j'}$, is **identical in form** to those obtained by Reynolds (1985), U_i,P and $\overline{(\tilde{u}_i+\hat{u}_i+u_i')(\tilde{u}_j+\hat{u}_j+u_j')}$ with the phase average here replacing the Reynolds average as was pointed out and stated earlier (Gatski and Liu 1980; Liu 1981). The U_i,P,R_{ij} system thus has the large-scale coherent structure taken out and considered explicitly, as suggested by Dryden (1948). The stresses $R_{ij} = \langle u_i' u_j' \rangle$ involves only the "real turbulence", thus second-order closure models, when suitably found, would most likely be more universal than the prevailing closure models for the Reynolds stresses $\overline{(\tilde{u}_i+\hat{u}_i+u_i')(\tilde{u}_j+\hat{u}_j+\hat{u}_j')}$ that include the contributions from the large-scale coherent structures. The latter are now well recognized as being non-universal because of the non-universality of hydrodynamic instability mechanisms (Liu 1981). As was shown in Section II, conservation equations can always be obtained for U_i,$\tilde{u}_i$ and $\hat{u}_i$, and transport equations for $\overline{u_i' u_j'}$, $\tilde{r}_{ij}$ and $\hat{r}_{ij}$. Within the U_i,P,R_{ij} framework, however, the study of mean flow,

coherent mode and fine-grained turbulence interactions can always be obtained by performing the Reynolds average **after** the results are found. As we have emphasized already, this procedure is really only practicable for the simplest problem, that is, the time dependent, mixing layer between two opposite parallel streams.

This problem was considered by Gatski and Liu (1980). The problem consists of the interaction of a monochromatic component of the large-scale coherent structure (so that $\tilde{u}_i + \hat{u}_i$ reduces only to $\tilde{u}_i$, say) with the fine-grained turbulence in a temporal mixing layer of horizontally homogeneous and oppositely directed streams. The coherent mode is horizontally periodic and develops in time. The physical significance of this class of problems is that it strongly resembles, but does not exactly correspond to, the spatially developing free shear layer in observations. The coherence enters into the periodic horizontal boundary conditions and the numerical problem is thus well-defined. This is in contrast to the numerical problem for the spatially developing mixing layer which is not as well-defined because of the unknown but necessary downstream boundary conditions. In this problem the vorticity axis of the large-scale structure lies in the spanwise, y-direction, with the velocities U,W in the streamwise and vertical directions, x,y, respectively. The spanwise velocity V is taken to be zero. (Relaxation of the monochromatic two-dimensional coherent structure to accommodate subharmonics, the coherent streamwise vortical coherent structures and the resulting generation of V and spanwise variations of U and W are certainly possible.) Here, all spanwise gradients of the phase-averaged quantities are also zero. Because of the two-dimensional coherent motions, it is possible to define the stream function

$$U = \frac{\partial \Psi}{\partial z}, \; W = -\frac{\partial \Psi}{\partial x}. \tag{4.4}$$

The vorticity is then related to the stream function via $\Omega = -\nabla^2\Psi$, where

$$\nabla^2 = \partial^2/\partial x^2 + \partial^2/\partial z^2 \tag{4.5}$$

is the Laplacian in the x,z plane. The nonlinear, total coherent vorticity equation then gives

$$\nabla^2\Psi_t + \Psi_z\nabla^2\Psi_x - \Psi_x\nabla^2\Psi_z = \langle u'w'\rangle_{xx} - \langle u'w'\rangle_{zz} + (\langle w'^2\rangle - \langle u'^2\rangle)_{xz}, \tag{4.6}$$

where subscripts indicate the appropriate partial differentiation. If we were to study the transition problem, (4.6) will then be augmented by the viscous diffusion mechanism $\nabla^4\Psi/Re$ on the right side. Here all velocities and coordinates are made dimensionless by the free stream velocity and the initial shear layer thickness (the pressure is made dimensionless by the free stream dynamic pressure). Viscosity effects have been neglected in the large-scale structure vorticity equation (4.6). Thus the phase-averaged stresses on the right of (4.6) take the place of viscous diffusion in the turbulent shear layer problem.

The two-dimensional vorticity equation (4.6) for $\Omega = -\nabla^2\Psi$ is merely the y-component of the total coherent vorticity $(\Omega_i+\tilde{\omega}_i+\hat{\omega}_i)$ given by equations (2.28) - (2.30) in the absence of the vorticity stretching/tilting mechanism and with the viscosity effects neglected. The net phase-averaged vorticity transport contributions

from the turbulence on the right sides of (2.28) - (2.30) would give

$$-\frac{\partial}{\partial x_j}\langle u_j'\omega_i'\rangle.$$

Its two-dimensional form, through the use of the continuity condition, reduces to the form on the right side of (4.6), in terms of the phase-averaged stresses $\langle u_i' u_j'\rangle$. Their transport equations are identical in form to the Reynolds system for $\overline{u_i' u_j'}$ (Gatski and Liu 1980; Liu 1981),

$$\left[\frac{\partial}{\partial t} + U_k\cdot\frac{\partial}{\partial x_k}\right]\langle u_i' u_j'\rangle = -\underbrace{\left[\langle u_j' u_k'\rangle\frac{\partial U_i}{\partial x_k} + \langle u_i' u_k'\rangle\frac{\partial U_j}{\partial x_k}\right]}_{\text{production}} + \underbrace{\langle p'\left(\frac{\partial u_i'}{\partial x_j} + \frac{\partial u_j'}{\partial x_i}\right)\rangle}_{\text{redistribution}}$$

$$\underbrace{-\frac{\partial}{\partial x_k}\left[\langle u_i' u_j' u_k'\rangle + \langle p'(u_i'\delta_{jk}+u_j'\delta_{ik})\rangle - \frac{1}{Re}\frac{\partial\langle u_i' u_j'\rangle}{\partial x_k}\right]}_{\text{transport}} \underbrace{- 2\frac{1}{Re}\left\langle\frac{\partial u_j'}{\partial x_k}\frac{\partial u_j'}{\partial x_k}\right\rangle}_{\text{dissipation}}, \qquad (4.7)$$

where the Reynolds number Re is based on the free stream velocity and initial shear layer thickness, δ_{ij} is the usual Kronecker delta. In the present problem (4.7) is equivalent to the sum of (2.42) and (2.43) for $\langle u_i', u_j'\rangle = \overline{u_i' u_j'} + (\tilde{r}_{ij}+\hat{r}_{ij})$. In Gatski and Liu (1980)'s framework the dominant large-scale coherent structure is sorted out distinctly from the fine-grained turbulence through phase averaging at the outset. This is in contrast to the prevalent numerical simulation methods where the entire flow is decomposed into succeeding, neighboring Fourier modes corresponding to the

horizontal periodic boundary condition. For lower Reynolds numbers the simulation is "exact", whereas for high Reynolds numbers an eddy viscosity subgrid closure is invoked (Reynolds 1976; Riley, et al 1981). In order to discover coherent structures additional limited spatial averaging is needed, as was done for the turbulent boundary layer problem by Kim (1983, 1984) and Moin (1984). In the simpler, explicit calculation of the dominant coherent structure in the mixing region (Gatski and Liu 1980) the phase-averaged, fine-grained turbulent stresses appear in the coherent structure vorticity equation as would be the Reynolds-averaged stresses in the Reynolds (1895) system. In this case, some form of the Reynolds stress closure arguments (e.g., Lumley 1978) could conceivably be adapted to the closure problem for (4.7). The eddy viscosity models were purposely avoided primarily because the consequences of such a model implies the a priori regulation of the direction of energy transfer to the smaller scales. Gatski and Liu (1980) used the formalism of Launder, et al (1975). This enabled them to obtain of the energy transfer mechanism between the coherent mode and turbulence, $\overline{\tilde{r}_{ij}(\partial\tilde{u}_i/\partial x_j + \partial\tilde{u}_j/\partial x_i)}$, on the basis that the coherent mode dynamics are obtained from conservation equations, coupled to the turbulenct stresses via their transport equations. The functional forms of the Reynolds stress closure should apply, though the detailed closure constants might not. However, the behavior of the fine-grained turbulence, with the non-universal coherent structure subtracted out, would be much more universal than the treatment of all oscillations, including the coherent structures, as "turbulence". In Gatski and Liu (1980), the transport equations for phase-averaged stresses include those for the single

shear stress $\langle u'w' \rangle$, three normal stresses $\langle u'^2 \rangle$, $\langle u'^2 \rangle$ and $\langle w'^2 \rangle$ and a modeled transport equation for the rate of viscous dissipation $\langle \epsilon \rangle$. The fine-grained turbulence is three-dimensional, but the spanwise derivatives $\partial \langle u_i' u_j' \rangle / \partial y$, vanish.

The vertical boundary conditions require all flow quantities vanish far away from the shear layer. Horizontal periodic boundary conditions are applied to all phase-averaged quantities, with the periodicity dictated by the wavelength of the initial coherent mode chosen. The initial conditions are arrived at through an initialization process described in Gatski and Liu (1980). In the absence of the coherent structure, the Reynolds-mean problem, consisting of the hyperbolic type mean shear flow and the Reynolds-averaged stresses and dissipation rate, is solved from "$t = -\infty$" to $t = t_0$ when self-preservation is very nearly achieved. This is to ensure self-consistency among the Reynolds-mean flow quantities when the initial conditions are to be imposed. The coherent disturbance imposed initially is obtained from the Rayleigh ("inviscid") equation corresponding to the initialized mean velocity profile and at an initial wave number corresponding to the most amplified mode for this profile ($\alpha \cong 0.275$); the initial kinetic energy content of the turbulence used in the computations was $E_t(0) = 1.2 \times 10^{-2}$ obtained from the initialization process and that of the coherent mode $E_\ell(0) = 10^{-4}$, where E_t and E_ℓ are defined by (4.8) and (4.9), respectfully. The disturbance is considered to be suddenly imposed, with the corresponding phase-averaged stresses and dissipation rate, which require finite time to respond, set equal to zero. The interaction between the Reynolds mean motion U, coherent structure $\tilde{u}_i$ and the structure Reynolds-averaged fine-grained turbulence

$\overline{u_i' u_j'}$ can be studied after the numerical results are obtained as already emphasized. The "strength" of the fluctuations and the mean flow are characterized by their kinetic energy content.

C. DIAGNOSTICS OF NUMERICAL RESULTS VIA REYNOLDS AVERAGING

The two-dimensional large-scale structure energy content is

$$E_\ell = \frac{1}{2} \int_{-\infty}^{\infty} (\overline{\tilde{u}^2} + \overline{\tilde{w}^2}) dz, \tag{4.8}$$

where the overbar is the Reynolds-average and is here the horizontal average over one wave length. Similarly, the fine-grained turbulence energy content is

$$E_t = \frac{1}{2} \int_{-\infty}^{\infty} (\overline{u'^2} + \overline{v'^2} + \overline{w'^2}) dz. \tag{4.9}$$

The mean flow kinetic energy defect is defined as

$$E_n = \int_{-\infty}^{0} (U^2 - U_{-\infty}^2) dz + \int_{0}^{\infty} (U^2 - U_{\infty}^2) dz. \tag{4.10}$$

where the dimensionless outerstream velocities are $U_{\pm\infty} = \pm 1$ in the present notation. The development of E_ℓ, E_t and E_m with time provides the insight into the nonequilibrium interactions among the three "components" of the energy. To this end, the diagnostics of the exact energy integral equations and the energy exchange mechanisms are obtained from the computational results via Reynolds averaging. The

energy integral equations, which follows from (2.21), (2.24) + (2.25) and (2.26), are:

$$\frac{dE_m}{dt} = -\tilde{I}_p - I'_p \tag{4.11}$$

$$\frac{dE_\ell}{dt} = \tilde{I}_p - I_{\ell t}, \tag{4.12}$$

$$\frac{dE_t}{dt} = I'_p + I'_{\ell t} - \overline{\phi'}. \tag{4.13}$$

We note that (4.11) - (4.13) were the starting point for an approximate consideration of the problem discussed in Liu and Merkine (1976). The energy exchanges between the mean flow and the fluctuations are given by the integrals

$$\tilde{I}_p = \int_{-\infty}^{\infty} -\overline{\tilde{u}\tilde{w}} \frac{\partial U}{\partial z} dz \tag{4.14}$$

$$I'_p = \int_{-\infty}^{\infty} -\overline{u'w'} \frac{\partial U}{\partial z} dz; \tag{4.15}$$

the energy exchange between the large-scale coherent structure and fine-grained turbulence is given by the integral

$$I_{\ell t} = \int_{-\infty}^{\infty} -\left[\overline{\tilde{r}_{xx} \frac{\partial \tilde{u}}{\partial x}} + \overline{\tilde{r}_{xz} \left(\frac{\partial \tilde{u}}{\partial z} + \frac{\partial \tilde{w}}{\partial x}\right)} + \overline{\tilde{r}_{zz} \frac{\partial \tilde{w}}{\partial z}}\right] dz. \tag{4.16}$$

The integrands in (4.14) - (4.16) have in common the product of stresses with the

appropriate rates of strain. The rate of viscous dissipation of the fine-grained turbulence is

$$\overline{\phi}' = \int_{-\infty}^{\infty} \overline{\epsilon}\, dz. \tag{4.17}$$

Consistent with (4.6), viscosity effects on the large-scales are not included. The sum of (4.11) - (4.13) gives

$$\frac{d}{dt}(E_m+E_\ell+E_t) = \overline{-\phi'}\,, \tag{4.18}$$

that the overall kinetic energy decays according to the rate of viscous dissipation of the fine-grained turbulence.

In spite of the local regions where energy is transferred from the fine-grained turbulence to the large-scale coherent structures indicated by structural results (see Figures 9 and 11-13 in Gatski and Liu 1980), the integral $I_{\ell t} > 0$ indicates that the global energy transfer is from the large to the fine scales of fluctuations. The time development of this integral is shown in Figure 5, which indicates that $I_{\ell t}$ peaks in the vicinity when the global energy transfer from the mean motion to the coherent mode changes sign. This latter mechanism, which is the integral of the energy exchange mechanism between the mean flow and the large-scale coherent structure is also shown in Figure 5; $\tilde{I}_p$ first increases, with energy feeding from the mean flow into the coherent mode, and then dcreases to below the axis as time increases, indicating an energy

transfer back to the mean flow. The evolution of such features is a familiar one in hydrodynamic stability problems of **developing** shear flows whether fine-grained turbulence is present or not. In laminar flows the development of positive and then negative disturbance production mechanism was first uncovered by Ko, Kubota and Lees (1970) in their approximate consideration of spatial, finite-disturbances in the laminar wake problem. Similar features were also recovered in the extensions of the Amdsen and Harlow (1964) computational problem by Patnaik et al (1976). It was also anticipated and shown that the devleopment of the positive and then negative coherent structure production mechanism would also exist in free turbulent shear flows (Liu 1971, Mankbadi and Liu 1981). This is essentially an "inviscid" or "dynamical" instability phenomenon in the hydrodynamic stability sense and can be anticipated when the kinematics of the growth rates from linear hydrodynamic stability theory are applied to the developing free shear flow through scaling by the local shear flow thickness. In the temporal problem for a fixed wave number disturbance, as the shear grows in time the rescaled local wave number increases, rendering the growth rates to eventually become negative. Similar interpretations also hold for the spatial problem where the local rescaled frequency increases with the downstream distance, the disturbance is eventually advected into the damped region. Experimentally, these features are not surprising either. As an example, the results of Fiedler, et al (1981) reproduced in Figure 2, taken along the line of most intense mean shear, very nearly approximates the integral $\tilde{I}_p$ (see also Weisbrot 1984). The theoretical results from the dynamics of the problem (see also Liu 1971, Mankbadi and Liu 1981) and experimental observed **evolution** of this energy

exchange mechanism is strikingly similar. There is no mistake that this "damped disturbance" phenomenon is one derived from ideas in hydrodynamic stability theory. The kinematical interpretation in terms of possible eddy orientations (Browand 1980) are summarized in Hussain (1983).

The time evolution of the coherent-mode energy dE_{ℓ}/dt is thus the difference $\tilde{I}_p - I_{\ell t}$ according to (4.12) and is also shown in Figure 5. It is clear from this numerical example that the fine-grained turbulence produces a global "turbulent dissipation" and augments the "damped disturbance" mechanism in causing the demise of coherent energy with time shown in Figure 6. The earlier vigorous amplification is due to extraction of energy from the Reynolds mean motion. The peak in the coherent-mode energy $E_{\ell}/E_{\ell 0}$ correspond to the vicinity when $\tilde{I}_p$ changes sign and $I_{\ell t}$ is maximum.

The fine-grained turbulence production rate I_p' starts out slightly larger than the dissipation rate $\overline{\phi'}$ as shown in Figure 7. This accounts for the initial small rate of growth of the turbulent kinetic energy E_t/E_{t0} shown in Figure 8. The production of turbulence from the mean flow is made more efficient by the presence of the coherent mode in the initial development stage although the direct energy transfer to the turbulence from the coherent mode is relatively small. But the net difference between production and destruction give rise to the evolution of a nonequilibrium development of the turbulence energy that evolves from an initial self-similar behavior to a new, higher level of self-similar behavior as shown in Figure 8. In terms of time development, the "burst" of fine-grained turbulence has taken place at the expense of the coherent mode.

The physical pictures derived here strongly suggest similar physical mechanisms, except for details, hold for the turbulent jet experiments of Favre-Marinet and Binder (1979) depicted in Figure 1, where the observed coherent mode grows and decays while the turbulence is enhanced.

As far as the coherent mode is concerned, the production and "dissipation" are in general not in balance during the time evolution in free shear flow problems. Thus marginal stability ideas would not be as useful here as would be for confined flow problems (e.g., Barcilon, et al 1979).

D. EVOLUTION OF LENGTH SCALES

The following definition of the shear layer thickness (which is not unique) is used

$$\delta(t) = \left[\int z^2 \partial\bar{U}/\partial z \, dz / \int \partial\bar{U}/\partial z \, dz \right]^{1/2} .$$

It is normalized by its initial value and is shown in Figure 9. Initially, the growth is self-similar in that $\delta \sim t$. Its subsequent modification is due to the nonlinear, nonequilibrium interactions that the Reynolds mean flow engages directly with the coherent mode and the fine-grained turbulence. Eventually, after subsidence of the coherent mode, the spreading is self-similar again $\delta \sim t$. From the structural results, the height of the closed streamline H, normalized by its initial value H_0, is also shown in Figure 9; it reaches a maximum at about $t \approx 2$ and subsequently decreases and is similar

to the development of the coherent-mode energy with time.

There is another "detail" of observations that can be qualitatively understood from Gatski and Liu (1980). That is, in the optical observations of Brown and Roshko (1974) the graininess of the fine-grained turbulence appears to enlarge as the shear layer spreads downstream. The size L_ϵ of the fine-grained turbulence from Gatski and Liu (1980) can be estimated by using a local equilibrium argument such that the eddy energy transfer rate down to the size L_ϵ just balances the viscous dissipation rate. This leads to $L_\epsilon \approx E_t^{3/2}/\overline{\phi'}$. Shown in Figure 9 is L_ϵ normalizing by its initial value $L_{\epsilon 0}$ as it evolves in time. Although L_ϵ rapidly decreases initially, as the coherent mode energy E_ℓ passes its maximum at about $t \approx 2$ (Figure 6), the scale of the fine-grained turbulence begins to increase with time at a rate similar to that for the shear layer thickness δ. In fact, L_ϵ/δ remains very nearly constant after $t \gtrsim 1.50$. The coarsing of the graininess of the fine-grained turbulence derived here accompanies the spreading of the shear layer (Gatski and Liu 1980). This appears to be entirely consistent with observations of Brown and Roshko (1974) that as the observed "strength" of the coherent mode weakens the spreading of the shear layer is maintained via the coarsing of the graininess of the fine-grained turbulence.

E. SOME STRUCTURAL DETAILS

We shall refer to Gatski and Liu (1980) for the details of the time evolution of structural results in terms of the phase-averaged stream function and vorticity

contours. We will illustrate here the instantaneous Ψ and Ω contours in Figures 10 and 11, respectively, for t = 1.50 when the coherent-mode energy is at its maximum and $dE_{\ell}/dt = 0$. There are strong vorticity nonuniformities within the "cat's eye" as would be expected for the t = $O(1)$ nonequilibrium stages of development. A similar nonlinear critical-layer theory (Benny and Bergeron 1969) for the present class of problems would require the vorticity within the cat's eye region to be uniform. This might be achieved as $t \to \infty$ for the idealized single event of the monochromatic problem as the fine-grained turbulence smooths out the inner coherent vorticity distribution. The coherent structure at the $t \to \infty$ neutral stage would have been significantly weakened that its participation in the shear layer dynamics would be of questionable interest.

Other structural details of the phase-averaged quantities that are of interest are those pertaining to the energy conversion mechanisms, the consequences of their Reynolds' average have already been discussed. At the phase-averaged level, the conversion of overall coherent mode energy to the horizontal fine-grained turbulence energy $\langle u'^2 \rangle/2$ is achieved primarily through the work done by the modulated turbulent shear stress against the coherent rate of strain, $-\langle u'w' \rangle \partial U/\partial z$. The contours of both of these quantities are shown in Figure 12a,b for the instant t = 1.50. The conversion mechanism due to the normal stress $-\langle u'^2 \rangle \partial U/\partial x$ is significantly weaker in this case and is not shown (see Gatski and Liu 1980). The rate of energy transfer in Figure 12a shows that there are local regions where turbulence energy is converted back to the coherent mode. The contributions to the vertical part of the turbulence energy $\langle w'^2 \rangle/2$ come from the dominant normal stress

conversion mechanism $-\langle w'^2\rangle \partial W/\partial x$, These are similar to the patterns for $\langle u'^2\rangle/2$ and we refer, again, to Gatski and Liu (1980) for details. These are the direct energy transfer mechanisms between the fine-grained turbulence and the two-dimensional overall coherent mode. The three-dimensional turbulence include also the spanwise contribution to its energy $\langle v'^2\rangle/2$. This is produced and maintained via the isotropizing mechanism of the pressure-velocity strain correlation $\langle p'\partial v'/\partial y\rangle$. The contours of these quantities are shown in Figure 13 for t = 1.50. The quantity $\langle p'\partial v'/\partial y\rangle$, however, was not an explicitly calculated quantity but was approximated via closure arguments, including the effects attributable to local rapid distortion due to the large-scale coherent structure (Gatski and Liu 1980; Launder et al 1975). Although this mechanism converts energy to $\langle v'^2\rangle/2$ on an overall basis, there are nevertheless local regions in which this energy conversion mechanism reverses sign.

V. THE ROLE OF LINEAR THEORY IN NONLINEAR PROBLEMS

A. INTRODUCTORY COMMENTS

The role of linearized theory in finite-amplitude, weakly nonlinear hydrodynamic stability problems is well known (Stuart 1958, 1960, 1962a,b, 1967, 1971a, 1972); particularly the parallel flow problem there serves as a valuable guide to the class of problems of interest here. In order to gain the necessary perspective as to how the linear hydrodynamic stability problems fit into and be made use of in nonlinear problems involving in **developing flows**, we purposely preceded this section by the discussion of a simple nonlinear problem in Section IV. The temporal mixing layer discussed in that section contains a vast richness in physical processes which could still be explored further. However, numerical extensions of the problem, though readily possible, are nevertheless tedious and it would be most worthwhile in exploring certain ideas and concepts derivable from the problem of Gatski and Liu (1980) in order to make progress, via simplification, towards the ambitious possibilities of describing the class of problems involving real, spatially developing flows found in the laboratory and in practical devices involving mixing-controlled situations. For purposes of introducing ideas, we shall mingle in our discussions ideas derived from the temporal problem with observable quantities in the laboratory without further qualifications.

The energy content of the coherent mode E_ℓ introduced in Section IV, equation (4.8), is a quantity measurable in the laboratory (Ho and Huang 1982) for different

modes. For a given initial energy level and shear layer thickness it is a quantity that depends on the mode content in its nonequilibrium evolution. Thus in the laboratory, high frequency modes' energy content peak further upstream then lower frequency modes (or the longer wavelength disturbances peak later in time). As such, E_ℓ is essentially related to an amplitude of the disturbance. It is the "slowly varying" wave envelope bounding the "fast" oscillations of the wave motion. There is strong observational evidence that for nonlinear problems while the wave envelope has to be obtained from a nonlinear theory with the physics of the problem participating fully, the wave characteristics are obtainable from the kinematics of a locally linearized theory (Michalke 1971). However, considerable confusion concerning the role of the linear theory would still result from the nonuniqueness of the "amplitude" associated with linear solution, the lack of distinguishability of the "wave envelope" from the "wave function" and the relative sensitivity of the wave-envelope to the real physical mechanisms in the shear flow evolution. Thus an extended discussion along these lines might help unravel some of the possible confusion that might result from reading the current literature (Wygnanski and Petersen 1985).

B. NORMALIZATION OF THE WAVE AMPLITUDE

In order to bring in the role of the linear theory it is thus essential that we provide the distinguishable roles of the wave envelope or amplitude, the hydrodynamical instability wave functions and the physically sensible manner in

which such functions are to be normalized. If we introduce a coherent-mode energy density as $E_\ell/\delta = |A|^2$, where $|A|^2$ would be a function of the mode number and mean motion evolutionary variable (wave number and time for the temporal problem, frequency and the streamwise distance for the spatial problem). Thus, according to our definition, (4.8) gives

$$|A|^2 = \frac{E_\ell}{\delta} = \frac{1}{2}\int_{-\infty}^{\infty} (\overline{\tilde{u}^2}+\overline{\tilde{w}^2})\, d(\frac{z}{\delta}). \tag{5.1}$$

We are using the two-dimensional coherent mode for simplified illustration, these ideas are easily extendable to include three-dimensional coherent modes. If we further assume that the velocities $\tilde{u},\tilde{w}$ are representable by the linear hydrodynamic stability theory, then the linear eigenfunctions are represented by the disturbance stream function ϕ in terms of local variables $\xi = x/\delta$, $\zeta = z/\delta$ with the local wave number α referred to δ. Then, in terms of the temporal mixing layer notation, for instance,

$$\begin{bmatrix} \tilde{u} \\ \tilde{w} \end{bmatrix} = A(t) \begin{bmatrix} \phi'(\zeta;\alpha) \\ -i\alpha\phi(\zeta;\alpha) \end{bmatrix} \exp(i\alpha\xi) + \text{c.c.}, \tag{5.2}$$

where ϕ' is the ζ-derivative of ϕ, the local ξ-derivative of ϕ is given by $-i\alpha\phi$, c.c. denotes the complex conjugate. In this case, the physical wavenumber is fixed but the local wavenumber changes as the shear layer thickness, δ, grows.

If we substitute (5.2) into (5.1), then

$$|A(t)|^2 = |A(t)|^2\left\{\frac{1}{2}\int_{-\infty}^{\infty}(|\phi'|^2 + |\alpha\phi|^2)d\zeta\right\}. \tag{5.3}$$

Thus, in order that we consistently attribute $|A|^2 = E_\ell/\delta$ indeed as the energy density, the local eigenfunctions must be normalized locally by the condition

$$\frac{1}{2}\int_{-\infty}^{\infty}(|\phi'|^2 + |\alpha\phi|^2)d\zeta = 1. \tag{5.4}$$

This addresses an appropriate normalization for the wave functions of the local linear theory for which the wave envelope would be given consistent physical meaning; this would not be the case with the "equal area" normalization (e.g., Wygnanski and Petersen 1985).

C. GLOBAL ENERGY EVOLUTION EQUATIONS

The above discussions follow those ideas put forth by Ko, Kubota and Lees (1970) in their generalizaiton of the shape assumption ideas of Stuart (1958) to real, developing free laminar shear flows with strongly amplified disturbances. While the cross-stream shape of the coherent mode would be given by the (properly normalized) linear theory, the overall evolution via the wave envelope, $|A(t)|^2$, must be solved by

the nonlinear theory with the proper physics involved. In Ko, Kubota and Lees (1970), the evolution of $|A|^2$ follows naturally from the disturbance energy integral equation. This is solved jointly with δ which follows from the mean flow kinetic energy equation following a similar shape assumption for the mean velocity profile. The problem is relatively much simpler in the absence of the participation of fine-grained turbulence in the dynamics.

From the diagnosis of the numerical results of Gatski and Liu (1980) for the turbulent shear layer, we see that if we were to obtain the evolution of $|A|^2 = E_\ell/\delta$, then the "exact" envelope equations (4.11) - (4.13) tell us that

$$\frac{dE_m}{dt} = -\tilde{I}_p - I_p' \tag{5.5}$$

$$\frac{d}{dt}\,\delta|A|^2 = \tilde{I}_p - I_{\ell t} \tag{5.6}$$

$$\frac{dE_t}{dt} = I_p' + I_{\ell t} - \overline{\phi'}\,. \tag{5.7}$$

From the diagnosed numerical results (Gatski and Liu 1980) discussed in Section IV, any approximate calculation for the wave envelope $|A|^2$ must necessarily involve the participation of the turbulenct kinetic energy content E_t and the mean flow kinetic energy defect E_m. Thus, strong nonlinear interactions occur among the "envelopes" $|A|^2$, E_t and E_m independently of whatever version of the linear hydrodynamical

stability equations that might have been used to generate the eigenfunctions ϕ in a possible assumption such as (5.2). We emphasize here that for nonlinear problems, the wave envelope must necessarily be obtained with the simultaneous nonlinear interactions between the mean motion, fine-grained turbulence and large-scale coherent structure properly (though approximately) taken into account.

D. SUBSIDIARY PROBLEMS. THE ROLE OF THE LINEARIZED THEORY

To further interpret (5.5) - (5.7) in terms of approximate considerations and in order to make practical the modelling of the "envelope" evolution problem we further postulate that, again using the temporal mixing layer as illustration (Liu and Merkine 1976), the mean flow behaves like

$$\frac{U}{\frac{1}{2}(U_\infty - U_{-\infty})} = F(\zeta) \tag{5.8}$$

where $F(\zeta)$ could conveniently be $\tanh \zeta$ or other function of ζ. From observations, the similarity behavior is almost established with the establishment of the mixing region profile. We introduce a similar energy density for the fine-grained turbulence as $E = E_t/\delta$, where E_t was defined by (4.9). Similar to the shape assumption for the coherent mode, we postulate (Liu and Merkine 1976) that the Reynolds stresses of the fine-grained turbulence be represented by

$$\overline{u_i' u_j'} = E(t) R_{ij}(\zeta) \tag{5.9}$$

such that the energy density E(t), like $|A(t)|^2$, bears the burden of the history of the nonequilibrium interactions, while the local shape functions $R_{ij}(\zeta)$ behaves according to observations $c_{ij} \exp(-\zeta^2)$. The constants c_{ij} would reflect the proper ratio between the turbulent kinetic energy and Reynolds shear stress as well as the necessary normalization to render indeed that $E = E_t/\delta$ is the turbulence energy density.

The rate of energy transfer between the large-scale coherent structure and fine-grained turbulence is provided by the integral $I_{\ell t}$ in (5.6), which is defined by (4.16). As the numerical results of Gatski and Liu (1980) illustrate, $I_{\ell t}$ contributes significantly towards the energy balances determining the evolution of the wave envelope $|A|^2$ or $\delta|A|^2$ in competition with the "inviscid" mechanism of energy exchanges between the coherent mode and the mean flow, $\tilde{I}_p$. Thus the participation of modulated fine-grained stresses, $\tilde{r}_{ij}$, which occur in the integrand of $I_{\ell t}$, must be taken into account. accounted.

From the general considerations discussed in Section II, illustrated by (2.14), the problem of $\tilde{u}_i$ and $\tilde{r}_{ij}$ are coupled through the action of the modulated stresses on the momentum problem of the large-scale coherent structure. Concurrently, $\tilde{r}_{ij}$ is given by its own transport equations, illustrated by (2.43). Thus, following the manner in which the coherent mode velocities were represented by the shape assumption such as (5.2), with the cross-stream shape given by the linear theory, $\tilde{r}_{ij}$

would necessarily take the following form (Liu and Merkine 1976):

$$\tilde{r}_{ij} = A(t)E(t)r_{ij}(\zeta,\alpha)\exp(i\alpha\xi) + \text{c.c.}, \tag{5.10}$$

with $r_{ij}(\zeta,\alpha)$ given by the local linear theory, jointly with $\phi(\zeta,\alpha)$.

Prior to discussing the nonlinear "envelope" problem, we shall briefly discuss the subsidiary, appropriate linear problem for ϕ and r_{ij} that has to be solved. The nonlinear problem that we have discussed thus far places the auxiliary linear problem in the proper perspective. The linear problem for a monochromatic large-scale disturbance follows directly from the linearized form of (2.13), (2.14) and (2.43). It was considered by Elswick (1971), Reynolds and Hussain (1972), and Legner and Finson (1980) in various forms. Liu and Merkine (1976), Alper and Liu (1978), Mankbadi and Liu (1981) considered the linear theory as an implement in nonlinear problems involving coherent mode-turbulence interactions. The local linear theory is obtained through the substitution of (5.2), (5.9) and (5.10) into the linearized vorticity and transport equations for $\tilde{r}_{ij}$ as already discussed. In terms of **local** variables, we obtain

$$i\alpha[(U-c)(\phi''-\alpha^2\phi) - \phi U''] = E[-\alpha^2 r_{xz} - r''_{xz} + i\alpha(r_{zz}-r_{xx})'] \tag{5.11}$$

$$i\alpha(U-c)\begin{bmatrix} r_{xx} \\ r_{yy} \\ r_{zz} \\ r_{xz} \end{bmatrix} = -(-i\alpha\phi)\begin{bmatrix} R'_{xx} \\ R'_{yy} \\ R'_{zz} \\ R'_{xz} \end{bmatrix} - \begin{bmatrix} 2r_{xz} \\ 0 \\ 0 \\ r_{xz} \end{bmatrix} U' + \begin{bmatrix} -R_{xx}2i\alpha\phi' - R_{xz}2\phi'' \\ 0 \\ R_{zz}2i\alpha\phi' - R_{xz}2\alpha^2\phi \\ -R_{zz}\phi'' - R_{xx}\alpha^2\phi \end{bmatrix} -$$

Advection by mean flow

Transport (vertical advection of mean stresses by wave)

"Production" from mean

Work done by mean stresses against wave rates of strain

$$- (p_{ji}+p_{ij}) - \frac{2}{Re}\phi_{ij}\,, \qquad (5.12)$$

where c is the wave speed, Re is a local Reynolds number, primes denote differentiation with respect to the local vertical variable ζ, the local ξ-differentiation is replaced by $i\alpha$. The subscripts x,y,z are associated with the streamwise, spanwise and vertical coordinates, respectively. The effect of viscous diffusion, which could be included, has been omitted from (5.11) and (5.12). The form of linear problem given by (5.11) and (5.12) holds for either the temporal problem (c complex, α real) or the spatial problem (αc = frequency, real) or for the "wave packet" problem (Gaster 1981). The linearized vorticity equation in terms of the stream function, (5.11), immediately bear resemblence to the nonlinear vorticity equation (4.6). If we subtract the Reynolds average of (4.6) from (4.6) itself and linearize, the resulting linear equation then forms the basis for (5.11). The right side of (5.11) in terms of

differentiation with respect to local variables, has the same interpretation as the right side of (4.6).

The linearized version of the transport equations for the modulated stresses (5.12) are written in a form with the right side resembling that of (2.43), (see also (2.44) and (2.45)). Comparing the forms of (2.43) and (5.12), the linearization circumvented the triple correlations as well as the transport of $\tilde{r}_{ij}$ by the fluctuations $\tilde{u}_k$ in the transport mechanisms, so that for local parallel flow the sole surviving transport effect is the advection of the mean stresses by the coherent vertical velocity. In the mechanism of "production" from the mean the only effect comes from the shear rate of strain of the mean flow, U'. The third group of terms on the right of (5.12) is the work done by the mean stresses against the coherent (wave) rates of strain. Absent in (5.12) is the work done by the modulated stresses against the coherent rates of strain in (2.43) which is a nonlinear effect. No empiricisms were present in these first three groups of effects. The action of the pressure gradients is represented by $(p_{ji}+p_{ij})$, defined (prior to the wave amplitude/wave function assumption) by (2.45) and (2.46). Similarly, the viscous dissipation rate ϕ_{ij} in (5.12) is related to the definition in (2.47). These two mechanisms, if included, would require closure arguments. Even without the effects of the action of pressure gradients and viscous dissipation, it is obvious from only the first three mechanisms on the right of (5.12) (a form of "rapid distortion" theory, free from empiricisms (Hunt 1973) that r_{ij} would not necessarily be in **phase** with rates of strain of the coherent mode. Thus any eddy-viscosity assumption in relating r_{ij} to the rates of strain of the coherent

mode might, according to (5.12), render such eddy viscosities to be complex with magnitudes changing sign depending on the location across the shear layer and the local coherent-mode number. The implications of the relative phases between the coherent mode velocity gradients and the modulated stresses in energy transfer will be discussed subsequently.

In order to make practical usage of the system (5.11) and (5.12), statements about the viscous dissipaton rate and pressure-gradient action must be made. Since the linear theory here is thought of as a valuable implement in the approximate consideration of the nonlinear "wave envelope" problem, the simplest form of such closure statements would suffice. We have, however, for good reasons already discussed, precluded an overall eddy viscosity treatment of r_{ij} as was done by Reynolds (1972) and Reynolds and Hussain (1972) for the linear problem. Elswick (1971) considered the wave modulated stresses as a perturbation upon the mean stress. In so doing, Elswick (1971) also considered the closure of the linear problem as a perturbation of the closure statements upon the mean motion problem. However, Elswick (1971) neglected viscous effects altogether in (5.12), including viscous dissipation. He also neglected the "transport" effect that constitute partially the sources or sinks for the wave modulated stresses. The perturbed form for the common assumption (e.g., Lumley 1970, 1978) about $(\tilde{p}_{ji}+\tilde{p}_{ij})$ appear for (5.12) in the form

$$\frac{1}{T}\left[\begin{bmatrix} r_{xx} \\ r_{yy} \\ r_{zz} \\ r_{xz} \end{bmatrix} - \frac{1}{3}\begin{bmatrix} \sum_i r_{ii} \\ \sum_i r_{ii} \\ \sum_i r_{ii} \\ 0 \end{bmatrix}\right]$$

where $\sum_i$ denotes the sum of the three normal stresses, $T^{-1} = sU'$ is the time scale for return to isotropy where the constant of proportionality is of order unity ($s \approx 1.445$). Elswick (1971) also partially perturbed this time scale. In the linearized form of the transport equations for r_{ij} presented by Reynolds and Hussain (1972), prior to their eddy viscosity assumption, the pressure-gradient action and the viscous dissipation were neglected; but the viscous diffusion, $(Re^{-1})\partial^2 r_{ij}/\partial x_k^2$, was retained for the wall-bounded shear flow problem. The perturbed form of the viscous dissipation rate in (5.12) would be of the form

$$\frac{d}{T}\begin{bmatrix} \sum_i r_{ii} \\ \sum_i r_{ii} \\ \sum_i r_{ii} \\ 0 \end{bmatrix}$$

where the constant is of the order $d \approx 0.1$ (see, for instance Liu and Merkine (1976), Alper and Liu (1978)).

For turbulent free shear flows, the presence of a mean inflectional profile strongly

suggests the consideration of the coherent oscillations $\tilde{u}_i$ in terms of "dynamical" or "inertial" instabilities (Liepmann 1962; Liu 1971b, 1974a). That is, arguments in this respect (Liu and Merkine 1976) leads to the "inviscid" or Rayleigh equation in place of (5.11). To this end, Elswick (1971) discussed an expansion procedure in inverse powers of an appropriately defined turbulent Reynolds number, which comes from "proper" scaling. The scale in our case here is set from the normalizations. In (5.11) all quantities were made dimensionless by the velocities associated with the free stream and the initial shear layer thickness. That the modulated stresses, $\tilde{r}_{ij}$, scale according to $|A|^2E$ comes from an examination of the "sources" or "sinks" for $\tilde{r}_{ij}$. For instance, this is naturally suggested by the transport mechanism in terms of the vertical advection of the mean stresses (~E) by the coherent motion (~A). The presence of the local value of the mean turbulence energy density $E = E_t/\delta$, defined by (4.9), on the right side of (5.11) suggests a similar scaling discussed by Elswick (1971). The energy density E is essentially estimated by the ratio of sum of the mean normal stresses to a mean velocity squared. This, therefore, has the interpretation of an inverse (local) turbulent Reynolds number, $E \sim R_T^{-1}$. From the numerical example of Gatski and Liu (1980), $R_T \sim 30$ when E is maximum and $R_T \sim 100$ at the "initialized" initial condition. However, these are not necessarily representative of the actual turbulent Reynolds numbers. Nevertheless, if we expand

$$\phi = \phi^{(0)} + R_T^{-1}\phi^{(1)} + \cdots, \tag{5.13}$$

$$r_{ij} = r_{ij}^{(0)} + R_T^{-1} r_{ij}^{(1)} + \cdots, \tag{5.14}$$

then $\phi^{(0)}$ satisfies the Rayleigh equation and immediately becomes uncoupled from r_{ij}. The first approximation for the shape of the modulated stresses $r_{ij}^{(0)}$ satisfies (5.12) but with the coherent wave streamfunction there replaced by $\phi^{(0)}$.

In this approximation, the outer boundary conditions for $\phi^{(0)}$ follows those of the Rayleigh equation and one seeks the outgoing wave solution. However, because of the presence of turbulent-nonturbulent interface associated with the outer "boundary", Reynolds (1972) formulated the necessary interfacial conditions for the more general problem. However, because the mean velocity is essentially continuous across the turbulent-nonturbulent flow interface according to measurements, this continuity is to order R_T^{-1}. The interface is actually "transparent" as far as the $\phi^{(0)}$ eigenvalue problem is concerned and the coherent mode velocities and pressure are continuous to order R_T^{-1}. The "instability" properties are primarily attributed to dynamical instabilities associated with the inflectional mean velocity profile that occur well within the turbulent fluid, and thus the outer boundary conditions are indeed those for the Rayleigh problem of decaying outgoing waves. The interface, if of interest, would be the subject of study at the higher order, $\phi^{(1)}$ and $r_{ij}^{(1)}$ level of description. This is expected from a physical view point also since the interface region is of much less importance energetically because of (1) the absence of sharpe gradients in the mean velocity in that region and (2) the fluctuations are much less

energetic there than in the vicinity of the mean velocity inflection point in the interior of the shear layer.

The role of the linear theory, (5.11) and (5.12) or its approximate, "dynamical instability" form, is now clear. The local eigenfunction ϕ' generate the local shape of the large-scale coherent velocity distributions across the shear layer. Michalke (1971) was the first to find that the local linear theory was able to generate the coherent velocity fluctuations that compare favorably with observations. However, in using the linear theory as a "curve fit", the local mean flow characteristic velocity and length scale are considered given (from measurements, say). As such, it does not, nor could it, address the wave envelope or amplitude **evolution** problem. Recent improvements on the linear theory to account for slight flow divergence (Crighton and Gaster 1976) has been applied, in the same spirit as that of Michalke (1971), to the turbulent mixing layer problem (Weisbrot 1984, Gaster, Kit and Wygnanski 1985, Wygnanski and Petersen 1985). Similar good fits were found between the eigenfunctions and experiments with those generated by the Rayleigh equation. However, in their normalization of such eigenfunctions the local "area" under the root mean square of the streamwise fluctuation velocity was set equal to that from measurements. This precludes the possibility of giving the wave envelope the physical interpretation discussed earlier. The wave amplitude problem follows a higher order correction due to slight flow divergence but excluded the essential physics of the turbulent shear flow problem that we have discussed. In regions where the coherent mode has grown to significant amplitudes so as to change the

mean flow spreading rate, such a "weak disturbance" procedure would not suffice. We shall soon see role of the linear theory, particularly the physical implications of the role of the modulated stresses, in the nonlinear problem.

E. NONLINEAR WAVE-ENVELOPE DYNAMICS

We continue to use the temporal mixing layer as a simple example. The nonlinear problem concerns the "wave envelope" development. From the coupled system (5.5) - (5.7), with the substitution of (5.2) and (5.8) - (5.10), we obtain

$$\frac{d}{dt}(-\delta) = -|A|^2 \tilde{I}_{rs}(\alpha) - E I'_{rs} \tag{5.15}$$

$$\frac{d}{dt}\delta|A|^2 = |A|^2 \tilde{I}_{rs}(\alpha) - |A|^2 E I_{wt}(\alpha) \tag{5.16}$$

$$\frac{d}{dt}\delta E = |A|^2 E I_{wt}(\alpha) + E I'_{rs} - \overline{\phi'}. \tag{5.17}$$

We will discuss the form of the dissipation integral $\overline{\phi'}$ subsequently. The initial conditions are $\delta(0) = 1$, $|A(0)|^2 = |A|_0^2$ and $E(0) = E_0$. The mean flow kinetic energy defect integral (4.10) became simply $(-\delta)$. The energy exchange mechanism between the mean flow and the coherent mode given by the integral defined in (4.14) has now become $\tilde{I}_p = |A|^2 I_{rs}(\alpha)$, where the integral $\tilde{I}_{rs}(\alpha)$ involves integration

over the eigenfunctions of the linear theory and the mean velocity gradient (Liu and Merkine 1976) and thus depends on the **local** wavenumber (in spatial problems, it would be the local frequency). See the Appendix for definitions of such integrals. The turbulence energy production integral, defined by (4.15), now becomes $I_p' = E\, I_{rs}'$, where I_{rs}' involves the integral over the shape distribution of the Reynolds shear stress R_{xz} and the mean velocity gradient and is a constant (Liu and Merkine 1976). The fine-grained turbulence, viscous dissipation integral was defined in (4.17). If we follow the standard local equilibrium argument for large Reynolds numbers (Townsend 1956), then $\overline{\phi'} = E^{3/2} I_\phi'$, were I_ϕ' is a constant. For simplicity, Liu and Merkine (1976) argued about the Reynolds-average shape function (5.9) on the basis of a **locally** homogeneous-shear problem (Champagne, Harris and Corrsin 1970) so that $\overline{\phi'} \cong E I_\phi'$ and that $I_{rs}' \cong I_\phi'$. In this case, the nonlinear interaction problem is somewhat simplified in that the only mechanism causing the change of δE would be its interaction with the coherent structure through $|A|^2 E\, I_{wt}(\alpha)$. In the context of the numerical work of Gatski and Liu (1980), only at the later stages of development would $I_\phi' \simeq I_p'$. In the present discussion of the approximate considerations of the wave-envelop evolution, the simplified version of Liu and Merkine (1976) $I_\phi' \simeq I_p'$ will be continued for purposes of illustrating ideas, leaving to subsequent discussions of application to real, spatially developing flows for a fuller account of $I_p' \neq I_\phi'$. The integrals $\tilde{I}_{rs}, I_{rs}'$, and I_ϕ' as well as I_{wt} introduced subsequently are defined in the Appendix and discussed in detail in Liu and Merkine (1976).

F. THE MECHANISMS OF ENERGY EXCHANGE BETWEEN COHERENT MODE AND FINE-GRAINED TURBULENCE

The energy exchange between the large-scale coherent structure and fine-grained turbulence is given by the integral $I_{\ell t}$ defined in (4.16), which now becomes $I_{\ell t} = |A|^2 E\ I_{wt}(\alpha)$, where the integral I_{wt} (Liu and Merkine 1976) involves the shape functions of the modulated stresses and those of the rate of strain of the coherent mode. The importance of the relative **phases** between the modulated stresses and the coherent mode rates of strain comes from the energy exchange mechanism discussed in Section III and IV,

$$\overline{\tilde{r}_{ij} \frac{\partial \tilde{u}_i}{\partial x_j}},$$

which comprise the integrand of $I_{\ell t}$. In the present context of using linearized theory to study the nonlinear "wave envelope" development, the integrand of I_{wt} consists of (Liu and Merkine 1976)

$$\overline{\tilde{r}_{xx} \frac{\partial \tilde{u}}{\partial x}} \Big/ |A|^2 E = 2\alpha |r_{xx}|\ |\phi'| \sin(\theta_{r_{xx}} - \theta_{\phi'}) \tag{5.18a}$$

$$\overline{\tilde{r}_{xz} \frac{\partial \tilde{u}}{\partial z}} \Big/ |A|^2 E = 2 |r_{xz}|\ |\phi''| \cos(\theta_{r_{xz}} - \theta_{\phi''}) \tag{5.18b}$$

$$\overline{\tilde{r}_{xz} \frac{\partial \tilde{w}}{\partial x}} \Big/ |A|^2 E = 2\alpha^2 |r_{xz}|\ |\phi| \cos(\theta_{r_{xz}} - \theta_{\phi}) \tag{5.18c}$$

$$\overline{\tilde{r}_{zz} \frac{\partial \tilde{w}}{\partial z}} \Big/ |A|^2 E = 2\alpha |r_{zz}| \, |\phi'| \sin(\theta_{\phi'} - \theta_{r_{zz}}). \qquad (5.18d)$$

The form above implies that we have represented complex shape functions of the modulated stresses, r_{ij} and the coherent mode eigenfunctions from the linear theory in the vector form in terms of magnitude and direction. Here θ, with the appropriate subscript, is the phase angle. In this representation the energy transfer then consists of the scalar products between modulated stresses and the appropriate coherent mode rates of strain. It is clear that the relative phases determine the directions of energy transfer. To illustrate this, the vector representation of the modulated stresses and coherent rates of strain is presented in Figure 14 for a wave number $\alpha = 0.4446$ which correspond to the most amplified mode for the hyperbolic tangent mean velocity profile. The qualitative behavior is similar for other values of α. The appropriate scalar products of the vectors in Figure 14, given by (5.18a) - (5.18d), are shown in Figure 15. In Figure 14 the curves represent the locus of vectors at different vertical positions across the shear layer. For instance, shown in Figure 14a are the vectors $2r_{xx}$ and $\alpha\phi'$. At $\zeta = 0$, $\theta_{r_{xx}} = 0$ and $\theta_{\phi'} = \pi/2$, thus giving a negative $\overline{\tilde{r}_{xx} \partial \tilde{u}/\partial x}$, indicating a local transfer of energy from the coherent mode to the fine-grained turbulence. At $\zeta \simeq 0.23$, $\theta_{r_{xx}}$ and $\theta_{\phi'}$ are out of phase by π so that $\overline{\tilde{r}_{xx} \partial \tilde{u}/\partial x} \to 0$. For $\zeta > 0.23$, $\theta_{\phi'}$ lags behind $\theta_{r_{xx}}$ so that locally energy is tranferred from the fined-grained turbulence to the coherent mode with a maximum at bout $\zeta \simeq 1$. Shown in Figure 14b are the vectors $2r_{xz}$, ϕ'' and $\alpha^2\phi$.

Because $U''(0) = 0$, then $\phi'' = \alpha^2\phi$ at $\zeta = 0$ according to the Rayleigh equation. Thus $\overline{\tilde{r}_{xz}\partial\tilde{w}/\partial x}$ are equal there (as shown in Figure 15). While the former of these remain positive, the latter becomes negative after $\zeta \approx 0.15$. The vectors $2r_{zz}$ and $\alpha\phi'$ are shown in Figure 14c. Their scalar product, $\overline{\tilde{r}_{zz}\partial\tilde{w}/\partial z}$, shown in Figure 15, this being very nearly equal and opposite in sign to $\overline{\tilde{r}_{xz}\partial\tilde{w}/\partial x}$. In Figure 15, it is shown that the mechanism of horizontal modulated normal stress - normal rate of strain dominates the energy transfer near the center of the shear layer ($\zeta = 0$), while the mechanism of modulated shear stress - shear rate of strain dominates the energy transfer away from the center of the shear layer. The net result of these four contributions is shown by the dot-dash line in Figure 15, which is positive over most of the shear layer indicating that for this case energy transfer is from the coherent mode to the fine-grained turbulence. The dot-dash line would fall slightly below the axis in the outer regions of the shear layer but the magnitude is not distinguishable within the width of the curve itself. We emphasize that from this consideration, there is significant energy transfer, within local vertical regions of the shear layer, from the turbulence to the coherent motion contributed by the individual mechanisms. The integral I_{wt} is then twice the area under the dot-dash curve, the ζ distribution being symmetrical about $\zeta = 0$. In principle, $I_{wt}(\alpha)$ depends on the local wave number, which, in turn, is scaled by the local developing shear layer thickness δ.

It is clear that, in general, the wave envelope development (5.16) is coupled to the spreading of the mean flow and the development of the fine-grained turbulence energy as indicated by (5.15) and (5.17), respectively. These approximate form of the

nonlinear interaction could be said to have been motivated by and bear strong resemblence to the diagnostics of the numerical problem (Gatski and Liu 1980) given by (4.11) - (4.13). The mean flow energy defect evolution (4.11) now reduces to the statement (5.15) that as long as energy is transferred to the fluctuating motions, $d\delta/dt > 0$. When $\tilde{I}_{rs}(\alpha)$ becomes negative, such as in the "damped disturbance" regime discussed in Section 4 ($\tilde{I}_p < 0$), the contribution to $d\delta/dt$ would be to arrest the growth of the shear layer or even decrease its growth (Weisbroth 1984, Fiedler and Mensing 1985) depending on the relative magnitude between the coherent mode and turbulence contributions. The steplike behavior of δ would come from peaking of $|A|^2\tilde{I}_{rs}$, as has been anticipated in Section III. These would account for the observed steplike shear layer thickness development discussed in Ho and Huang (1982), Fiedler and Mensing (1985) and Wygnanski and Petersen (1985). The observed momentary depression (Weisbrot 1984, Fiedler and Mensing 1985) in the shear layer thickness is attributed to the dominance of the "damped disturbance" mechanism relative to others (such as turbulence and viscosity) affecting the spreading rate. Some of these aspects will be quantitively addressed in the next section.

G. WAVE ENVELOPE AND TURBULENCE ENERGY TRAJECTORIES. A SIMPLE ILLUSTRATION

Another feather of the wave-envelope problem exhibited by the observations depicted in Figure 1, could be qualitatively deduced from the much simplified framework here. If we assume that the right side of (5.15) is in some sense "small"

so that the shear layer growth rate is correspondingly small $d\delta/dt \to 0$, the change in δ is then ignored entirely. Thus δ remains at the initial value $\delta = 1$ and the interaction integrals $\tilde{I}_{rs}, I_{wt}$ are fixed by the initial wave number α. In this case, (5.15 - 5.17) reduce to

$$\frac{d}{dt} |A|^2 = |A|^2 \tilde{I}_{rs} - |A|^2 E\, I_{wt} \tag{5.19}$$

$$\frac{dE}{dt} = |A|^2 E\, I_{wt}. \tag{5.20}$$

We have retained the approximation (Liu and Merkine 1976) that locally $E\, I'_{rs} = \overline{\phi'}$. The simple essentials here state that the energy transfer from the coherent structure to the fine-grained turbulence is the only mechanism causing E to change from its original value. The evolution of the coherent structure amplitude is determined by the local balances between energy extraction from the mean flow and energy transfer to the fine-grained turbulence. In the $|A|^2$ - E plane the system (5.19), (5.20) admits the solution

$$\frac{|A|^2}{|A|_0^2} = 1 + \frac{1}{L_0 M_0} \ell n \frac{E}{E_0} - \frac{1}{M_0} \left[\frac{E}{E_0} - 1 \right] \tag{5.21}$$

where $L_0 = E_0 I_{wt}/\tilde{I}_{rs}$ and $M_0 = |A|_0^2/E_0$. The dimensonless time t is obtained from

$$t = \frac{1}{E_0 I_{wt}} \int_0^{\chi} \frac{d\chi'}{(1+M_0) + \chi'/L_0 - \exp \chi'} \tag{5.22}$$

where $\chi = \ell n\ E/E_0$. In this special example the equilibrium values, denoted by the subscript e, for $|A|^2$,E are such that $|A|_e^2 = 0$ deduced from setting the right sides of (5.19) and (5.20) to zero and that for E_e directly from (5.21)

$$L_e \exp(-L_e) = L_0 \exp[-L_0(1+M_0)],$$

where $L_e = E_e I_{wt}/\tilde{I}_{rs}$. We expect that $L_e > L_0$ because we found $I_{wt} > 0$ and the fine-grained turbulence energy would be increased, $E_e > E_0$, due to the presence of the coherent structure. For a fixed ratio of initial amplitudes M_0, as $L_0 = E_0 I_{wt}/\tilde{I}_{rs}$ increases the turbulence equilibrium aplitude ratio E_e/E_0 decrease. This can be interpreted as follows. If we fix the wave number thus $I_{wt}/\tilde{I}_{rs}$ is fixed, so that as E_0 is increased more energy is transferred to the turbulence from the coherent motion, thereby limiting the coherent mode amplitude. This in turn decreases the the efficiency of the coherent mode as an intermediary in taking energy from the mean flow and transferring it to the turbulence. On the other hand, if E_0 is fixed and $I_{wt}/\tilde{I}_{rs}$ is increased then the energy transfer from the coherent mode to the turbulence becomes more efficient than that from the mean motion to the coherent mode. This again gives a lower E_e. If L_0 and E_0 are fixed and M_0 is increased

through increasing $|A|_0^2$, E_e is increased because the coherent mode is made more efficient in drawing energy from the mean flow and transferring it to the turbulence. In this special consideration, the equilibrium amplitude of the coherent mode $|A|_0^2 \to 0$ as long as $E_0 > 0$, and is independent of initial conditions. From the physical considerations discussed, E_e is not independent of initial conditions. From (5.21) it is seen that L_0 and M_0 fix the trajectory in the $|A|^2/|A|_0^2$, E/E_0 plane. The wave envelope or amplitude $|A|^2/|A|_0^2$ reaches a maximum when $E/E_0 = 1/L_0$ for $L_0 < 1$ whereas $|A|^2/|A|_0^2$ decays at the outset for $L_0 > 1$. The latter situation is because energy transfer to the turbulence overwhelms that extracted from the mean flow. The trajectories in the $|A|^2/|A|_0^2$ - E/E_0 plane are shown in Figure 16 for $M_0 = 1$ and various values of $L_0 < 1$. The time development begins at (1,1), and follows the trajectory. Not shown are the decaying $|A|^2/|A|_0^2$ trajectories starting at (1,1) for the strong initial turbulence ($L_0 > 1$) situation. The interesting physical picture that emerges from this consideration is that under conditions where the coherent mode amplitifes, its amplitude first grows "exponentially" due to extraction of energy from the mean motion and subsequently decays due to energy transfer to the fine-grained turbulence. The fine-grained turbulence energy relaxes from an original equilibrium level to a final, higher level due to energy supplied by the coherent mode. This recovers some of the physical mechanisms derived more laborously from the numerical work of by Gatski and Liu (1980) and could, in part, explain the observations depciting large-scale coherent structures interacting with turbulence reported, for instance, by Favre-Marinet and Binder (1979) and shown in

Figure 1. Other, semi-analytical models of this equilibration picture are given in Liu and Merkine (1976) for the temporal mixing layer.

We have already appreciated the shortcomings of the temporal mixing layer relative to the real, laboratory situations of the spatially developing free turbulent shear flows. The expected lack of a legitimate one-to-one transformation (rather than mimicking) coincide with the similar situation in hydrodynamic stability theory (Gaster 1962, 1965, 1968). However, the physical similarities between the relatively simple approximate considerations of "wave envelopes" and the numerical computational results thus strongly encourage the further development of the former, principally directed at the realistic spatially-developing free shear flows.

VI. SPATIALLY DEVELOPING FREE SHEAR FLOWS

A. GENERAL COMMENTS

Some aspects of the quantitative observations of turbulent free shear flows discussed in Section III pertain to laboratory, spatially developing flows. Although certain qualitative explanations of physical features are possible from the considerations of Sections IV and V, we shall address directly the spatial problem in this section. No attempt will be made here for a complete survey of the literature, but that aspects of the literature will again be drawn to put forth a consistent "point of view" for the problem of large-scale coherent structures in free turbulent shear flows. Because many of the symptoms of such structures in turbulent flows share those of hydrodynamically unstable disturbances in an otherwise laminar flow, many of the physical features of the former can be inferred from the latter. In the context of Sections IV and V, such inferences must necessarily be made with considerable care rather than with unaffected simplicity. For instance, one must differentiate carefully between (1) the dynamical instability mechanism for the "fast oscillations" that could generate local coherent mode velocity profiles from linear wave functions and (2) the slowly varying wave envelope or amplitude distribution that necessarily require the participation of the real physics of the problem, including turbulence, nonlinearities and mean flow development.

In the case of finite amplitude disturbances, J. T. Stuart (1958) advanced the idea that the kinematics and shape of the disturbances in shear flow instability could

be approximated by the linear theory but that the amplitude or wave envelope is to be obtained by the nonlinear theory. Its observational basis and application to the turbulent free shear layer problem has been discussed in Section V in connection with the work of Liu and Merkine (1976). The generalization of Stuart (1958) to the finite disturbance problem in a **spatially** developing free (wake) laminar shear flow was given by Ko, Kubota and Lees (1970). Some of their results are worth emphasizing since they anticipated many of the obvious aspects of the coherent structure problem in turbulent shear layers. Although only a single (fundamental) physical frequency was considered, they have shown how the nonlinear disturbance and the coupled mean flow would respond to several parameters. A simplified version of the wave envelope problem of Ko, et al (1970) (in the absence of fine-grained turbulence), in the context of the mixing region problem appears in the form

$$\bar{I}\,\frac{d\delta}{dx} = |A|^2\,\tilde{I}_{rs}(\delta) + \frac{1}{Re}\,\bar{I}_{\phi}/\delta \tag{6.1}$$

$$\overline{\tilde{I}(\delta)}\,\frac{d}{dx}(\delta|A|^2) = |A|^2\,\tilde{I}_{rs}(\delta) - \frac{1}{Re}\tilde{I}_{\phi}(\delta)\;|A|^2/\delta \tag{6.2}$$

where x is the dimensionless streamwise distance; $\bar{I}_{\ell},\tilde{I}_{\ell}(\delta)$ are the mean flow and fluctuation advection integrals; $\bar{I}_{\phi}$ and $\tilde{I}_{\phi}(\delta)$ are the mean flow and fluctuation viscous dissipation integrals. Integrals involving instability modes are dependent on the shear layer thickness $\delta(x)$ through the dependence of local instability properties.

on the local frequency parameter β, whereas mean flow integrals $\bar{I}$ and $\bar{I}_\phi$ are constant for the similar mean flow shape distribution. Since $\tilde{I}(\delta) > 0$ and is slowly varying, it is replaced by a mean value indicated in (6.2). We refer to the Appendix for further details regarding the integrals. Here, the Reynolds number is $Re = \bar{U}\delta_0/\nu$, where $\bar{U}$ is the average over the upper and lower free stream velocities. In the incipient instability region $|A|^2 \to 0$ so that the second term on the right of (6.1) initially dominates and provides the basic viscous shear layer spreading $\delta \sim \sqrt{x}$. The deviation from this parabolic spreading would indicate the onset of finite disturbance levels as the first term on the right of (6.1) competes with the second. This is indeed the case found theoretically by Ko, et al (1970) and experimentally by Sato and Kuriki (1961) for the wake problem. Thus a dominating peak in the energy extraction from the mean flow would bring about a steplike development of $\delta(x)$. The observed steplike growth of transitional shear layers (e.g., Ho and Huang 1982), and forced turbulent shear layers (Fiedler, et al 1981; see also Wynganski and Petersen 1985) is attributed to this mechanism. However, in the turbulent shear layer problem the basic spreading of the shear layer is due to the fine-grained turbulence with the mechanism depicted by $E\, I'_{rs}$ discussed in Section IV which tends to give a linear growth in the absence of other "nonequilibrium" energy loss from the mean flow.

Ko, et al (1970) found that for a fixed Reynolds number and initial wake thickness, the peak in the fluctuation energy density, $|A|^2$, moves closer to the start of the wake as the initial fluctuation level is increased. For the same initial

fluctuation energy level, the growth, peak and decay process is hastened in the streamwise direction as the Reynolds number is increased. Accompanying these properties of $|A|^2$ would be the moving upstream of the steplike growth of the shear layer.

B. THE SINGLE COHERENT MODE IN FREE TURBULENT SHEAR FLOWS

The observed growth and decay of a single dominant coherent mode in turbulent free flows, the coherent mode "negative" production mechanism and the eventual increase in the fine-grained turbulence level, illustrated in Figures 1 and 2, were explanable by the single mode considerations of Sections V. There are several more detailed features of experimental observations that could be explained within the considerations of this section. Following the forced plane turbulent mixing layer experiments of Oster and Wygnanski (1982), Weisbrot (1984) continued with quantitative measurements of the coherent mode energy exchange with the mean motion in addition to the mean flow spreading rate, at high amplitudes of forcing. Subsequent subharmonic formation was however, not detected further downstream. Although higher homonics of the forcing frequency were present, these decayed rapidly with distance downstream. A significant rise in the level of the background broadband turbulence occurred with increasing downstream distance. The coherent mode at the forcing frequency appeared to be functioning as a monochromatic disturbance in the turbulent mixing layer. As anticipated in the discussions in

Section V, even if the comparison of measured disturbance velocity distributions across the shear layer with those obtained from a local inviscid linear stability theory appeared good, the same "theory" is not capable in describing the amplitude or wave-envelope evolution in the streamwise direction.

The nonlinear wave-envelope problem for a single coherent mode in a spatially developing turbulent shear layer, in the spirit of Section V, is in the form (Alper and Liu 1978)

$$\bar{I}\,\frac{d\delta}{dx} = |A|^2\,\tilde{I}_{rs}(\delta) + E\,I'_{rs} \tag{6.3}$$

$$\overline{\tilde{I}(\delta)}\,\frac{d\delta}{dx} = |A|^2\,\tilde{I}_{rs}(\delta) - |A|^2\,I_{wt}(\delta) \tag{6.4}$$

$$I'\,\frac{d\delta E}{dx} = E\,I'_{rs} + |A|^2 E\,I_{wt}(\delta) - E^{3/2} I'_{\phi} \tag{6.5}$$

where $\bar{I}, I'$ and I_{ϕ}, are the mean flow energy advection and turbulence energy advection and dissipation integrals, respectively and are constants for a nominally similar mean velocity and Reynolds stress profiles; the local shear-layer thickness dependent, coherent mode integrals were previously defined. We again refer to the Appendix for details of the integrals. Mean motion and coherent mode viscous dissipation have not been included for the turbulent shear layer problem.

The observed (Weisbrot 1984) behavior of the spreading rate of the "highly excited" turbulent mixing layer can be diagnosed directly by (6.3), which is obtained

from kinetic energy considerations. The sum $(|A|^2 \tilde{I}_{rs}+E\, I'_{rs})$ is the integral of the total energy exchange mechanism between the mean flow and the coherent plus turbulent fluctuaitons, across the shear layer. It has been evaluated from measurements by Weisbrot (1984) as a function of the streamwise distance. In terms of his notation

$$[|A|^2 \tilde{I}_{rs}+E\, I'_{rs}] = \left[\int_{-\infty}^{\infty} \overline{-u'v'}\, \frac{\partial U}{\partial y}\, dy\, \frac{1}{(U_2-U_1)^3}\right] \frac{(U_2-U_1)^3}{[(U_1+U_2)/2]^3} \qquad (6.6)$$

where $U_\infty \to U_2$, $U_{-\infty} \to U_1$, $z \to y$, $w \to v$. We have assumed, for simplicity, that the mean flow develops similarly so that $\bar{I}$ = constant = $2R^2(3/2 - \ln 2)$ for a hyperbolic tangent profile, where for $U_{-\infty} > U_\infty$, $R = (U_{-\infty}-U_\infty)/(U_{-\infty}+U_\infty)$. Thus, the shear layer thickness obtained from (6.3) becomes

$$\delta - \delta_0 = \frac{1}{\bar{I}} \int_{x_0}^{\infty} [|A|^2 \tilde{I}_{rs} + E\, I'_{rs}]dx. \qquad (6.7)$$

If nonsimilarities of the mean velocity profile were to be included, then $\bar{I}(x)$ would appear in (6.3) within the differential $d(\bar{I}\delta)/dx$. In the experiments, the mean velocity profiles were indeed not entirely similar. In order to make use of the idea developed from energy considerations that the mean flow will spread as long as energy is taken away and would contract if energy were supplied to it by "damped" disturbances, we integrate the "raw" experimental data (Weisbrot 1984, Figure 5.3.1) to obtain the features of shear layer growth (and contraction) via

$$\theta - \theta_0 \cong \frac{2(U_2-U_1)^3}{\bar{I}\,\bar{U}^3}\left\{\int_{x_0}^{x}\left[\int_{-\infty}^{\infty} -\overline{u'v'}\,\frac{\partial U}{\partial y}\,dy\,\frac{1}{(U_2-U_1)^3}\right]_{exp} dx\right\}. \qquad (6.8)$$

The multiplication of the velocity ratio factor is to make (6.8) consistent with the way in which $\bar{I}$ was originally made dimensionless. The subscript exp denotes the experimental data mentioned. Here both θ and x are considered dimensional. We show the integral (6.8) in Figure 18. It amazingly resembles that of the measured shear layer momentum thickness given in Figure 5.1.1 of Weisbrot (1984). We have deliberately avoided "matching constants" leading to direct comparisons. Weisbrot (1984) also obtained the "phase locked" contribution to the shear stress "production" mechanism. From this consideration it is thus shown conclusively that the excited coherent fluctuation causes the shear layer to spread rapidly and that even in the "damped" region it dominated the overall energy extraction/supply rate to the mean motion and causes the shear layer to contract. The eventual linear spreading rate is due to the broad-band turbulence. The features of the evolution of coherent mode energy "production" mechanism is similar to that of Fiedler, et al (1982) shown in Figure 2 and anticipated by the calculations of Gatski and Liu (1980) shown in Figure 5. In the formulation (6.3) - (6.5) only the dominant energy exchange mechanism between the mean flow and the fluctuations were retained. Because the mean flow is rapidly expanding and changing in the streamwise direciton in the

experiments, the remaining energy exchange mechanisms for a two-dimensional mean flow (in the present notation)

$$(\overline{u^2}-\overline{w^2})\,\frac{\partial U}{\partial x} + \overline{\tilde{u}\tilde{w}}\,\frac{\partial W}{\partial x}$$

would need to be assesed in the diagnosis of the observed spreading rate in Figure 18. The dominant energy exchange mechanism included in (6.3) - (6.5), as well as that having been measured (Weisbrot 1984), was sufficient to uncover the basic effect but not intended for an "accurate prediction". Of the mechanisms responsible for the coherent mode wave-envelope evolution depicted in (6.4), only $|A|^2\,\tilde{I}_{rs}$ is relatively easily measured. The measurement of the wave-turbulence energy transfer mechanism, depicted by $|A|^2 E\, I_{wt}$ in (6.4) or $I_{\ell t}$ in (4.12) and (4.16), is difficult (see, for instance, Hussain 1983). It would involve taking spatial derivatives of phase-averaged quantities and the subtraction between large numbers. Nevertheless, it is an important mechanism in the turbulent shear flow problem. In this situation we must rely on the insights developed from theoretical considerations, such as in Sections IV and V, to help towards the understanding of the coherent mode wave-envelope **evolution** problem (Alper and Liu 1978).

The shear layer growth, which is explained here from dynamical considerations, is the result of the overall energy drain or resupply to the mean kinetic energy. The spectrum of Weisbrot's (1984) observation indicate that several higher frequency harmonics undergo growth and decay process earlier in the streamwise distance than

the component at the forced frequency. A "phase-locked" subharmonic was not observed over the length of the streamwise distance measured. We shall delay to the following section to discuss the theoretical aspect of multiple-coherent mode interactions. The growth and decay of higher frequency coherent modes occurring in regions closer to the start of the mixing layer and lower frequency components further downstream from such observations have been borne out by theoretical considerations (e.g., Liu 1974a, Merkine and Liu 1975, Alper and Liu 1978, Mankbadi and Liu 1981, 1984) on the basis of single, independent modes interacting with fine-grained turbulence.

The effect of initial conditions on single, independent coherent mode development in terms of the initial Strouhal frequency, coherent mode amplitude and turbulence level were discussed by Alper and Liu (1978). For the same initial energy levels, the higher frequency coherent components which have shorter streamwise lifetimes and attain higher wave-envelope peaks than lower frequency components. However, the higher frequency modes may not necessarily enhance the fine-grained turbulence energy as vigorously as the lower frequency modes. This is because the mode-turbulence energy transfer depends not only on the magnitude of $|A|^2$ but also on the lifetime of the coherent mode as well. For the same frequency, increasing the coherent mode amplitude moves the peak of $|A|^2$ upstream. Aside from controlling the large-scale coherent structure and the fine-grained turbulence through direct perturbation at definite frequencies and coherent mode amplitudes, the use of fine-grained turbulence to control its development can also be achieved (Alper and

Liu 1978). For the same coherent mode frequency but different initial turbulence energy levels, the higher turbulence level case supresses the coherent mode downstream devleopment. Consequently, the fine-grained turbulence would achieve a relative lower enhancement downstream. The very-large initial coherent mode amplitude forcing would effect a subsequent decay of the coherent mode. This limiting-forcing amplitude threshold effect has been found experimentally by Fiedler and Mensing (1985). Although the calculations were performed for coherent modes in a round turbulent jet, Mankbadi and Liu (1981) theoretically found that such an initial-amplitude threshold effect does indeed exist. We shall refer to Mankbadi and Liu (1981) for the elucidation of initial condition effects and the possible control of the free turbulent shear flow.

C. COHERENT MODE INTERACTIONS

To begin the discussion of mode interactions it would be most helpful to first recall the streakline patterns obtained calculationally by Williams and Hama (1980) from the superposition of kinematically obtained wavy disturbances of the fundamental mode and its subharmonic upon a hyperbolic tangent mean velocity profile. Such streaklines are also obtained from the local eignefunctions of inviscid linear theory by Weisbrot (1984) (see also Wygnanski and Petersen 1985), resolving in some sense the usefulness of the local linear theory in mimicking flow visualization (the quantitative wave-envelope problem was not resolvable from this consideration,

however). We shall discuss Williams and Hama (1980) for illustrative purposes. They obtained streakline patterns from the superposition of subharmonic to fundamental with certain constant-amplitude ratios. These patterns bear striking resemblance to the visual observation of dye streak behavior in a mixing layer (e.g., Freymuth 1966; Winant and Browand 1974; Ho and Huang 1982). However, the streakline calculations of William and Hama (1980) come from a linear superposition of two constant amplitude wave disturbances, the pairing and roll up are the consequence of wave interference. The simulated wave amplitudes of the fundamental and subharmonic are both constant and the abrupt switching of modal structure, as the visual appearance of streaklines would suggest, is entirely absent. We are thus cautioned by this illustration, that dye streak behavior are not necessarily indicative of unique physical circumstances without the guidance from simultaneous quantitative measurements. Quantitative measurements suggesting mode-mode interactions between the fundamental disturbance wave and its subharmonic in a shear layer are reported by Ho and Huang (1982). Their shear layer is essentially one undergoing transition and the presence of such distinct modes is brought about by forcing at the subharmonic frequency. The significance of Ho and Huang's (1982) work lies in the identification of the visually observed location of "pairing", indicated by the accumulation of dye streaks, with the occurrence of the measured cross-sectional energy maximum of the subharmonic (actually, they measured the kinetic energy associated with the streamwise velocity fluctuation, integrated across the shear layer). There was no abrupt switching from the fundamental frequency and wavelength to

those of the subharmonic. Reproduced in Figure 4, corresponding to Mode II of Ho and Huang (1982), is the evolution of the measured secitonal-energy associated with the streamwise velocity fluctuation. The 2.15 Hz curve corresponds to the forced, subharmonic component, the 4.30 Hz curve is the fundamental. Although the peak amplitudes of the two modes are distinct, the fading in of the subharmonic occurs in regions of active fundamental devleopment and, in turn, the fading out of the fundamental takes place in regions where the subharmonic is active. The measurements suggest a natural occurrence of the switch-on and switch-off processes, in contrast to the suggestive, abrupt switch in the modal content from visual observations of dye streaks alone.

The theoretical formulation of mode-mode interactions in a spatially devleoping shear layer was undertaken for a laminar viscous shear flow, without the involvement of the fine-grained turbulence at the outset, by Nikitopoulos (1982), Liu and Nikitopoulos (1982). The measureable sectional energy content of each mode is essentially $\delta_1 A_1^2$, related to the square of the amplitude of the coherent structure. The cross-sectional energy content (Ho and Huang 1982) thus **reconciles** measurements with the theoretical ideas about wave-envelope evolution. For each frequency and the same initial conditions, the amplitude is a fixed streamwise envelope under which the propagating wavy disturbance enters from its initiation upstream and exits downstream. The aim here is to understand the direction of energy transfer between the modes, its effect on establishing the spatial distribution of wave envelopes and the consequential rate of spread of the shear flow.

In order to bring out the role of coherent-mode interactions in a dveloping shear flow, we shall delay considering the simultaneous presence of fine-grained turbulence. In this case, the rate of viscous dissipation is included for the "low" Reynolds number incipient transitional problem. Following the general discussions of Section II, we first consider that an essemble of disturbances exist in a shear flow and split the modes into "odd" (denoted by $\tilde{q}$) and "even" (denoted by $\hat{q}$), then the rate of energy transfer from the even to the odd modes is given by (Stuart 1962a; see also Section II.C)

$$\overline{\tilde{u}_i \tilde{u}_j \frac{\partial \hat{u}_i}{\partial x_j}} > 0$$

where the average is taken over the largest periodicity of the disturbances. The mechanism is the work done (by the stresses of the odd modes) against the appropriate rate of strain (of the even modes). It is clear that the **phase** relation between the stresses and the rate of strain determines the direction of energy transfer and that the amplitudes determine the strength of this transfer (the **"Kelly mechanism"**, Kelly 1967; Liu 1981).

For a spatially developing shear layer, Liu and Nikitopoulos (1982) considered the interaction between the subharmonic mode (a single "odd" mode) and its fundamental (a single "even" mode), If the energy content of the fundamental mode across the shear layer is denoted by $E_2 = \delta |A_2|^2$ and that of the subharmonic by $E_1 = \delta |A_1|^2$, then the overall energy transfer mechanism between the modes is

proportional to $|A_1|^2|A_2|$. In contrast, the respective fluctuation energy production rate from the mean flow is proportional to $|A_1|^2$ and to $|A_2|^2$. The rate of viscous dissipation scales like $|A|^2/\delta$. The dimensionless energy density $|A|^2$ is much less than unity according to observations. In this case, the estimate here shows that the individual energy production from the mean motion would seem to dominate over that of the mode-mode energy transfer except in regions where the former changes sign at a later stage of development. In the early stages of development, the mode interactions are dominated by implicit nonlinear interactions via the mean motion rather than by the more explicit direct energy transfer mechanism. At the later stages mode interactions are most certainly important towards affecting the details of the amplitude distribution in the streamwise direction. In the experiments of Ho and Huang (1982) there are modes other than the fundamental and the subharmonic present, including initially weak fine-grained turbulence disturbances and these are not included in this initial analysis.

To begin, use is made of the kinetic energy equations (2.21), (2.24) and (2.25) in Section II.C with the fine-grained turbulence omitted (Nikitopoulos 1982, Liu and Nikitopoulos 1982), with the spatial interpretaiton of the advective derivative $\bar{D}/Dt$. We again address the wave-envelope problem and specialize the odd modes to a single-plane subharmonic mode and the even modes to the plane fundamental. The appropriate kinetic energy equaitons integrated across the plane shear layer then take the form

mean flow:

$$\frac{1}{2}\frac{d}{dx}\left[\int_{-\infty}^{0} U(U^2-U_{-\infty}^2)dz + \int_{0}^{\infty} U(U^2-U_{+\infty}^2)dz\right] - \int_{-\infty}^{\infty}(-\overline{\tilde{u}\tilde{w}}-\overline{\hat{u}\hat{w}})\frac{\partial U}{\partial z}\,dz - \bar{\Phi}, \qquad (6.9)$$

subharmonic:

$$\frac{1}{2}\frac{d}{dx}\int_{-\infty}^{\infty} U(\overline{\tilde{u}^2}+\overline{\tilde{w}^2})dz = \int_{-\infty}^{\infty}(-\overline{\tilde{u}\tilde{w}})\frac{\partial U}{\partial z}\,dz -$$

$$-\int_{-\infty}^{\infty}\left[\overline{\tilde{u}^2\frac{\partial\hat{u}}{\partial x}} + \overline{\tilde{u}\tilde{w}\left(\frac{\partial\hat{u}}{\partial z}+\frac{\partial\hat{w}}{\partial x}\right)} + \overline{\tilde{w}^2\frac{\partial\hat{w}}{\partial z}}\right]dz - \bar{\tilde{\phi}}, \qquad (6.10)$$

fundamental:

$$\frac{1}{2}\frac{d}{dx}\int_{-\infty}^{\infty} U(\overline{\hat{u}^2}+\overline{\hat{w}^2})dz = \int_{-\infty}^{\infty}(-\overline{\hat{u}\hat{w}})\frac{\partial U}{\partial z}\,dz +$$

$$+\int_{-\infty}^{\infty}\left[\overline{\tilde{u}^2\frac{\partial\hat{u}}{\partial x}} + \overline{\tilde{u}\tilde{w}\left(\frac{\partial\hat{u}}{\partial z}+\frac{\partial\hat{w}}{\partial x}\right)} + \overline{w^2\frac{\partial\hat{w}}{\partial z}}\right]dz - \bar{\hat{\phi}}, \qquad (6.11)$$

all quantities are made dimensionless in the manner previously discussed. We recall that x is the streamwise coordinate measured from the start of the mixing layer, z is the vertical coordinate measured from the center of the mixing layer, u,w are the x,z

fluctuation velocities, U is the mean velocity with $\pm\infty$ denoting the upper and lower streams, respectively. Here $\bar{\Phi}$ is integral of mean flow viscous dissipation rate, the lower case ϕ represents the corresponding integral of the fluctuation dissipation rates. Equations (6.9) - (6.11) are stated here for completeness and also form the basis for subsequent discussions of the mode interaciton problem in the presence of fine-grained turbulence. Here, they form the basis for obtaining the evolution equations for the cross-sectional energies or energy densities of the disturbances. Following earlier work (see, for instance, Liu 1981 and Section V), the disturbances are assumed to take the separable form of the product of an unknown amplitude $A_i(x)$ with a **vertical distribution** function given by the local linear stability theory (which has found experimental justification, e.g. Michalke 1971, Weisbrot 1984) as was done for the single mode in (5.2),

$$\begin{bmatrix} \tilde{u} \\ \tilde{w} \end{bmatrix} = A_1(x) \left[\begin{bmatrix} \phi_1' e^{-i\beta t} \\ -i\alpha_1 \phi_1 e^{-i\beta t} \end{bmatrix} + \begin{bmatrix} c.c. \\ c.c. \end{bmatrix} \right], \tag{6.12}$$

$$\begin{bmatrix} \hat{u} \\ \hat{w} \end{bmatrix} = A_2(x) \left[\begin{bmatrix} \phi_2' e^{-2i\beta t - i\theta} \\ -i\alpha_2 \phi_2 e^{-2i\beta t - i\theta} \end{bmatrix} + \begin{bmatrix} c.c. \\ c.c. \end{bmatrix} \right]. \tag{6.13}$$

We again recall the definition that ϕ_i denotes the eigenfunction of the local linear

theory and is a function of the rescaled vertical variable $\zeta = z/\delta(x)$, where $\delta(x)$ is a length scale of the mean flow, to be identified as the half-vorticity thickness, $(\,)'$ denotes differentiation with respect to ζ; $\beta = 2\pi f\delta(x)/\bar{U}$ is the dimensionless local frequency, f is the physical frequency and we again recall that $\bar{U} = (U_\infty+U_{-\infty})/2$, the local wavenumbers α are also scaled by $\delta(x)$; θ is the relative phase between the fundamental component (2β) and its subharmonic (β) and c.c. denotes the complex conjugate. We are again reminded that the velocities and lengths are considered to be made dimensionless by $\bar{U}$ and δ_0 (so that $\delta(0) = 1$), and time by $\delta_0/\bar{U}$. The mean velocity profile is taken to be the hyperbolic tangent profile $U = 1 - R\tanh\zeta$. The sectional-energy content is defined similarly as in (5.1)

$$E_1(x) = \frac{1}{2}\int_{-\infty}^{\infty} (\overline{\tilde{u}^2}+\overline{\tilde{w}^2})dz = |A_1(x)|^2\delta(x) \tag{6.14}$$

$$E_2(x) = \frac{1}{2}\int_{-\infty}^{\infty} (\overline{\hat{u}^2}+\overline{\hat{w}^2})dz = |A_2(x)|^2\delta(x). \tag{6.15}$$

This is similar to E(f) measured by Ho and Huang (1982), except that their sectional energy refers to the contributon by u alone. The normalization of the local eigenfunctions according to (5.4) is implied, which allow us to relate the energy content to the amplitude or wave envelope. Alternatively, the square of the amplitude is an "energy density". Equations (6.9) - (6.11) then yield three first-order nonlinear differential equations describing the streamwise evolution of δ, $|A_1|^2$ and

$|A_2|^2$ or in the alternative form δ, E_1 and E_2:

mean flow:

$$\bar{I}\frac{d\delta}{dx} = [\tilde{I}_{rs2}(\delta)E_2 + \tilde{I}_{rs1}(\delta)E_1]/\delta + \frac{1}{Re}\bar{I}_{\Phi}/\delta \qquad (6.16)$$

visc. dissip.

subharmonic:

$$\overline{\tilde{I}_1(\delta)}\frac{dE_1}{dx} = \tilde{I}_{rs1}(\delta)E_1/\delta - I_{21}(\delta)E_1E_2^{1/2}/\delta^{3/2} - \frac{1}{Re}\tilde{I}_{\phi 1}(\delta)E_1/\delta^2, \qquad (6.17)$$

production; Sub.-Fund. energy exchange; visc. dissip.

fundamental:

$$\overline{\tilde{I}_2(\delta)}\frac{dE_2}{dx} = \tilde{I}_{rs2}(\delta)E_2/\delta + I_{21}(\delta)E_1E_2^{1/2}/\delta^{3/2} - \frac{1}{Re}\tilde{I}_{\phi 2}(\delta)E_2/\delta^2, \qquad (6.18)$$

production; visc. dissip.

The relevant integrals in (6.16) - (6.18) are again defined in the Appendix. The "slowly varying" advection integrals $I_1(\delta)$ and $I_2(\delta)$ are approximated by their "mean" values. Not previously introduced are the mode-energy exchange integral $I_{\phi i}(\delta)$ and the viscous dissipaton integrals $\tilde{I}_{\phi i}(\delta)$. The Reynolds number is again $Re = \bar{U}\delta_0/\nu$. The subscripts 1 and 2 denote the subharmonic and fundamental, respectively. Following arguments of inertial or dynamical instability reasoning (Section V), it is sufficient to use the Rayleigh equation in obtaining the characteristics of such integrals (see, for instance, Liu & Merkine 1976) and thus they are not functions of

the Reynolds number. Equations (6.16) - (6.18) are subject to the initial conditons $E_1(0) = E_{10}$, $E_2(0) = E_{20}$ and $\delta(0) = 1$; with $\beta(0) = \beta_0$ choosen to correspond to the physical frequency of the subharmonic (or any other mode), the specified $\bar{U}$ and the initial physical length scale of the mean flow δ_0. This length scale has been identified with the initial half-maximum slope thickness.

There are many other less dominant disturbance modes present in the experiments of Ho & Huang (1982), including weak fine-grained turbulence, to which the shear layer is sensitive. The relative phase between the fundamental and subharmonic is left arbitrary in the experiments. Thus, the **dctails** of the real shear layer is not expected to be described by the idealized two-mode problem in the absence of weak fine-grained turbulence and other (not necessarily weak) modes. However, the problem solved by Nikitopoulos (1982) and Liu and Nikitopoulos (1982) brings out the dominant physical mechanisms in the growth and decay and the effect of the relative phases of the overlapping fundamental and subharmonic disturbances in the absence of other complications. Some of these earlier qualitative results were discussed by Ho and Huerre (1984). Subsequent calculations and quantitative comparisons with experiments (Nikitopoulos and Liu 1986) are discussed here. The initial subharmonic frequency parameter is taken to be $\beta_0 = 0.26$, giving a fundamental of $2\beta_0 = 0.52$ which is very nearly at the maximum amplification rate according to the linear theory. In the experiments (Ho and Huang 1982), only the u-contribution to the cross-secitonal energy were measured. The calculations (Nikitopoulos and Liu 1986) were obtained for the overall energy E but subsequently

partitioned to obtain E_u via the local linear theory. The initial conditions were applied at the streamwise station corresponding to where the mixing layer profile has been established from a previous wake-like region behind the splitter plate. The initial values used, in the notation corresponding to the theoretical formulation, correspond to those of Ho and Huang (1982) and are $E_{u1}(0) = 0.16 \times 10^{-4}$, $E_{u2}(0) = 0.48 \times 10^{-3}$, Re = 81 and R = 0.31. Three relative phase angles were used ($\theta = 0^\circ$, 80°, 180°) in the calculations. The development of the cross-sectional energy, $E_{un}(x)/E_{un}(0)$, where n = 1 (subharmonic) and n = 2 (fundamental), is shown in Figure 19 as a function of x/δ_0, where x = 0 correspond to where the initial condition was applied as already discussed. Because the fundamental component is (by definition) the most amplified disturbance at the outset, the extraction of energy from the mean flow is its dominant energy supply and is responsible for the first peak in E_{u2}. In the strong nonlinear region the subharmonic feeds energy into the fundamental component for $\theta = 0^\circ$. Thus, the second peak in E_{u2} for $\theta = 0^\circ$ occurs in the vicinity of the peak in E_{u1}. This mechanism is responsible for the relatively weaker E_{u1} shown in Figure 19. For $\theta = 180^\circ$, the fundamental feeds energy into the subharmonic and this is responsible for the much earlier decay of the fundamental energy E_{u2}. In this case, the mode-interaction mechanism augments the direct energy supply from the mean motion to the subharmonic energy and causes E_{u1} to peak earlier. In the intermediate case is $\theta = 80^\circ$ the subharmonic energy transfer to the fundamental is not as vigorous as in the $\theta = 0^\circ$ case and compares favorably with the measurements of Ho and Huang (1982). The resulting growth of

the shear layer thickness is shown in Figure 20. The first plateau is due to the peak in the fundamental, the second due to the peaking of the subharmonic according to (6.16). Because the interaction between the mean flow and the amplified disturbances is strong, the rapid spreading rate is a part of the nonlinear interaction process and thus ought not be presumed as a known input for the nonlinear amplitude problem. This significant interaction feature, which is lacking in the "small divergence theory" (Gaster, Kit and Wygnanski 1985, Wygnanski and Petersen 1985, Weisbrot 1984), is an essential feature in for the wave function rather than be used for the description of the wave-envelope problem. We note that the shear layer spreading due to the subharmonic very nearly doubles that due to the fundamental in Figure 20. That is, the ratio of the two plateaus is nearly two. However, this is dependent upon the initial conditions and mode numbers and should not be a general "rule of thumb". The plateaus are clearly attributed to the net energy loss from the mean flow directly to the disturbances according to (6.16). The interaction between the coherent modes has but an **indirect** effect. The continued subsequent spreading of the mean flow (Figure 20) in the experiments are attributable to other fluctuations which are not accounted here. These simple ideas are extended to include the presence of fine-grained turbulence subsequently. In the absence of any fluctuations, or course, the shear flow spreads because of viscosity alone as is evident from (6.16). In Liu (1981), the Kelly mechanism was discussed in a much broader context than the weakly nonlinear theory from which it was obtained as is illustrated here. In order to show consistency with the pioneering work of Kelly

(1967) for parallel flows, Nikitopoulos and Liu (1986) discussed the properties of the mode interaction integral I_{12} in detail. We shall summarize here that $I_{12} < 0$ for small β and θ, covering the range of β when the fundamental is most amplified and when $\theta = 0^\circ$ (Kelly 1967), indicating that the fundamental energy is transferred to the subharmonic. As β increases this energy transfer mechanism changes sign for the same θ, a feature attributable to the developing, spatial problem. For large θ and small β, energy is transferred from the subharmonic to the fundamental and again, this transfer mechanism changes sign as β increases. In the context of strongly amplified disturbances in a **developing mean shear flow**, however, the original Kelly mechanism for **parallel flows** is largely academic as the integral I_{12} changes sign as the flow evolves. However, in the broader sense the Kelly mechanism is intepreted as having pointed out the importance of both the relative phase and amplitudes in the subharmonic - fundamental mode interactions. Nikitopoulos and Liu (1984) have also sutdied the three-mode interaction problem. This, and the two-mode problem briefly discussed here, shall appear elsewhere in greater detail (Nikitopoulos and Liu 1986).

We have already emphasized that the spreading rate of the mean flow is proportional to the rate at which energy is removed from the mean flow. For a purely laminar viscous flow only viscous dissipation contributes to the spreading rate $I_\Phi/(\bar{I}\ Re\ \delta)$ as indicated by (6.16), thus $\delta \sim \sqrt{x}$ as expected. For a laminar flow undergoing transition, the rate of energy transfer to originally small disturbances, reflected by the $-\overline{\tilde{u}\,\tilde{w}}$ Reynolds stress conversion mechanism (including, for simplicity

in notation, an "essemble" of coherent modes), now competes with the viscous dissipation. When the disturbances have become sufficiently finite, a marked deviation from the purely viscous spreading rate would be noticed (see, for instance, Sato & Kuriki 1961; Ko, Kubota & Lees 1970). In the presence of both a fundamental disturbance and its subharmonic, such as the case discussed here (Ho and Huang 1982), where the peak in the finite amplitudes are distinctively separated in space, the growth of the shear layer undergoes successive plateaus; the vigorous shear layer growth regions are associated with active energy extraction from the mean flow for the disturbance amplification and the plateau regions associated with decaying disturbance amplitudes. In Ho and Huang's (1982) experiments, the shear layer continues to spread after the plateau regions (see Figures 3 and 20), it is most likely that transition to fine-grained turbulence has taken place in that the existing fine-grained turbulence having been sufficiently strained by the coherent structures is now contributing towards the mean flow spreading rate via their Reynolds stress fine-grained turbulence $-\overline{u'w'}$. For large-scale coherent structures in a turbulent shear flow both $-\tilde{u}\tilde{w}$ and $-\overline{u'w'}$, but depending on their relative strength, contribute to the growth of the mean shear flow. In the downstream region where a particular mode of choherent structure has rearranged its velocity distribution such that $-\tilde{u}\tilde{w}$ is opposite the sign of $\partial U/\partial z$, then energy is returned to the mean motion from this particular mode and this contributes to the decrease of the spreading rate. We have already seen this using Weisbrot's (1984) observation as example.

Kaptanoglu (1984) and Liu and Kaptanoglu (1984) studied the dominant two-dimensional coherent-mode interactions in a two-dimensional **turbulent mixing layer** by extension of the corresponding problem in a laminar, viscous layer (Nikitopoulos 1982, Liu and Nikitopoulos 1982, Nikitopoulos and Liu 1986) through the specialization of the basic equations in Section II. The individual mode-turbulence interations are entirely similar to the single coherent mode problem discussed in Section V and Section VI.B. Of particular interest is the application of these ideas to the transition problem (e.g., Ho and Huang 1982) in which the initial fine-grained turbulence is sufficiently weak so as to render coherent mode-interactions to develop initially unhindered by the fine-grained turbulence. Depending on the initial level of the turbulence and the relative strengths of the initial coherent mode energy levels and the initial mode content, the fine-grained turbulence would eventually be amplified to a fully participating role in the dynamics of the shear layer through energy transfer from the mean flow and the coherent modes. We return to the eventual linear spreading of the shear layer in the transition problem (Ho and Huang 1982) discussed earlier (see, Figures 3 and 20). We emphasize here that Kaptanoglu's model still retains the simple two-dimensional coherent modes as dominant without considering the spanwise standing waves found to exist observationally as streamwise "streaks". As such, the comparison with observations (e.g. Huang 1985) is not likely to be meaningful as the three-dimensional wave disturbances are starting to play a significant role in the dynamics of the shear layer. We shall address this problem in Section VI.D. Nevertheless, we shall be

contented here to illustrate the transition problem via the simple two-dimensional coherent mode-interaciton model in the presence of fine-grained turbulence.

Kaptanoglu (1984) and Liu and Kaptanoglu (1984) first consider an "experiment" in which the "fundamental" mode is initiated at a relatively higher energy level $A_{20}^2 = 17 \times 10^{-5}$ at the initial frequency $2\beta_0$, whereas its "subharmonic" at the initial frequency β_0 is initiated at a lower level $A_{10}^2 = 3 \times 10^{-5}$; with other parameters set at $R = 0.31$, $Re = 62$, $\theta = 0°$, $E_0 = 10^{-6}$. The initial Strouhal frequency was chosen to be $\beta_0 = 0.149$ so that $2\beta_0 = 0.298$. The latter is slightly less than the Strouhal frequency of 0.4426 for the maximum initial amplification rate according to the linear theory. We shall continue to refer to the initial $2\beta_0$-mode as the fundamental and the initial β_0-mode as the subharmonic even if $2\beta_0 \neq 0.4426$ and $\beta_0 \neq 0.2213$. The numerical values of the above parameters are fixed and each variation from fixed values will be explicitly stated. The results from the above fixed set of parameters are shown in Figure 21. The energy densities in Figure 21a are denoted by "2" for A_2^2 (the initial $2\beta_0$-mode), "1" for A_1^2 (the initial β_0-mode) and "0" for E. The shear layer thickness (normalized by the initial shear layer thickness) is shown in Figure 21b. For this set of parameters, the maximum magnitudes of A_2^2 and A_1^2 reaches the same level approximately; in terms of maximum "amplificaiton", $(A_2^2/A_{20}^2)_{max} \approx 206$ and $(A_1^2/A_{10}^2) \approx 1200$. The respective coherent mode amplitudes grow by extraction of energy from the mean flow and decay by return of energy to the mean flow ("negative production"), viscous dissipation net energy transfer to the fine-grained turbulence. The relative phase was $\theta = 0°$ so that initially energy is

is transferred from the $2\beta_0$-mode to the β_0-mode and this reverses sign with increasing streamwise distance. The mode interaction effect, which is proportional to amplitude cubed, is relatively effective in the vicinity where the mean flow production of wave-disturbance, proportional to amplitude squared, is nearly zero and about to reverse in sign. The production of fine-grained turbulence is slightly larger than its viscous dissipation; the turbulence growth is augmented by the energy transfer from the coherent modes giving rise to the mild but noticable maximum in the turbulence energy density in Figure 21a. The noticable two bumps in the shear layer thickness in Figure 21b is due to the peaking of the energy drain from the two coherent modes. The eventual linear growth is due to the fine-grained turbulence. In the far downstream region, the balance between the fine-grained turbulence production, dissipation and the effect of shear layer spreading give an equilibrium fine-grained turbulence energy density $E_e \approx 0.18\ R^2$ and an equilibrium spreading rate $d\delta/dx \approx 0.025\ R$ due to the fine-grained turbulence. The effect of mean flow dissipation not being important and was neglected. These are estimated from the appropriate equation for $d\delta/dx$ and $d\delta E/dx$ with the coherent modes having equilibrated to zero in this case. We see that the equilibrium behavior of E and $d\delta/dx$ in Figure 21 very nearly follow from the estimates given.

We consider next the effect of initial turbulence levels, E_0, on the subsequent shear layer development. When the turbulence energy level is exceedingly weak, $E_0 = 10^{-10}$, we see in Figure 22 that the coherent modes and the initial shear layer development are essentially unaffected by the turbulence. The subsequent linear

spreading rate far downstream is caused by the rising turbulence energy level. As the initial turbulence level is increased to $E_0 = 10^{-8}$ in Figure 23, the linear spreading rate and steep rise in turbulence energy level moves upstream; with the coherent modes still somewhat unaffected. These are to be comapred to the "standard experiment" for $E_0 = 10^{-6}$ in Figure 21 where the coherent modes are already modified by the fine-grained turbulence. As the turbulence energy level is increased to $E_0 = 10^{-4}$ in Figure 24, the β_0-mode maximum-A_1^2 level is significantly modified and its occurrence is moved upstream; the A_2^2 maximum level and location is slightly modified. As the initial turbulence level is increased to $E_0 = 10^{-2}$ in Figure 25, corresponding to r.m.s. velocity ratios of about 7% of the averaged mean velocity, the coherent modes' energy levels are significantly reduced. The steplike growth of the shear layer thickness is very nearly obliterated by the strong turbulence levels. The qualitative effects are consistent with observations of Browand and Latigo (1979). In the experiments, however, it is difficult to preserve the same β_0 while changing the initial turbulence levels. In general, as the turbulence level is increased, the coherent mode peaks tend to move upstream.

With all other parameters fixed as in the "standard experiment" of Figure 21, the Reynolds number is changed increased Re = 500 in Figure 26. Results for Re > 500 shows only very modest differences. In this case, the viscous dissipation of the coherent modes and of the mean flow are not important. This results in a significant development of the $2\beta_0$-mode and, consequently, because $\theta = 0^\circ$, there is significant energy transfer from the β_0-mode resulting in the supression of the latter.

The "nonequilibrium" peak in the turbulence energy level (Figure 26a) is due to energy transferred from the coherent modes. The pronounced first step in the shear layer thickness (Figure 26b) is due to the pronounced peak in the $2\beta_0$–mode. The second step, merging immediately into the linear growth region, is attributed to the combined peaks of the β_0-mode and turbulence. As the Reynolds number is lowered to Re = 100 in Figure 27, the A_2^2 level is lowered due to viscous dissipation and the supression of the A_1^2 level from mode-interaction is thus to a lesser extent; the turbulence level development is milder as shown in Figure 27a. In this case, the pronounced steplike growth (Figure 26b) has become milder (Figure 27b). These are to be compared, again, to the "standard experiment" of Re = 62 shown in Figure 21. As the Reynolds number is lowered to Re = 40, the $2\beta_0$-mode is significantly surpressed at the outset due to viscous dissipation and the β_0-mode, in the presence of weak intermode energy drain, is allowed to develop as shown in Figure 28a. The pronounced step in the shear layer thickness is due to the peak in A_1^2. We note that as the Reynolds number is increased, the location of the peak of the $2\beta_0$-mode moves upstream, whereas that of the β_0-mode remains more or less unchanged.

The "standard experiment" (Figure 21) was initiated at the initial dimensionless frequencies β_0 = 0.149 and $2\beta_0$ = 0.298; both modes are on the lower frequency side of the most amplified freuqency of 0.4426. Shown in Figure 29 is the case when β_0 = 0.25 and $2\beta_0$ = 0.50, the latter falling to the higher frequency side of 0.4426. Consequently, the $2\beta_0$ has little to travel downstream before it is advected into the "negative production" region and is thus unable to develop to any significant extent

as shown in Figure 29a, the second mild peak is due to the energy transfer from the β_0-mode. In this case, the β_0-mode develop almost independently of the $2\beta_0$-mode and it gives rise to the single pronounced steplike shear layer thickness in Figure 29b prior to the linear growth region. As the initial frequencies are lowered to $\beta_0 = 0.2$ and $2\beta_0 = 0.4$, the A_2^2 is able to develop further before being advected into the "damped" region shown in Figure 30a; but still the steplike structure in the shear layer thickness is due to the strong levels of A_1^2 (Figure 30b). In the "low frequency" initiation at $\beta_0 = 0.05$ and $2\beta_0 = 0.10$, the $2\beta_0$-mode is able to develop significantly and consequently supressing the β_0-mode via mode interaction (Figure 31a). The pronounced step in the shear layer thickness (Figure 31b) and the peak in the turbulence level (Figure 31a) is attributed to the $2\beta_0$-mode. The initially lower frequency modes are stretched out in their streamwise evolution compared to the higher frequency modes as was expected (Liu 1974, Mankbadi and Liu 1981, 1984) from single-mode considerations.

Although not shown, imposing very large initial amplitudes upon one of the modes causes the maximum of that mode to be precisely the initial amplitude; whereas the maximum amplification is achieved by imposing very small initial amplitudes. The amplification of the remaining other mode is only moderately affected. Such resulting properties of mode-forcing upon single, independent modes were already obtained by Mankbadi and Liu (1981) in connection with the round turbulent jet problem. The recent experiments of Fiedler and Mensing (1985) indicate also such interesting properties of possible control. Similar mode interactions in a

round turbulent jet between two-frequency, axially symmetric (n = 0) modes were recently considered by Mankbadi (1985). The interactions between axially symmetric and helical modes ($n \neq 0$) in a round jet are very much similar to mode interactions involving two-dimensional and spanwise periodic three-dimensional modes in an otherwise two-dimensional shear layer. The issues with regard to such three-dimensional effects is addressed in the next section.

D. THREE-DIMENSIONAL NONLINEAR EFFECTS IN LARGE-SCALE COHERENT MODE INTERACTIONS

In the previous sections we have discussed the mechanisms of interaction between plane, large-scale coherent modes with the three-dimensional fine-grained turbulence. Although the two-dimensional coherent structures are still the dominant coherent modes in two-dimensional shear flows, there is increasing observational evidence that three-dimensional coherent modes, in the form of spanwise periodicities or standing waves, persit (Miksad 1972; Bernal, et al 1980; Bernal 1981; Breidenthal 1981; Browand and Troutt 1980, 1984; Roshko 1981, Konrad 1977; Jimenez 1983; Alvarez and Martinez-Val 1984; Huang 1985). The experiments dealt primarily with transitional shear layers and it is clear that coherent three-dimensionality is most likely to provide additional sites for the straining and amplification of preexisting fine-grained turbulence, however initially weak (Huang 1985). This would augument the direct production of fine-grained turbulence from the mean flow and from the two-dimensional coherent motions. The three-dimensional coherent motions persist

well into the region where fine-grained turbulence has become active (Bernal 1981, Roshko 1981). On the basis of the discussions in the previous sections, it is entirely conceivable that such spanwise periodicities, again appearing as a manifestation of hydrodynamic instability, would also develop in an initially turbulent shear layer, depending on the balances between mechanisms of energy supply and "dissipation". From this discussion, we are lead carefully to distinguish the two very distinct three-dimensional motions. One is the fine-grained turbulence and the other is the large-scale coherent motion in the form of spanwise standing waves in a two-dimensional mean shear flow or helical modes in the round jet (e.g., Mankbadi and Liu 1981, 1984). It is an experimental fact that the spanwise wavelength of the three-dimensional coherent modes increases further downstream (Barnel 1981, Jimenez 1983, Huang 1985), as if evolving through the emergence of a spanwise subharmonic formaiton, much in the same spirit as the subharmonic formation in terms of frequency and streamwise wavelength for two-dimensional coherent modes (Freymuth 1966, Winant and Browand 1974). Quantitative observations (e.g., Jimenez 1983, Huang 1985) indicate that the combined spanwise, three-dimensional modes develop downstream in a nonequilibrium fashion resembling, though not in detail, that of the two-dimensional modes. The wave-envelope amplifies and eventually decays. Jimenez (1983) showed that the three-dimensional disturbances are imposed by upstream disturbance such as the inherent waviness of the trailing edge of the plate separating the two streams or the screens placed upstream of the trailing edge. As such the upstream initial conditions on the spanwise modes are uncontrolled. Unlike the

situation with the wavenumber or frequency selection mechanism for the two-dimensional coherent modes, the spanwise wavenumber selection mechanism is still unsettled in spite of recent works on the temporal mixing layer from the point of view of computational-hydrodynamic stability (Pierrehumbert and Widnall 1982, Corcos and Lin 1984) and numerical simulation (Riley and Metcalfe 1980, Cain, et al 1981, Couet and Leonard 1980, Metcalfe, et al 1985). Corcos and Lin (1984) suggest that perhaps the nonlinear interactions between spanwise modes and the role of initial conditions might uncover the mechanism of the spanwise wavenumber selection. To this end, we shall return to a brief discussion of the classical nonlinear analyses of three-dimensional disturbances in shear flows. This would form the basis that naturally leads to the discussion from our point of view in focusing attention on real, spatially developing shear flows.

Three-dimensional disturbance effects in temporal, parallel shear flows have been studied by Benney and Lin (1960) and Benney (1961). This body of work is a second-order theory rather than one of finite amplitude in that the amplitudes are taken as exponentials. They considered the temporal problem consisting of two interacting fundamentals, a two-dimensional wave disturbance of the form $\exp(i\alpha(x-c_1t))$ and a three-dimensional disturbance of the form $\exp(i\alpha(x-c_2t))\cos\gamma y$, where γ is the spanwise wavenumber, c_1 and c_2 are the complex phase velocities and α is the streamwise wavenumber associated with the fundamental two-dimensional disturbance. For simpliticity, Benney and Lin (1960) assumed that $c_1 = c_2$ for a given Reynolds number and this leads to harmonics that are stationary rather than

periodic in time. Other second-order effects include the formation of harmonics of the two fundamentals and the distortion of the mean flow. The combination of nonlinear effects on amplitude and three-dimensional wave disturbance effects were studied by Stuart (1962b) and presented at the 1960 Second International Congress in Aeronautical Science in Zurich. Stuart (1962b) found that there are at least eight physically distinct "modes". This can best be characterized by attaching the subscipts m and n to the relevant flow quantities, say, the velocity u_{mni} (where i is retained to indicate the components of the velocity). The first subscript m indicates the streamwise wavenumber for the temporal problem, whereas n would indicate the spanwise wavenumber. For instance, m = 1 denotes the fundamental streamwise wavenumber α, m = 2 its first harmonic 2α; n = 1 denotes the $\cos\gamma y$ mode and n = 2 denotes the $\cos 2\gamma y$ mode. The three streamwise nonperiodic modes consist of the 00, 01 and 02 modes. The first refers to the modification of the temporal mean motion which is here the combined streamwise- and spanwise-averaged flow. The 01 and 02 modes are the streamwise-independent but spanwise-periodic harmonics generated by the three-dimensional wave disturbance. The 10 and 20 modes are the two-dimensional fundamental and harmonic components respectively. The 11 mode is the three-dimensional fundamental and the 22 and 21 modes are the associated harmonics. Following earlier work on finite-amplitude effects for two-dimensional disturbances (Stuart 1960), Stuart (1962b) obtained amplitude equations for the two complex two-amplitude functions A(t) and B(t) for the temporal two- and three-dimensional disturbances respectively, in a parallel flow,

$$\frac{dA}{dt} = A(a_0+a_1^{(1)}|A|^2+a_1^{(2)}|B|^2+\cdots) + a_1^{(3)}\tilde{A}B^2 + \cdots \tag{6.19}$$

$$\frac{dB}{dt} = B(b_0+b_1^{(1)}|A|^2+b_1^{(2)}|B|^2+\cdots) + b_1^{(3)}\tilde{B}A^2 + \cdots . \tag{6.20}$$

In (6.19) and (6.20), the constants $a_0 = -i\alpha c_1$ and $b_0 = -i\alpha c_2$ come from the linear theory and the remaining constants from the nonlinear theory. Stuart (1962b) showed how these constants could be evaluated. He argued that for finite values of the spanwise wavenumber γ, the constants $a_1^{(3)}$ and $b_1^{(3)}$ may be choosen to be zero. In this case, the "wave envelope" equations then appear in the form

$$\frac{d|A|^2}{dt} = 2|A|^2(\alpha c_{1i}+a_{1r}^{(1)}|A|^2+a_{1r}^{(2)}|B|^2+\cdots) \tag{6.21}$$

$$\frac{d|B|^2}{dt} = 2|B|^2(\alpha c_{2i}+b_{1r}^{(1)}|A|^2+b_{1r}^{(2)}|B|^2+\cdots) \tag{6.22}$$

where the subscripts i and r denote imaginary and real parts, respectively. The amplitude equations from weakly nonlinear theory are stated here for later reference for purposes of showing the contrast with the wave-envelope equations of three-dimensional disturbances in spatially developing shear flows for strongly amplified disturbances.

We have seen in Section VI.C how ideas from weakly nonlinear theory could

be used as a valuable guide for mode interactions in a developing shear flow. There the single, odd- and even-mode were given their individual amplitudes, as would be motivated by observations (e.g., Ho and Huang 1982), rather than in terms of an expansion in terms of ascending powers of a single amplitude function of the weak, nonlinear theory. The nonlinear effects being of amplitude to the fourth power reflects such an expansion procedure. This will be contrasted to the anticipated third power in amplitude for the present class of problems. In order to study the interaction between an initial fundamental component and its subharmonic in the spatial problem, the mode interaction is in terms of frequency and calls for the reinterpretation of the the single even-mode as the fundamental component and the single-odd mode as its subharmonic at half the fundamental frequency. The same interpretation is used to denote three-dimensional wave disturbance interactions. The even and odd modes here refer to the frequency only and the basic equations devleoped in Section II applies. The Reynolds mean motion is, by definition, obtained via averaging over all periodicities. In this case, the average is taken with respect to time and over the spanwise distance for two-dimensional shear flows. For round jets, the latter average is replaced by the circumferential average. The conditional average used to separate the coherent modes and the fine-grained turbulence is still the phase-averaging procedure geared to the coherent frequencies or periods for the spatial problem.

In order to study subharmonic/fundamental interactions (in the frequency sense) and the downstream evolution of at least two spanwise periodic scales for the

spatially developing shear flow, it is not difficult to confirm that the minimum number of frequency-periodic modes required is five. Using similar notation as that of Stuart (1962b) we denote the coherent dynamical quantities as q_{mn} (with u_{mni} as the velocity, i is the component indicator), m refers to the frequency and n the spanwise periodicity. The even frequency mode is denoted by m = 2 (reinterpreted as the fundamental mode in frequency) and odd frequency mode by m = 1 (the reinterpreted subharmonic mode in frequency). The two-dimensional modes are denoted by n = 0. It is not essential to take the spanwise periodicity indication $n \neq 0$ literally as long as we identify modes with n = 1 to have spanwise wavelengths twice that of the modes with n = 2. For instance, n = 2 and 1 could be taken to indicate $\cos 2\gamma y$ and $\cos \gamma y$, respectively or $\cos \gamma y$ and $\cos(\gamma/2)y$, respectively. In both cases, the spanwise wavelength (λ_n) is such that $\lambda_1 = 2\lambda_2$. In observations (e.g., Jimenez 1983, Huang 1985), λ_1 eventually prevails over λ_2 downstream. The five minimum frequency periodic ($m \neq 0$) modes consistant with Stuart (1962b), would be: three modes belonging to the fundamental frequency (even, m = 2) 20, 21, 22 and two modes belonging to the subharmonic frequency (odd, m = 1) 10, 11. These modes still belong to the family of binary-frequency interactions (Liu and Nikitopoulos 1982, Nikitopoulos 1982). Inclusion of other $m \neq 0$ modes would necessitate tertiary-frequency interactions but which could still be formulated from the basic equations of Section II as was done for triple-frequency mode interactions for two-dimensional wave disturbances (Nikitopoulos and Liu 1984). The remaining frequency-independent modes (00,01 and 02) are modifications to the time-averaged

mean flow; the 01 and 02 are modifications prior to spanwise averaging. modifications prior to spanwise averaging. Before we continue with the three-dimensional wave disturbance problem, we shall insert a brief comment about accounting only for binary-frequency interactions which shows that it could be more general than would be anticipated.

The basis for our implicit hypothesis that only binary-frequency mode interactions suffice for the spatially developing shear flow lies in the earlier theoretical confirmation (Liu 1974a) of observations that progressively lower frequency modes develop and peak further downstream relative to higher frequency modes. For mode-interactions of the sub- and super-harmonic type to take place, modes of only integral multiples of the frequency participate. As demonstrated by Ho and Huang (1982), the peaks of the fundamental and subharmonic do not overlap. The first subharmonic, peaking further downstream than the fundamental, would eventually serve as the fundamental to the second subharmonic but in a region where the original fundamental has significantly weakened. In this case interactions between neighboring frequency modes would dominate. Situations where binary-frequency interactions would not suffice are elucidated by Nikitopoulos and Liu (1984).

The spanwise periodicities are considered to be standing waves. To help understand the physical mechanisms of mode interactions within the limited framework described, we obtain and state the energy equations for the five coherent modes. The energy equations of the even-frequency modes are obtained from (2.25). These modes are considered to be the fundamental-frequency modes and are given

$$\frac{\bar{D}}{Dt}\overline{u_{20i}^2}/2 = -\frac{\partial}{\partial x_j}\left[\overline{p_{20}u_{20j}} + \overline{(u_{10i}u_{10j}+u_{11i}u_{11j})u_{20i}} + \overline{u_{20i}r_{20ij}}\right]$$

$$+\left[-\overline{u_{20i}u_{20j}}\frac{\partial U_i}{\partial x_j} - \overline{\left[r_{20ij}\frac{\partial u_{20i}}{\partial x_j}\right]} - \overline{(-u_{10i}u_{10j}-u_{11i}u_{11j})\frac{\partial u_{20i}}{\partial x_j}}\right]$$

$$+\nu\frac{\partial^2\overline{u_{20i}^2}/2}{\partial x_j^2} - \nu\overline{\left[\frac{\partial u_{20i}}{\partial x_j}\right]^2}. \qquad (6.23)$$

The averaging, as already discussed, is with respect to both time and spanwise distance. The symbol ($\hat{}$) denoting even modes in Section II is identified here with the first subscript m = 2 denoting the fundamental frequency whereas ($\tilde{}$) denoting the odd modes is identified here with m = 1 as the frequency-subharmonic. In the second group of terms on the right side of (6.23), there is direct energy exchanges between the 20-mode with the mean flow and the fine-grained turbulence as well as direct energy exchanges with the two-dimensional and three-dimensional (n = 1) subharmonic modes, 10 and 11, respectively. The fundamental frequency, n = 1 three-dimensional 21-mode energy equation is

$$\frac{\bar{D}}{Dt}\overline{u_{21i}^2}/2 = -\frac{\partial}{\partial x_j}\left[\overline{p_{21}u_{21j}} + \overline{(u_{10i}u_{11j}+u_{11i}u_{10j})u_{21i}} + \overline{u_{21i}r_{21ij}}\right]$$

$$+\left[\overline{-u_{21i}u_{21j}}\frac{\partial U_i}{\partial x_j} - \left[\overline{r_{21ij}\frac{\partial u_{21i}}{\partial x_j}}\right] - \overline{(-u_{10i}u_{11j}-u_{11i}u_{10j})\frac{\partial u_{21i}}{\partial x_j}}\right]$$

$$+\nu\frac{\partial^2}{\partial x^2}\overline{u_{21i}^2}/2 - \nu\overline{\left[\frac{\partial u_{21i}}{\partial x_j}\right]^2} \qquad (6.24)$$

Again, direct energy exchanges of the 21-mode energy with the mean flow and fine-grained turbulence are obvious in the second group of terms on the right of (6.24). The last item in this group refelects, as will be confirmed subsequently, the energy exchange between the 21-mode with the 10-mode through interference of the 11-mode $-\overline{u_{10i}u_{11j}\partial u_{21i}/\partial x_j}$, and with the 11-mode through interference of the 10-mode $-\overline{u_{11i}u_{10j}\partial u_{21i}/\partial x_j}$; the net rate of these energy exchanges are the same. The fundamental-frequency, n = 2 three-dimensional 22-mode energy equation is

$$\frac{\bar{D}}{Dt}\overline{u_{22i}^2}/2 = -\frac{\partial}{\partial x_j}\left[\overline{p_{22}u_{22j}} + \overline{u_{11i}u_{11j}u_{22i}} + \overline{u_{22i}r_{22ij}}\right]$$

$$+\left[\overline{-u_{22i}u_{22j}}\frac{\partial U_i}{\partial x_j} - \left[\overline{-r_{22ij}\frac{\partial u_{22i}}{\partial x_j}}\right] - \overline{(-u_{11i}u_{11j})\frac{\partial u_{22i}}{\partial x_j}}\right]$$

$$+ \nu \frac{\partial^2}{\partial x_j^2} \overline{u_{22i}^2}/2 - \nu \overline{\left[\frac{\partial u_{22i}}{\partial x_j}\right]^2} . \qquad (6.25)$$

Again, in addition to energy exchanges with the mean flow and fine-grained turbulence, the last term in the second group of energy exchange mechanisms on the right of (6.25) reflects a direct energy exchange between the 22-mode and the 11-mode. We note that there are no direct energy exchanges between the three fundamentals 20, 21 and 22.

The energy equation for the two-dimensional subharmonic 10 mode is

$$\frac{\bar{D}}{Dt} \overline{u_{10i}^2}/2 = - \frac{\partial}{\partial x_j} \left[\overline{p_{10}u_{10j}} + \overline{u_{20}u_{10i}^2}/2 + \overline{u_{10i}r_{10ij}}\right]$$

$$+ \left[\overline{-u_{10i}u_{10j}} \frac{\partial U_i}{\partial x_j} - \left(\overline{-r_{10ij} \frac{\partial u_{10i}}{\partial x_j}} \right) \right.$$

$$\left. + \left(\overline{-u_{10i}u_{21j} \frac{\partial u_{11i}}{\partial x_j}} - \overline{u_{10i}u_{10j} \frac{\partial u_{20i}}{\partial x_j}} - \overline{u_{10i}u_{11j} \frac{\partial u_{21i}}{\partial x_j}} \right) \right]$$

$$+ \nu \frac{\partial^2}{\partial x_j} \overline{u_{10i}^2}/2 - \nu \overline{\left[\frac{\partial u_{10i}}{\partial x_j}\right]^2} . \qquad (6.26)$$

Again, in addition to direct energy exchanges with the mean flow and fine-grained turbulence, the two-dimensional subharmonic 10-mode exchanges energy with the frequency-subharmonic, three-dimensional 11-mode via the interference of the fundamental 21-mode. It exchanges energy with the fundamental two-dimensional 20-mode directly but with the fundamental three-dimensional 21-mode via interference by the 11-mode. The frequency-subharmonic, n = 1 three dimensional 11-mode energy equation is

$$\frac{\bar{D}}{Dt}\,\overline{u_{11i}^2}/2 = -\frac{\partial}{\partial x_j}\left[\overline{p_{11}u_{11j}} + \overline{(u_{20j}+u_{22j})u_{11i}^2}/2 + \overline{u_{21j}u_{10i}u_{11i} + u_{11i}r_{11ij}}\right]$$

$$+ \left[\overline{-u_{11i}u_{11j}}\,\frac{\partial U_i}{\partial x_j} - \left[\overline{-r_{11ij}\,\frac{\partial u_{11i}}{\partial x_j}}\right]\right.$$

$$+ \left[\overline{u_{10i}u_{21j}\,\frac{\partial u_{11i}}{\partial x_j}} - \overline{u_{11i}u_{11j}\,\frac{\partial u_{20i}}{\partial x_j}} - \overline{u_{11i}u_{10j}\,\frac{\partial u_{21i}}{\partial x_j}} + \overline{u_{11i}u_{11j}\,\frac{\partial u_{22i}}{\partial x_j}}\right]$$

$$+ \nu\,\frac{\partial^2}{\partial x_j^2}\,\overline{u_{11i}^2}/2 - \nu\overline{\left[\frac{\partial u_{11i}}{\partial x_j}\right]^2}\,. \qquad (6.27)$$

The energy exchange with other modes are given by the second group of terms on the right side of (6.27). The 11-mode exchanges energy with the two-dimensional

10-mode through the interference of the 21-mode and with the 21-mode through the interference of the 10-mode. As already noted, the 11-mode exchanges energy directly with the 20- and 22-mode. Again, the 11-mode exchanges energy directly with the mean flow and fine-grained turbulence as depicted, respectively, by the first two terms in this same group.

We have, in Figure 21, depicted the mn-mode energy transfer mechanisms. The direction of the arrow in the figure is associated only with the manner in which the sign of the energy exchange term occur in the individual energy equation, not the actual direction of individual energy exchange mechanism. As we have learned from our previous considerations, the direction of energy transfer lies in the relative phase relations between the fluctuations that make up this mechanism.

The energy exchanges between the coherent modes and with the fine-grained turbulence is summarized in Table 1. The n = 0 two-dimensional mode energy exchanges between the coherent modes and with fine-grained turbulence have been the subject of discussions in Sections IV, V and in the present section. It is not difficult to see that the n = 1,2 three-dimensional modes provide additional modulated turbulent stresses and coherent rates of strain for such exchange mechanisms. The energy exchange mechanisms with the mean flow is summarized in Table 2. We have already shown how energy extraction by two-dimensional modes from the mean flow causes its thickness to grow. The additional mechanisms due to the three-dimensional modes would augment this spreading rate if wave disturbances continue to take energy from the mean flow.

From the special form of (6.23) - (6.27) for which the mean flow is two-dimensional we can obtain the spatial evolution equations for the five coherent modes; and, in addition, those of the fine-grained turbulence energy and the mean flow thickness similar to the two-dimensional coherent mode problem. The notation used for the advection and interaction integrals are similar to those previously defined except for the subscripts mn, where m = 1,2 and n = 0,1,2 (but there is no 12-mode within the present framework). The wave-envelope equations for the five modes can be written in the form

$$\bar{I}_{mn} \frac{d\,\delta A_{mn}^2}{dx} = \underbrace{A_{mn}^2 \tilde{I}_{rsmn}}_{\substack{\text{energy exchange} \\ \text{with mean flow}}} - \underbrace{A_{mn}^2 EI_{wtmn}}_{\substack{\text{energy exchange} \\ \text{with} \\ \text{turbulence}}} - \underbrace{\frac{1}{Re} A_{mn}^2 \tilde{I}_{\phi\,mn}/\delta}_{\substack{\text{viscous} \\ \text{dissipation}}} +$$

$$+ \underbrace{\vartheta_{mn}}_{\substack{\text{energy exchange} \\ \text{with} \\ \text{other modes}}} . \qquad (6.28)$$

The mode interaction mechanisms, ϑ_{mn}, is summarized in Table 3. The mean flow kinetic energy equation gives

$$\bar{I} \frac{d\delta}{dx} = \underbrace{\sum_m \sum_n A_{mn}^2 \tilde{I}_{rsmn}}_{\substack{\text{energy exchange} \\ \text{with overall coherent} \\ \text{modes}}} + \underbrace{EI'_{rs}}_{\substack{\text{energy} \\ \text{exchange} \\ \text{with turbulence}}} + \underbrace{\frac{1}{Re} \bar{I}_{\phi}/\delta}_{\substack{\text{viscous} \\ \text{dissipation}}} . \qquad (6.29)$$

The fine-grained turbulence kinetic energy equation gives

$$\overline{I'}\,\frac{d\delta E}{dx} = \underbrace{EI'_{rs}}_{\substack{\text{energy exchange}\\ \text{with mean flow}}} + \underbrace{E\sum_{m}\sum_{n} A_{mn}^{2} I_{wtmn}}_{\substack{\text{energy exchange with}\\ \text{overall coherent modes}}} - \underbrace{E^{3/2} I'_{\phi}}_{\substack{\text{viscous}\\ \text{dissipation}}} \tag{6.30}$$

Equations (6.28) - (6.30) would be subjected to the initial conditions $A_{mn}^2(0) = A_{mno}^2$, $\delta(0) = 1$, $E(0) = E_0$; supplemented by choosing the initial frequency of the wave disturbance β_0 (and $2\beta_0$), the relative spanwise wave number γ/β_0 and the relative phases between the coherent modes. We comment here that in the case of the round jet the physical mechanisms, except for details with regard to curvature effects in the downstream region, and formulation appear in the same form as (6.28) - (6.30) with $n = 0$ identified with the axially symmetric modes and $n \neq 0$ with helical modes. Although the numerical aspects of this problem is under active pursuit by S. S. Lee* (Lee and Liu 1985), a number of relevant and meaningful interpretations can be directly inferred from the formulation and results of a preliminary nature. It is now well known that higher frequency wave disturbances grow, peak and decay in a region closer to the start of the shear flow than lower frequency disturbances. In this situation, the entire $m = 2$ higher fundamental frequency group of 20, 21 and 22 modes accomplish such growth and decay activities early on in the streamwise

*Graduate Student, The Division of Engineering, Brown University.

direction than the m = 1 group of 10 and 11 modes for not disparately different initial mode-energy levels. Within the m = 2 group it is expected that the n = 0 dimensional 20-mode would persist the longest in the streamwise distance then the 21-mode; the latter, in turn prevails over the 22-mode. In this case, although the $\cos 2\gamma y$ and $\cos \gamma y$ modes would initially develop at about the same level, the shorter wavelength ($2\pi/2\gamma$), three-dimensional spanwise mode disappears first, giving way to the longer wavelength ($2\pi/\gamma$) spanwise mode associated with the higher, fundamental frequency group. Eventually in the streamwise development, the m = 2 frequency group of modes give way to the m = 1 subharmonic frequency group of 10 and 11 modes. The development of the 11-mode, of wavelength $2\pi/\gamma$, then persists further downstream (until they succumb to subsequent subharmonics or turbulence). Thus, the present multiple-mode interaction model gives the important observational feature (Bernal 1981, Jimenez 1983, Huang 1985) that the number of streamwise, longitudinal streaks lessens with the downstream distance. Although this important feature is inferred from the formulation of the problem, preliminary numerical results (Lee and Liu 1985) confirm this. Characteristically with coherent modes in developing shear flows, the problem is one of nonequilibrium interactions and is sensitive to initial conditions. Perhaps, when the full numerical results become available, a study based on the variaiton of initial conditions and mode numbers might provide us with an understanding of the spanwise-mode selection mechanisms in **dcvlcoping** shear flows.

In the recent measurements of Huang (1985), frequency-fundamental and subharmonic mode energies were obtained but without differentiating between two-

and three-dimensional modes in the present context. Thus, the sectional energy measured, in terms of the present interpretation, reflects the sum within each frequency group of modes: $(E_{20}+E_{21}+E_{22})$ for the fundamental and $(E_{10}+E_{11})$ for the subharmonic. Further decomposition along the lines discussed here would be helpful towards the understanding of the important modal-interaction mechanisms that we have elucidated.

There are several temporal mixing layer studies that would be of interest to the present point of view. We delayed discussions of these until the present nonlinear interaction problem is fully stated. In this case, we will be able to place these temporal problems in proper perspective with respect to the spatial problem that we have discussed. To this end, the mode number in the temporal problem refers to the streamwise wavenumber and is taken to be analogous to the frequency in the spatial problem. This "common" mode number will be denoted by m in the mn-notation. The spanwise mode number is identical in both cases and is denoted by n. The basic flow for Pierrehumbert and Widnall's (1982) linear three-dimensonal stability studies is a class of finite-amplitude, steady two-dimensional solutions to the Liouville equation obtained by Stuart (1967, 1971b). The class of solutions is obtained by variations of a so-called vorticity concentration parameter, ϵ, which when set equal to zero the hyperbolic tangent profile, which could be considered as the mean flow, is obtained. For small but finite ϵ, an expansion in powers of ϵ reveal that the mean flow is perturbed by a steady, spatially-periodic fundamental

component at the ϵ order, at the ϵ^2 order there is a first harmonic component and a correction to the mean flow, and so on. When $\epsilon \to 1$, the flow due to a row of point vorticies is recovered. The $\epsilon \to 0$ range is relevant to our discussion. Because the flow is steady, the problem is neutral in that no energy exchange exist among the disturbance components and the mean flow. In our notation, in addition to the mean flow, this basic flow also consists of neutrally noninteracting 20 and 10 components (where we now revert to interpreting 20 as the 1st harmonic and 10 as the fundamental). The translative mode corresponds to a three-dimensional perturbation at the same m. In this case, the modes consist of the basic 20- and 10-mode plus the 11-mode. In the linear problem only direct energy transfers are possible. Form Figure 32 we see that there is no direct connection between the 11-mode perturbation with the basic 10-mode, but that there is a direct connection between the 11-mode with the basic 20-mode. One concludes in this situation that the amplification of the 11-mode comes from the basic mean flow and the 20-mode, while the 10-mode remain dormant in this process. As the parameter ϵ is further lowered, the present first harmonic, the 20-mode, being of order ϵ^2, becomes unimportant so that the only energy supply to the 11-mode would be the mean flow. This loss of an additional source of energy supply for $\epsilon \to 0$ may well be the reason why the 11-mode amplification rate is lowered with decreasing values of ϵ in the Pierrehumbert and Widnall (1982) translative-mode problem (see, also Ho and Huerre 1984). This translative mode is not equivalent to the second-order interactions described by Benney and Lin (1960) and Benney (1961) in that they included the

21-mode which interacts with and causes interaction between the 10- and 11-mode. To interpret the linearized helical-mode instability of Pierrehumbert and Widnall (1982), we now reinterpret the 20-mode as the two-dimensonal fundamental and 11-mode as the subharmonic, three-dimensional perturbation. From Figure 32, there is a direct interaction between the 20- and the 11-mode, in addition to the direct participation of the mean flow. Corcos and Lin (1984) considered similar three-dimensional linear perturbations but upon a time evolving two-dimensional flow consisting of equivalently, the mutually interacting mean shear flow and the two-dimensional mo-modes. In the equivalent translative mode interactions, they included the 20- and 21-mode, or alternatively, the 10- and 11-mode (cases 1 through 4); in these cases there are no direct mode interactions but that the three-dimensional mode derives its energy from the mean flow. In the translative-mode interaction with presence of a subharmonic, the 20-, 10- and 21-mode (cases 7-10) are included; again, there are no direct three- and two-dimensional mode interactions. Whereas, in the helical-mode interaction, modes 20, 10 and 11 were involved (cases 5, 6) where there is direct interaction between the 20- and 11-mode. Unfortunately, the rate of energy supply to the three-dimensional disturbance given by Corcos and Lin (1984) is the overall rate and thus does not elucidate these important individual mechanisms.

The resonant triad of Craik (1971, 1980), originally discussed in terms of boundary layers, is essentially a two-mode interaction in the context of spanwise standing-wave disturbances, involving the 20- and 11-mode for which there is a direct interaction (Figure 32). For a discussion of the work on resonant interactions

between three-dimensional disturbances due to Raetz, which remain unpublished, we refer to Stuart (1962a).

VII. OTHER WAVE-TURBULENCE INTERACTION PROBLEMS

It seems more appropriate to conclude this article by briefly pointing out a few examples to confirm that "...the more research in mechanics* expands, the more interconnections of seemingly far distant fields become apparant". This was an observation and a spirit infused upon this series by the founding editors, von Karman and von Mises, in their preface to the first volume.

In the structural aspects of the turbulent boundary layer there is no dearth for problems involving the interactions between various scales of large-scale motions and fine-grained turbulence (Willmarth 1975). Although the situation there is considerably more complicated and involved relative to the free shear flows, many of the interaction ideas share the same fundamental basis. The prospects of control naturally leads to the attempt to understand various perturbations upon turbulent boundary layers. One of such perturbations is through interaction of sound with wall turbulent shear layers (Howe 1986), to which some progress for its understanding is beginning to take place (Quinn and Liu 1985).

Interaction between wave motions and turbulence has recently taken on important roles in the meteorological context in mesospheric dynamics (Holton and Matsuno 1984, Fritts 1984) and in the oceanographic context in the mixing mechanism in the interior ocean and the microstructure problem. In fact Munk (1981)

---

*in the present case, research in the large-scale organized aspects in free turbulent shear flows.

underscores the connection between internal waves and small scale processes as "where the key is". Recent laboratory experiments (Stillinger, et al 1983) in a stratified fluid points to the necessity of the separation between waves and turbulence towards the understanding of their internal interaction processes. As an illustration of the turbulence-modified internal wave problem, similar conditional averaging procedures can be used to obtain the equation for linear internal waves (Quinn and Liu 1986):

$$\frac{\partial^2}{\partial t^2}\left[\nabla_H^2 + \frac{\partial^2}{\partial z^2}\right]\tilde{w} + N^2\nabla_H^2\,\tilde{w} = -\nabla_H^2\,\frac{\partial}{\partial x_j}\left[\frac{g}{T_0}\,\tilde{q}_j + \frac{\partial}{\partial t}\,\tilde{r}_{zj}\right]$$

$$+ \frac{\partial^2}{\partial t\partial z}\,\frac{\partial}{\partial x_j}\left[\frac{\partial \tilde{r}_{xj}}{\partial x} + \frac{\partial \tilde{r}_{yj}}{\partial y}\right] \qquad (7.1)$$

where $\tilde{w}$ is the vertical wave velocity, ∇_H^2 the horizontal Laplacian, z is the vertical coordinate, x and y are horizontal coordinates, N^2 the Brunt frequency taken as constant, g the acceleration of gravity, T_0 the temperature of the undisturbed (hydrostatic) fluid taken as constant as far as the wave motion is concerned, $\tilde{q}_j$ is the wave-modulated turbulence heat flux vector; $\tilde{r}_{ij}$ has the same meaning as in the previous discussions. Equation (7.1) would be augmented by the transport equations for $\tilde{r}_{ij}$, $\tilde{q}_j$ and for the wave-modulated, square of the turbulence temperature fluctuation $\tilde{h}$. These would be a rational replacement of the standard eddy-viscosity assumptions where, particularly in geophysical problems, the madnitude and sign of

such viscosities are difficult to estimate. Wave-turbulence interaction problems in the lower atmosphere in the vicinity of the atmospheric boundary layer has received attention (Einaudi and Finnegan 1981; Finnegan and Einaudi 1981; Fua, et al 1982). The onset of turbulence in Kelvin-Helmholtz billows is addressed by Sykes and Lewellen (1982) and by Klaassen and Peltier (1985), similar to the temporal homogeneous fluid problem of Gatski and Liu (1980).

ACKNOWLEDGMENT

This work is partially supported by the National Science Foundation, Fluid Dynamics and Hydraulics Program, Grant MSM83-20307 and the National Aeronautics and Space Administration, Langley Research Center Grant NAG1-379 and Lewis Research Center Grant NAG3-673. The partial support of NATO Research Grant 343/85 in association with J. T. Stuart of Imperial College, U. K. and the National Science Foundation, U. S.-China Cooperative Research Program, Grant INT85-14196 in association with H. Zhou of Tianjin University, China is also gratefully acknowledged.

REFERENCES

Alper, A. and Liu, J. T. C. (1978). On the interactions between large-scale structure and fine-grained turbulence in a free shear flow. Part II. The development of spatial interactions in the mean. Proc. Royal Soc. Lond. A359, 497-523.

Alvarez, C. and Martinez-Val, R. (1984). Visual measurement of streamwise vorticity in the mixing layer. **Phys. Fluids 27**, 2367-2368.

Amsden, A. A. and Harlow, F. H. (1964). Slip instability. **Phys. Fluids 7**, 327-334.

Barcilon, A., Brindley, J., Lessen, M. and Mobbs, F. R. (1979). Marginal instability in Taylor-Couette flows at a very high Taylor number. **J. Fluid Mech. 94**, 453-463.

Benney, D. J. (1961). A non-linear theory for oscillations in a parallel flow. **J. Fluid Mech. 10**, 209-236.

Benney, D. J. and Lin, C. C. (1960). On the secondary motion induced by oscillations in a shear flow. **Phys. Fluids 3**, 656-657.

Benney, D. J. and Bergeron, R. F., Jr. (1969). A new class of nonlinear waves in parallel flows. **Stud. Appl. Math. 48**, 181.

Bernal, L. P., Breidenthal, R. E., Brown, G. L., Konrad, J. H. and Roshko, A. (1980). On the development of three-dimensional small scales in turbulent mixing layers, **in** "Turbulent Shear Flows" **2**, 305-313. Springer-Verlag, Berlin.

Bernal, L. P. (1981). The coherent structure of turbulent mixing layers: II. Secondary streamwise vortex structure. Ph.D. Thesis, California Institute of Technology.

Binder, G. and Favre-Marinet, M. (1973). Mixing improvement in pulsating turbulent jets, **in** "Fluid Mechanics of Mixing" (eds. E. M. Uram and V. W. Golschmidt), pp. 167-172. New York: A.S.M.E.

Bishop, K. A., Ffowcs Williams, J. E. and Smith, W. (1971). On the noise sources of unsuppressed high speed jet. **J. Fluid Mech. 50**, 21-31.

Blackwelder, R. F. and Kaplan, R. E. (1972). Intermittent structures in turbulent boundary layers. NATO-AGARD CP 93. Tech. Ed. and Reprod., London.

Blackwelder, R. F. and Kaplan, R. E. (1976). On the wall structure of the turbulent boundary layer. **J. Fluid Mech. 76**, 89-112.

Bradshaw, P. Ferriss, D. H. and Johnson, R. F. (1964). Turbulence in the noise-producing region of a circular jet. **J. Fluid Mech. 19**, 591-624.

Bradshaw, P. Ferriss, D. H. and Johnson, R. F. (1964). Turbulence in the noise-producing region of a circular jet. **J. Fluid Mech. 19**, 591-624.

Bradshaw, P. (1966). The effect of initial conditions on the development of free shear layer. **J. Fluid Mech. 26**, 225-236.

Briedenthal, Jr. R. (1982). Structure in turbulent mixing layers and wakes using a chemical reaction. **J. Fluid Mech. 158**, 489-509.

Broadwell, J. E. and Breidenthal, R. E. (1982). A simple model of mixing and chemical reaction in a turbulent shear layer. **J. Fluid Mech. 125**, 397-410.

Browand, F. K. and Latigo, B. O. (1979). Growth of the two-dimensional mixing from a turbulent and non-turbulent boundary layer. **Phys. Fluids 22**, 1011-1019.

Browand, F. K. (1980). The mixing layer - A physical description. Invited Lecture. **33rd Annual Meeting, Division of Fluid Dynamics, Am. Phys. Soc.**, Cornell University.

Browand, F. K. and Troutt, T. R. (1980). A note in spanwise structure in the two-dimensional mixing layer. **J. Fluid Mech. 97**, 771-781.

Browand, F. K. and Troutt, T. R. (1984). The turbulent mixing layer: geometry of large vorticies. **J. Fluid Mech. 158**, 489-509.

Bradshaw, P. (1966). The effect of initial conditions on the development of free shear layer. **J. Fluid Mech. 26,** 225-236.

Briedenthal, Jr. R. (1982). Structure in turbulent mixing layers and wakes using a chemical reaction. **J. Fluid Mech. 158**, 489-509.

Broadwell, J. E. and Breidenthal, R. E. (1982). A simple model of mixing and chemical reaction in a turbulent shear layer. **J. Fluid Mech. 125**, 397-410.

Browand, F. K. and Latigo, B. O. (1979). Growth of the two-dimensional mixing from a turbulent and non-turbulent boundary layer. **Phys. Fluids 22**, 1011-1019.

Browand, F. K. (1980). The mixing layer - A physical description. Invited Lecture. **33rd Annual Meeting, Division of Fluid Dynamics, Am. Phys. Soc.**, Cornell University.

Browand, F. K. and Troutt, T. R. (1980). A note in spanwise structure in the two-dimensional mixing layer. **J. Fluid Mech. 97,** 771-781.

Browand, F. K. and Troutt, T. R. (1984). The turbulent mixing layer: geometry of large vorticies. **J. Fluid Mech. 158,** 489-509.

Brown, G. and Roshko, A. (1971). The effect of density difference on the turbulent mixing layer, in **A.G.A.R.D. Conf. on Turbulent Shear Flows**, pp.

23/1-23/12. Conf. Proc. no. 93.

Brown, G. and Roshko, A. (1972). Structure of the turbulent mixing layer, in "Proc. 13th Int. Conf. Theor. Appl. Mech.", (E. Becker & G. K. Mikahilov, eds.). Springer-Verlag, Berlin.

Brown, G. and Roshko, A. (1974). On density effects and large structure in turbulent mixing layers, **J. Fluid Mech 64**, 775-816.

Cain, A. B., Reynolds, W. C. and Ferzigen, J. H. (1981). A three-dimensional simulation of transition and early turbulence in a time-developing mixing layer. Stanford Univ. Dept. Mech. Engrg. Rept. TF-14.

Cantwell, B. J. (1981). Organized notion in turbulent flow. **A. Rev. Fluid Mech. 13**, 457-515.

Carrier, G. F., Fendell, F. E. and Marble, F. E. (1975). The effect of strain rate on diffusion flames. **SIAM J. 28**, 463-4 .

Champagne, F. H., Harris, V. G. and Corrsin, S. (1970). experiments on nearly homogeneous turbulent shear flow. **J. Fluid Mech 41**, 81-139.

Corcos, G. M. and Sherman, F. S. (1984). The mixing layer: deterministic models of a turbulent flow. Part 1. Introduction and the two-dimensional flow. **J. Fluid Mech. 139**, 29-65.

Corcos, G. M. and Lin, S. J. (1984). The mixing layer: deterministic models of a turbulent flow. Part 2. The origin of the three-dimensional motion. **J. Fluid Mech. 139**, 67-95.

Corrsin, S. (1943). Investigations of flow in an axially symmetric heated jet of air. **N. A. C. A. Adv. Conf. Rep. No. 3123** (also W-94).

Couet, B. and Leonard, A. (1980). Mixing layer simulation by an improved three-dimensional vortex-in-cell algorithm.

Craik, A. D. D. (1971). Nonlinear resonant instability in boundary layers. **J. Fluid Mech. 50**, 393-413.

Craik, A. D. D. (1980). Nonlinear evolution and breakdown in unstable boundary layers. I. **Fluid Mech. 99**, 247-265.

Crighton, D. G. and Gaster, M. (1976). Stability of slowly diverging jet flow. **J. Fluid Mech. 77**, 397-413.

Crow, S. C. and Champagne, F. H. (1971). Orderly structure in jet turbulence. **J. Fluid Mech. 48**, 547-591.

Davis, P. O. A. L., Fisher, M. J. and Barratt, M. J. (1963). The characteristics of turbulence in the mixing region of a round jet. **J. Fluid Mech. 15**, 337-367. **(Corrigendum, 15**, 559).

Dryden, H. L. (1948). Recent advances in the mechanics of boundary layer flow. "Advances in Applied Mechanics", (R. von Mises and Th. von Karman, eds.), pp. 1-40. Academic Press, N.Y.

Einaudi, F. and Finnegan, J. J. (1981). The interaciton between an internal gravity wave and planetary boundary. Part I. The linear analysis. **Quart. J. R. Met. Soc. 107**, 793-806.

Elswick, Jr., R. C. (1971). Wave-induced Reynolds stress in turbulent shear layer instability. The Pennsylvania State University Ph.D. Thesis.

Favre-Marinet, M. and Binder, G. (1975). Structure des jets pulsants. L'Universite Scientifique et Medicale de Grenoble. Docteur-Ingenieur These.

Favre-Marinet, M. and Binder, G. (1979). Structure des jets pulsants. **J. Mec. 18**, 357-394.

Fiedler, H. E., Dziomba, B., Mensing, P. and Rosgen, T. (1981). Initiation, evolution and global consequences of coherent structures in turbulent shear flows, in "The Role of Coherent Structures in Modelling Turbulence and Mixing" (J. Jimenez, ed.), **Lecture Notes Phys. 136**, 219-251. Springer-Verlag, Berlin.

Fiedler, H. E. and Mensing, P. (1985). The plane turbulent shear layer with

periodic excitation. **J. Fluid Mech. 150**, 281-309.

Finnegan, J. J. and Einaudi, F. (1981). The intersection between an internal gravity wave and the planetary boundary layer. Part II. Effect of the wave on the turbulence structure. Quart. J. R. Met. Soc. **107**, 807-832.

Freymuth, P. (1966). On transition in a separated boundary layer. **J. Fluid Mech. 25**, 683-704.

Fua, D., Chimonas, Einaudi, F. and Zeman, O. (1982). An analysis of wave-turbulence interaction. J. Atmos. Sci. **39**, 2450-2463.

Gaster, M. (1962). A note on the relation between temporally-increasing and spatially-increasing disturbances in hydrodynamic stability. **J. Fluid Mech. 14**, 222-224.

Gaster, M. (1965). The role of spatially growing waves in the theory of hydrodynamic stability. **Progr. Aeron. Sci. 6**, 251-270.

Gaster, M. (1968). Growth of disturbances in both space and time. **Phys. Fluids 11**, 723-727.

Gaster, M. (1981). On transition to turbulence in boundary layers, in "Transition and Turbulence" (R. E. Meyer, ed.), pp. 95-112. Academic Press, N.Y.

Gaster, M., Kit, E. and Wygnanski, I. (1985). Large-scale structures in a forced

turbulent mixing layer. **J. Fluid Mech. 150**, 23-39.

Gatski, M. and Liu, J. T. C. (1977). Numerical solution for the large-scale coherent structure in a turbulent shear layer. **Bull. Am. Phys. Soc. 22**, 1284.

Gatski, T. B. and Liu, J. T. C. (1980). On the interactions between large-scale structure and fine-grained turbulence in a free shear flow. Part III. A numerical solution. **Phil. Trans. Royal Soc. Lond.** A **293**, 473-509.

Grant, H. L. (1958). The large eddies of turbulent motion. **J. Fluid Mech. 4**, 149-190.

Ho, C. M. and Huang, L. (1982). Subharmonics and vortex merging in mixing layers. J. Fluid Mech. 119, 443-473.

Ho, C.M. and Huerre, P. (1984). Perturbed free shear layers. **Ann. Rev. Fluid. Mech. 16**, 365-424.

Howe, M. S. (1986). On the absorption of sound by turbulence and other hydrodynamic flows, **in** "Recent Advances in Aeroacoustics" (A. Krothapalli and C. A. Smith, eds.), pp. 53-83. Springer-Verlag, Berlin.

Huang, L. S. (1985). Small scale transition in a two-dimensional mixing layer. University of Southern California Ph.D. Thesis.

Hunt, J. C. R. (1973). A theory of turbulent flow round two-dimensional

bluff bodies. **J. Fluid Mech. 61**, 625-706.

Hussain, A. K. M. F. and Reynolds, W. C. (1970a). The mechanics of an organized wave in turbulent shear flow. **J. Fluid Mech. 41**, 241-258.

Hussain, A. M. F. K. (1983). Coherent structures - reality and myth. **Phys. Fluids 26**, 2816-2850.

Hussain, A. M. F. K. and Reynolds, W. C. (1970a). The mechanics of an organized wave in turbulent shear flow. **J. Fluid Mech. 41**, 241-258.

Hussain, A. M. F. K. and Reynolds, W. C. (1970b). The mechanics of a perturbation wave in turbulent shear flow. Stanford University, Dept. Mech. Eng. Thermosciences, Div. Rep. FM-6.

Hussain, A. M. F. K. and Zaman, K. B. M. Q. (1980). Vortex paving in a circular jet under controlled excitation. Part 2. Coherent structure dynamics. **J. Fluid Mech. 101**, 493-544.

Jimenez J. (1983). A spanwise structure in the plane shear layer. **J. Fluid Mech. 132**, 319-336.

Kaptanoglu, H. T. (1984). Coherent mode interactions in a turbulent shear layer. Brown University, Division of Engineering, Sc.M. Thesis.

Kelly, R. E. (1967). On the stability of an inviscid shear layer which is periodic

in space and time. **J. Fluid Mech. 27**, 657-689.

Kendall, J. M. (1970). The turbulent boundary layer over a wall with progress surface waves. **J. Fluid Mech. 41**, 259-281.

Kim, J. (1982). On the structure of wall-bounded turulent flows. **Phys. Fluids 26**, 2088-2097.

Kim, J. (1983). On the structure of wall-bounded turbulent flows. **Phys. Fluids 26**, 2088-2097.

Kim, J. (1984). Vortical structures associated with the bursting even. **Bull. Am. Phys. Soc.** 1520. (Paper AH-1, 37th Annual Division of Fluid Dynamics Meeting, Am. Phys. Soc., Brown University, 18-20 November 1984).

Klassen, G. P. and Peltier, W. R. (1985). The onset of turbulence in finite-amplitude Kelvin-Helmholtz billows. **J. Fluid Mech. 155**, 1-35.

Knight, D. D. (1979). Numerical investigation of large scale structures in the turbulent mixing layer. Proc. Sixth Biennial Symp. Turbulence, 241-249. Univ. Missouri-Rolla.

Knight, D. D. and Murray, B. T. (1981). Theoretical investigation of interaction and coalescence of large scale structures in the turbulent mixing layer. **in** "The Role of Coherent Structures in Modelling Turbulence and Mixing"

(J. Jimenez, ed.), Lect. Notes Phys. **136**, 62-92. Springer-Verlag, Berlin.

Ko, D. R. S. Kubota, T. and Lees, L. (1970). Finite disturbance effect in the stability the staility of laminar incompressible wake behind a flat plate. **J. Fluid Mech. 40**, 315-341.

Konrad, J. H. (1977). An experimental investigation of mixing in two-dimensional turbulent shear flows with applications to diffusion-limited chemical reactions. Ph.D. Thesis, California Institute of Technology. (Also as Project SQUID Tech. Rep. CIT-8-PU (1976).)

Kovasznay, L. S. G. (1970). The turbulent boundary layer. **Ann. Rev. Fluid Mech. 2**, 95.

Kovasznay, L. S. G. Kibens, V. and Blackwelder, R. F. (1970). Large-scale motion in the intermittent region of a turbulent boundary layer. **J. Fluid Mech. 41**, 283-325.

Landahl, M. T. (1967). A wave-guide model for turbulent shear flow. **J. Fluid Mech. 29**, 441-459.

Laufer, J. (1975). New trends in experimental turbulence research. **Ann. Rev. Fluid Mech. 7**, 307-326.

Launder, B. E., Reece, G. J. and Rodi, W. (1975). Progress in the development of a Reynolds-stress turbulence closure. **J. Fluid Mech. 68**, 537-566.

Lee, S. S. and Liu, J. T. C. (1985). Multiple mode interactions in a round jet. **Bull. Am. Phys. Soc. 30**, 1715.

Legner, H. H. and Finson, M. L. (1980). On the stability of fine-scaled turbulent free shear flows. **J. Fluid Mech. 100**, 303-319.

Liepmann, H. W. (1952). Aspects of the turbulence problem. Part II. Z. Angew. **Math. Phys. 3**, 407-426.

Liepmann, H. W. (1962). Free turbulent flows. In **Mecanique de la turbulence**, Int. Symp. Nat. Sci. Res. Centre, Marseille 1961, pp. 211-227, CNRS, Paris.

Lighthill, M. J. (1952). On sound generated aerodynamically. I. General theory. **Proc. Roy. Soc. A 211**, 564-587.

Lighthill, M. J. (1962). Sound generated aerodynamically. (The Bakerian Lecture, 1961.) **Proc. Roy. Soc. A 267**, 147-182.

Lighthill, M. J. (1969). The outlook for a wave theory of turbulent shear flow. **in** "Proc. Comp. Turbulent Boundary Layers", vol. 1 (S. J. Kline, M. V. Morkovin, G. Sovran and D. J. Cockrell, eds.), p. 511. Stanford University Press.

Lin, C. C. (1955). "The Theory of Hydrodynamic Stability". Cambridge University Press.

Lin, S. J. and Corcos, G. M. (1984). The mixing layer: deterministic models of a turbulent flow. Part 3. The effect of plane strain on the dynamics of streamwise vorticies. **J. Fluid Mech. 141**, 139-178.

Liu, J. T. C. (1971a). On eddy-Mach wave radiation source mechanism in the jet noise problem. **A.I.A.A. Paper** no. 71-150.

Liu, J. T. C. (1971b). Nonlinear development of an instability wave in a turbulent wake. **Phys. Fluids 14**, 2251-2257.

Liu, J. T. C. (1974a). Developing large-scale wavelike eddies and the near jet noise field. **J. Fluid Mech. 62**, 437.

Liu, J. T. C. (1974b). A nonlinear instability description of the coherent structure in free turbulent shear flows. Colloquium on Coherent Structures in Turbulence, Southampton, England 26-29 March, 1974. (See Corrigendum, **J. Fluid Mech.** (1976) **74**, 797.

Liu, J. T. C. and Merkine, L. (1976). On the interactions between large-scale structure and fine-grained turbulence in a free shear flow. Part I. The development of temporal interactions in the mean. **Proc. Royal Soc. Lond.** A **352**, 213-247.

Liu, J. T. C. (1981). Interactions between large-scale coherent structures and

fine-grained turbulence in free shear flows, **in** "Transitions and Turbulence" (R. E. Meyer, ed.), pp. 167-214. Academic Press, New York.

Liu, J. T. C. and Nikitopoulos, D. E. (1982). Mode interactions in developing shear flows. **Bull. Am. Phys. Soc. 27**, 1192.

Liu, J. T. C. and Kaptanoglu, H. T. (1984). Multiple-mode interactions in a turbulent mixing layer. Abstract in **Bull. Am. Phys. Soc. 29**, 155 (Paper DH-1, 37th Annual Division Fluid Dynamics Meeting/Am. Phys. Soc., Brown University, 18-20 November 1984).

Lumley, J. L. (1967). The structure of inhomogeneous turbulent flows, **in** "Proc. Int. Coll. Atmospheric Turbulence and Radio Wave Propagation" (A. M. Yaglom and V. L. Tatarsky, eds.), p. 166, Nauka Press, Moscow.

Lumley, J. L. (1970). Toward a turbulent constitutive relation. **J. Fluid Mech. 41**, 413-434.

Lumley, J. L. (1978). Computational modeling of turbulent flows. **Ad. Appl. Mech. 18**, 128-176.

MacPhail, D. C. (1941). Turbulence in a distorted passage and between rotating cylinders. Ph.D. dissertation, University of Cambridge. (Also in **Proc. 6th Int. Congr. Appl. Mech.**, Paris, 1946.)

Malkus, W. V. R. (1956). Outline of a theory of turbulent shear flow. **J. Fluid**

Mech. 1, 521-539.

Mankbadi, R. and Liu, J. T. C. (1981). A study of the interactions between large-scale coherent structures and fine-grained turbulence in a round jet. **Phil. Trans. Royal Society London**, A **298**, 541-602.

Mankbadi, R. and Liu, J. T. C. (1984). Sound generated aerodynamically revisited: Large-scale structures in a turbulent jet as a source of sound. **Phil. Trans. Royal Soc. Lond.** A **311**, 183-317.

Mankbadi, R. (1985). On the interaction between fundamental and subharmonic instability waves in a turbulent round jet. **J. Fluid Mech. 160**, 385-419.

Marble, F. E. and Broadwell, J. E. (1977). The coherent flame model for turbulent chemical reacitons. Project SQUID Tech. Rep. No. TRW-9-PU.

Merkine, L. (1974). Nonlinear interactions of the large-scale coherent structure and turbulence in a free shear flow. Brown University, Division of Engineering Ph.D. thesis, Part III.

Merkine, L. and Liu, J. T. C. (1975). On the development of noise producing large-scale wavelike eddies in a turbulent jet. **J. Fluid Mech. 70**, 353-368.

Metcalfe, R. W., Orszag, S. A., Bracket, M. E., Menon, S. and Riley, J. J. (1985). Secondary instability of a temporally growing mixing layer. **J. Fluid Mech.**

(submitted).

Michalke, A. (1971). Instabilitat eines kompressiblen runden Freistrahls under Berucksichtigung des Einflusses der Strahlgrenzschichtidcke. Z. **Flugwissenchaften 19**, 319-328. (English translation as NASA TM-75190, 1977).

Miksad, R. W. (1972). Experiments on the nonlinear stages of free shear-layer transition. **J. Fluid. Mech. 56**, 695-719.

Miksad, R. W. (1973). Experiments on nonlinear interactions in the transition of a free shear layer. **J. Fluid Mech. 59**, 1-21.

Moffatt, H. K. (1967). The interaction of turbulence with strong wind shear **in** "Proc. Int. Coll. Atmospheric Turbulence and radio Wave Propagation" (A. M. Yaglom and V. L. Tatarsky, eds.), p. 139. Nauka Press, Moscow.

Moffatt, H. K. (1969). Waves versus eddies **in** "Proc. Comp. Turbulent Boundary Layers", vol. 1 (S. J. Kline, M. V. Morkovin, G. Sovran and D. J. Cockrell, eds.), p. 495. Stanford University Press.

Moin, P. (1984). Hairpin vorticies in wall-bounded turbulent flows. **Bull. Am. Physc. Soc. 29**, 1520. (Paper AH-2, 37th Annual Division of Fluid Dynamics Meeting, Am. Phys. Soc., Brown University, 198-20 November

1984).

Mollo-Christensen, E. (1967). Jet noise and shear flow instability seen from an experimenter's viewpoint. **A.S.M.E. J. Appl. Mech.** E **89**, 1-7.

Mollo-Christensen, E. (1971). Physics of turbulent flow. **A.I.A.A. J. 9**, 1217-1228.

Mollo-Christensen, E. (1973). Intermittency in large-scale turbulent flows. In. **A. Rev. Fluid Mech. 5**, 101-118.

Murray, B. T. (1980). Numerical simulation of large scale coherent structure interaction in the two-dimensional mixing layer. Rutgers University Dept. Mech. Aerospace Engineering M.Sc. thesis.

Nikitopoulos, D. E. (1982). Nonlinear interactions between two instability waves in a developing shear layer. Brown University, Divison of Engineering Sc.M. Thesis, Providence.

Nikitopoulos, D. E. and Liu, J. T. C. (1984). Triple-mode interactions in a developing shear layer. **Bull. Am. Phys. Soc. 29**, 1548.

Nikitopoulos, D. E. and Liu, J. T. C. (1986). Nonlinear binary-coherent mode interactions in a developing mixing layer. (To be published).

Oster, D. and Wygnanaski, I. (1982). The forced mixing layer between parallel streams. **J. Fluid Mech. 123**, 91-130.

Pai, S. I. (1939). Turbulent flow between rotating cylinders. California Institute of Technology Ph.D. thesis. (Also as 1943. N. A. C. A. Tech. Note, no. 892).

Papailiou, D. D. and P. S. Lykoudis (1974). Turbulent vortex streets and the entrainment mechanism of the wake. **J. Fluid Mech. 62**, 11-31.

Patnaik, P. C., Sherman, F. S. and Corcos, G. M. (1976). A numerical simulation Kelvin-Helmholtz waves of finite amplitude. **J. Fluid Mech. 73**, 215-240.

Pedlosky, J. (1979). "Geophysical Fluid Dynamics". Springer-Verlag, Berlin.

Pierrehumbert, R. T. and Widnall, S. G. (1982). The two- and three-dimensional instabilities of a spatially periodic shear layer. **J. Fluid Mech. 114**, 59-82.

Phillips, O. M. (1967). The maintenance of Reynolds stress in turbulent shear flow. **J. Fluid Mech. 27**, 131-144.

Phillips, O. M. (1969). Shear-flow turbulence. **A. Rev. Fluid Mech. 1**, 245-264.

Quinn, M. C. and Liu, J. T. C. (1985). The interaction of sound with wall turbulent shear layers. **Bull. Am. Phys. Soc. 30**, 1743 (paper EB-3).

Quinn, M. C. and Liu, J. T. C. (1986). Internal waves and turbulence in a stratified fluid - their mutual interactions. IUTAM Symposium in Fluid Mechanics in the Spirit of G. I. Taylor. Cambridge University, 24-28

March 1986.

Reynolds, O. (1895). On the dynamical theory of incompressible viscous fluids and the determination of the criterion. **Phil. Trans. R. Soc. Lond.** A **186**, 123-164.

Reynolds, W. C. and Tiederman, W. G. (1967). Stability of turbulent channel flow, with application to Malkus' theory. **J. Fluid Mech. 27**, 253-272.

Reynolds, W. C. (1972). Large-scale instabilities of turbulent wakes. **J. Fluid Mech. 54**, 481-488.

Reynolds, W. C. and Hussain, A. K. M. (1972). The mechanics of an organized wave in turbulent shear flow. 3. Theoretical models and comparisons with experiments. **J. Fluid Mech. 54**, 263-288.

Reynolds, W. C. (1976). Computations of turbulent flows. **Ann. Rev. Fluid Mech. 8**, 183-208.

Riley, J. J., Metcalfe, R. W. and Weissman, M. A. (1981). Direct numerical simulations of homogeneous turbulence in density-stratified fluids, **in** "Nonlinear Properties of Internal Waves (B. J. West, ed.), pp. 79-112. Am. Inst. Phys., New York.

Roshko, A. (1952). On the development of turbulent wakes from vortex streets.

California Institute of Technology Thesis.

Roshko, A. (1954). On the devleopment of turbulent wakes from vortex streets. **N.A.C.A. Rep.**, 1191.

Roshko, A. (1961). Experiments on the flow past a circular cylinder at very high Reynolds number. **J. Fluid Mech. 10**, 356-366.

Roshko, A. (1976). Structure of turbulent shear flows: a new look. (Dryden Research Lecture). **A.I.A.A. J. 14**, 1349-1357.

Roshko, A. (1981). The plane mixing layer: flow visualizaiton results and three-dimensional effects **in** "The Role of Coherent Structures in Modelling Turbulence and Mixing" (J. Jimenez, ed.). Springer-Verlag, Berlin.

Sato, H. and Kuriki, K. (1961). The mechanism of transition in the wake of a thin flat plate placed parallel to a uniform flow. **J. Fluid Mech. 11**, 321-352.

Schubauer, G. B. and Skramstad, H. K. (1948). Laminar boundary layer oscillations and transition on a flat plate. **NACA Rep.** no. 909.

Stillinger, Helland, K. N. and Van Atta, C. W. (1983). Experiments on the transition of homogeneous turbulence to internal waves in a stratified fluid. **J. Fluid Mech. 131**, 91-122.

Stuart, J. T. (1958). On the nonlinear mechanics of hydrodynamic stability. **J. Fluid Mech. 4**, 1-21.

Stuart, J. T. (1960). On the nonlinear mechanics of wave disturbances in stable and unstable parallel flows. Part 1. The basic behavior in plane Poiseuille flow. **J. Fluid Mech. 9, 353-370.**

Stuart, J. T. (1962a). Nonlinear effects in hydrodynamic stability, in **Proc. Xth Int. Congr. Appl. Mech., Stresa, 1960.**, pp. 63-97. Elsevier, Amsterdam.

Stuart, J. T. (1962b). On the three-dimensional nonlinear effects in the stability of parallel flow **in** "Advances in Aeronautical Sciences", vol. 3, pp. 121-142. Pergamon, London.

Stuart, J. T. (1967). On finite amplitude oscillations in laminar mixing layers. **J. Fluid Mech. 29**, 417-440.

Stuart. J. T. (1971a). Nonlinear stability theory. **A. Rev. Fluid Mech. 3**, 347-370.

Stuart, J. T. (1971b) . Stability problems in fluids, **in** "Mathematical Problems in Geophysical Sciences", 1. Geophysical Fluid Dynamics (W. H. Reid, ed.), pp. 139-155. Am. Math. Soc., Providence, R.I..

Sykes, R. I. and Lewellen, W. S. (1982). A numerical study of breaking

Kelvin-Helmholtz billows using a Reynolds-stress turbulence closure model. **J. Atmos. Sci. 39**, 1506-1520.

Tennekes, H. and Lumley, J. L. (1972). "A First Course in Turbulence." MIT Press, Cambridge.

Thomas, A. S. W. and Brown, G. L. (1977). Large structure in a turbulent boundary layer, **in Proc. 6th Australasian Hydraulics and Fluid Mechanics Conference**, pp 407-410, Adelaide, Australia.

Thorpe, S. A. (1971). Experiments on the instability of stratified shear flows-miscible fluids. **J. Fluid Mech. 46**, 299-319.

Townsend, A. A. (1947). Measurements in the turbulent wake of a cylinder. **Proc. R. Soc. Lond. A 190**, 551-561.

Townsend, A. A. (1956). "The Structure of Turbulent Shear Flow." Cambridge University Press (Second Edition, 1976).

Von Kármán, Th. (1938). Some remarks on the statistical theory of turbulence, in Proc. 5th Inst. Congress for Applied Mechanics, (J. P. Den Hartog and H. Peters, eds.), pp. 347-351. Wiley, N.Y. (1939).

Weisbrot, I. (1984). A highly excited turbulent mixing layer. Tel-Aviv University, Faculty of Engineering M.S. Thesis.

Williams, D. R. and Hama, F. R. (1980). Streaklines in a shear layer perturbed by two waves. **Phys. Fluids 23**, 442-447.

Willmarth, W. W. (1975). Structure of turbulence in boundary layers. **Adv. Appl. Mech. 15**, pp. 159-254.

Winant, C. D. and Browand, F. K. (1974). Vortex pairing: the mechanism of turbulent mixing layer growth at moderate Reynolds numbers. **J. Fluid Mech. 63**, 237-255.

Wygnanski, I. and Petersen, R. A. (1985). Coherent motion in excited free shear flows. **A. I. A. A. Paper no.** 85-0539.

APPENDIX

The integrals for the spatially developing plane turbulent mixing layer are explicitly defined here for completeness. These integrals are similar in form to certain of those that occur in the temporal problem except that there integrals involving the eigenfunctions depend on the local wavenumber. The dominant coherent mode here is also taken as two-dimensional and the spatial eigenfunctions are evaluated "locally" and depend on the local frequency parameter. The mean velocity profile and Reynolds stresses are taken to be of the form (5.8) and (5.9), respectively. Specifically, we have taken $u_i u_j \sim e^{-\zeta}$ and $U = 1 - R \tanh \zeta$, where $R = (U_{-\infty}-U_{\infty})/(U_{-\infty}+U_{\infty})$, $\zeta = z/\delta(x)$. Generalizations to other profiles are certainly possible. The local shear layer thickness $\delta(x)$ measured in terms of the initial shear layer thickness (δ_0), and is half of the maximum slope or mean vorticity thickness

$$\delta_\omega = \frac{1}{|\Omega|_{max}} \int_{-\infty}^{\infty} |\Omega| dz = \frac{U_{-\infty} - U_{\infty}}{|\partial U/\partial z|_{max}}$$

where $\Omega = -\partial U/\partial z$ (see Brown and Roshko 1974); $\delta(x)$ is also twice the momentum thickness (Winant and Browand 1974) for the hyperbolic tangent profile. The appropriate initial Reynolds number is $Re = \delta_0 \bar{U}/\nu$, where $\bar{U}$ is the average velocity $(U_{-\infty}+U_{\infty})/2$. All velocities are normalized by $\bar{U}$ and lengths by δ_0. The integrals involving the local eigenfunctions reflect the normalization defined by (5.4).

(1) Kinetic energy advection integrals

Mean flow:

$$\bar{I} = -\frac{1}{2}\left\{\int_{-\infty}^{0}(1 - R\tanh\zeta)[(1 - R\tanh\zeta)^2 - (1+R)^2]d\zeta\right.$$

$$\left. + \int_{0}^{\infty}(1 - R\tanh\zeta)[(1 - R\tanh\zeta)^2 - (1-R)^2]d\zeta\right\}$$

$$= (3 - 2\,\ell n\,2)R^2.$$

Coherent mode:

$$\tilde{I}(\delta) = 1 - R\int_{-\infty}^{\infty}\tanh\zeta(|\phi'|^2 + |\alpha\phi|^2)d\zeta.$$

In the binary mode interactions, I_2 is associated with eigenfunctions with subscript 2, I_1 with subscript 1. In general I_2 and I_1 do not change sign are very nearly "constant" and will be replaced by their respective meanvalue over the range of δ of interest.

Fine-grained turbulence:

$$I' = \frac{1}{\sqrt{\pi}}\int_{-\infty}^{\infty}(1 + \tanh\zeta)e^{-\zeta^2}\,d\zeta = 1.$$

(2) Fluctuation "production" integrals

Coherent mode:

$$\tilde{I}_{rs}(\delta) = 2R \int_{-\infty}^{\infty} \vartheta m(\alpha\phi\overline{\phi'}) \, \mathrm{sech}^2\zeta d\zeta$$

where $\bar{\phi}$ denotes the complex conjugate of ϕ. In the "damped" disturbance region $\vartheta m(\alpha\phi\bar{\phi}')$ changes sign and $I_{rs} < 0$. In binary mode interactions, I_{rs2} will be associatd with $\alpha_2,\phi_2,\ldots$ and I_{rs1} with $\alpha_1,\phi_1,\ldots$.

Fine-grained turbulence:

$$I'_{rs} = \frac{a_1 R}{\sqrt{\pi}} \int_{-\infty}^{\infty} e^{-\zeta^2} \mathrm{sech}^2\zeta = 0.7263 a_1 R.$$

(3) Viscous dissipation integrals

Mean flow:

$$\bar{I}_{\phi} = R^2 \int_{-\infty}^{\infty} \mathrm{sech}^4\zeta d\zeta = \frac{4\,R^2}{3} .$$

Coherent mode:

$$\tilde{I}_{\phi} = 2\left[|\alpha|^2 + 2\int_{-\infty}^{\infty} (|\phi''|^2 + |\alpha\phi'|^2)d\zeta\right].$$

Fine-grained turbulence:

$$I'_{\phi} = \frac{a_2}{2\pi^{3/2}} \int_{-\infty}^{\infty} e^{-3\zeta^2/2}\, d\zeta = 0.3066 a_2.$$

(4) Coherent mode-turbulence energy exchange integral

$$I_{wt}(\delta) = -2 \int_{-\infty}^{\infty} \mathcal{R}e[r_{xx}(-i\bar{\alpha}\overline{\phi'}) + r_{xz}(\bar{\phi}''+\bar{\alpha}^2\bar{\phi}) + r_{zz}(i\bar{\alpha}\overline{\phi'})]d\zeta.$$

(5) Binary-coherent mode energy exchange integral

$$I_{21} = I^{1}_{12} = 2 \int_{-\infty}^{\infty} \mathcal{I}m\left\{ e^{i\theta}\left[\phi_1'^2\bar{\alpha}_2\bar{\phi}_2' + \alpha_1\phi_1\phi_1'(\bar{\alpha}_2^2\bar{\phi}_2' + \bar{\phi}_2'') + \alpha_1^2\phi_1^2\bar{\alpha}_2\bar{\phi}_2' \right] \right\} d\zeta.$$

The integrands of I_{wt} and I_{21} are grouped to reflect "similar" stress-rates of strain products.

TABLE 1. Energy exchanges with fine-grained turbulence:

	n = 0	n = 1	n = 2
m = 1	$-\overline{r_{10ij}\frac{\partial u_{10i}}{\partial x_j}}$	$-\overline{r_{11ij}\frac{\partial u_{11i}}{\partial x_j}}$	
m = 2	$-\overline{r_{20ij}\frac{\partial u_{20i}}{\partial x_j}}$	$-\overline{r_{21ij}\frac{\partial u_{21i}}{\partial x_j}}$	$-\overline{r_{22i}\frac{\partial u_{22i}}{\partial x_j}}$

TABLE 2. Energy exhanges with mean flow:

	n = 0	n = 1	n = 2
m = 1	$-\overline{u_{10i}u_{10j}}\,\frac{\partial U_i}{\partial x_j}$	$-\overline{u_{11i}u_{11j}}\,\frac{\partial U_i}{\partial x_j}$	
m = 2	$-\overline{u_{20i}u_{20j}}\,\frac{\partial U_i}{\partial x_j}$	$-\overline{u_{21i}u_{21j}}\,\frac{\partial U_i}{\partial x_j}$	$-\overline{u_{22i}u_{22j}}\,\frac{\partial U_i}{\partial x_j}$

TABLE 3. Mode interaction mechanisms ϑ_{mn}:

	n = 0	n = 1	n = 2
m = 1	$A_{10}A_{21}A_{11}(I_{11}^{10} + I_{21}^{10})$ + $A_{10}^2 A_{20} I_{20}^{10}$	$A_{10}A_{21}A_{11}(-I_{11}^{10} + I_{21}^{11})$ + $A_{11}^2(A_{20}I_{20}^{11} + A_{22}I_{22}^{11})$	
m = 2	$-A_{10}^2 A_{20} I_{20}^{10} - A_{11}^2 A_{20} I_{20}^{11}$	$-A_{10}A_{11}A_{21}(I_{21}^{10} + I_{21}^{11})$	$-A_{11}^2 A_{22} I_{22}^{11}$

FIGURE CAPTIONS

Figure 1. Coherent mode and turbulence measurements on the jet centerline. ●: unforced, 0,Δ forced at Strouhal number St = 0.18 (Favre-Marinet and Binder 1979).

Figure 2. Measured streamwise development of fluctuation production mechanism along the line most intense mean velocity gradient in a turbulent mixing layer. x: coherent mode production mechanism; ●: overall production mechanism. (Fiedler, Dziomba, Mensing and Rösgen 1981).

Figure 3. Streamwise development of mixing layer thickness (Ho and Huang 1982, "Mode II").

Figure 4. Streamwise development of coherent mode energy (u-component only), corresponding to the shear layer thickness development in Figure 3 (Ho and Hunag 1982, "Mode II").

Figure 5. Evolution of energy exchange mechanisms between the large-scale structure and the mean flow ($\tilde{I}_p$) and the fine-grained turbulence ($I_{\ell t}$).

Figure 6. Evolution of large-scale coherent structure energy.

Figure 7. Evolution of fine-grained turbulence energy production (I_p'), viscous dissipation ($\overline{\phi'}$) and energy transfer from the large-sale coherent structure ($I_{\ell t}$).

Figure 8. Evolution of fine-grained turbulence energy.

Figure 9. Evolution of length scales: shear layer thickness (δ), fine-grained turbulence scale (L_ϵ), large-scale coherent structure closed streamline height (H).

Figure 10. Large-scale coherent structure streamlines at t = 1.50.

Figure 11. Large-scale coherent structure vorticity at t = 1.50.

Figure 12. Horizontal contribution of the phase-averaged turbulent kinetic energy and its dominant production mechanism at t = 1.50: (a) $\langle u'^2 \rangle/2$; (b) $-\langle u'w' \rangle \partial U/\partial z$.

Figure 13. Spanwise contribution of the phase-averaged turbulent kinetic energy and its "production" mechanism at t = 1.50: (a) $\langle v'^2 \rangle/2$; (b) $\langle p' \partial u'/\partial y \rangle$.

Figure 14. Locus of vectors representing the shape distribution of modulated turbulent stresses and coherent-mode rates of strain across the mixing layer. $\alpha = 0.4446$

(a) Streamwise normal stress and rate of strain;

(b) Shear stress and shear rates of strain;

(c) Vertical normal stress and rate of strain.

Figure 15. Relative contributions to the coherent mode and fine-grained turbulence energy exchange mechanisms. $\alpha = 0.4446$.

Figure 16. Coherent mode and fine-grained turbulence energy trajectories for the parallel flow model. $M_0 = 1$.

Figure 17. Evolution of coherent mode and fine-grained turbulence energy for a given wavenumber ($\alpha = 0.4446$), parallel flow model.

Figure 18. Illustrating that observed growth and contraction of observed shear thickness is attributed to wave disturbance energy extraction from and supply to the mean flow. exp: Weisbrot 1984, "theory": present explanation.

Figure 19. Evolution of u-contribution to the coherent mode energy, n = 2: fundamental; n = 1: subharmonics; comparison with measurements of Ho and Huang (1982) "Mode II" conditions.

Figure 20. Evolution shear layer thickness; comparison with measurements of Ho and Huang (1982) "Mode II" conditions.

Figure 21. Evolution of (a) coherent mode and fine-grained turbulence energy densities and (b) shear layer thickness for a "standard experiment".

Figure 22. Shear layer development at a weak initial turbulence level $E_0 = 10^{-10}$. (a) Energy densities; (b) Shear layer thickness.

Figure 23. Shear layer development at a weak initial turbulence level $E_0 = 10^{-8}$. (a) Energy densities; (b) Shear layer thickness.

Figure 24. Shear layer development at a moderate initial turbulence level $E_0 = 10^{-4}$. (a) Energy densities; (b) Shear layer thickness.

Figure 25. Shear layer development at a strong initial turbulence level $E_0 = 10^{-2}$. (a) Energy densities; (b) Shear layer thickness.

Figure 26. High Reynolds number effect in the shear layer development, Re = 500. (a) Energy densities; (b) Shear layer thickness.

Figure 27. "Moderate" Reynolds number effect in the shear layer development, Re = 100. (a) Energy densities; (b) Shear layer thickness.

Figure 28. "Low" Reynolds number effect in the shear layer development, Re = 40. (a) Energy densities; (b) Shear layer thickness.

Figure 29. "High" initial frequency effect on shear layer development, β_0 = 0.25. (a) Energy densities; (b) Shear layer thickness.

Figure 30. "Moderate" initial frequency effect on shear layer development, β_0 = 0.20. (a) Energy densities; (b) Shear layer thickness.

Figure 31. "Low" initial frequency effect on shear layer development, β_0 = 0.05. (a) Energy densities; (b) Shear layer thickness.

Figure 32. Two- and three-dimensional coherent mn-mode energy transfer mechanisms.

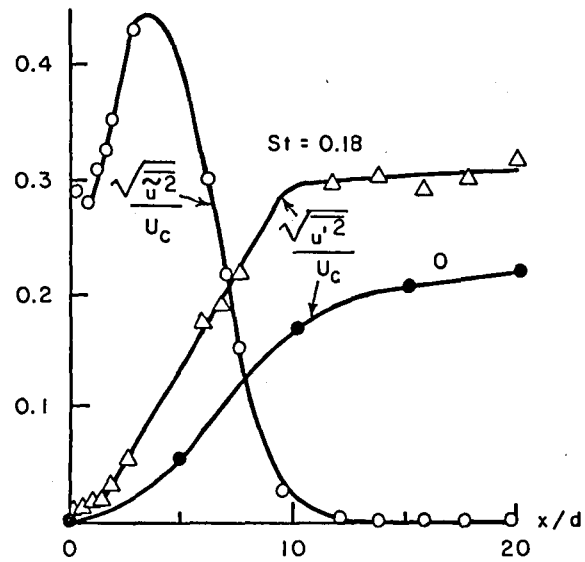

Fig. 1

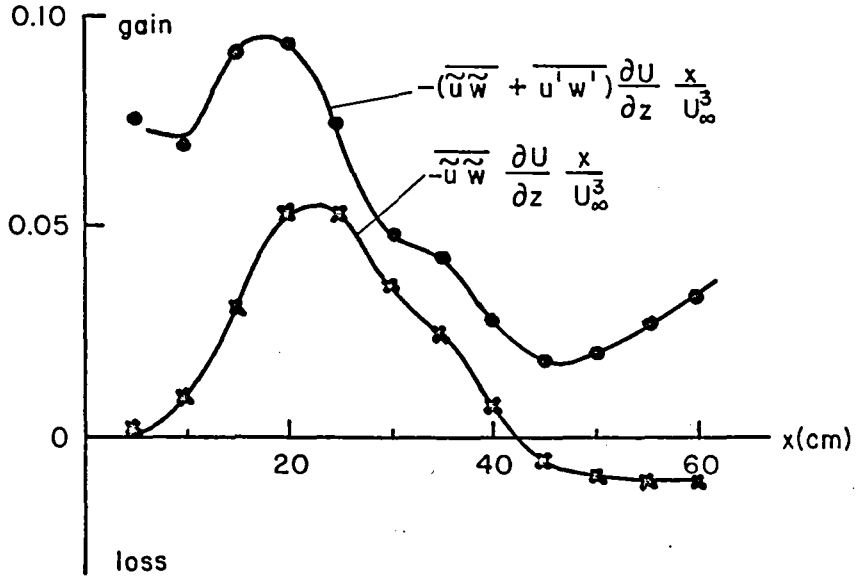
0.10
gain
$-(\overline{\tilde{u}\tilde{w}} + \overline{u'w'})\frac{\partial U}{\partial z}\frac{x}{U_\infty^3}$
$-\overline{\tilde{u}\tilde{w}}\frac{\partial U}{\partial z}\frac{x}{U_\infty^3}$
0.05
0
20
40
60
x(cm)
loss

Fig. 2

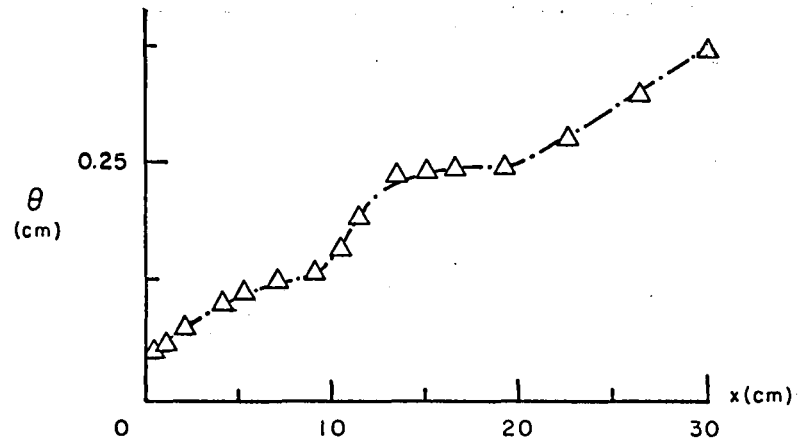

Fig. 6.3

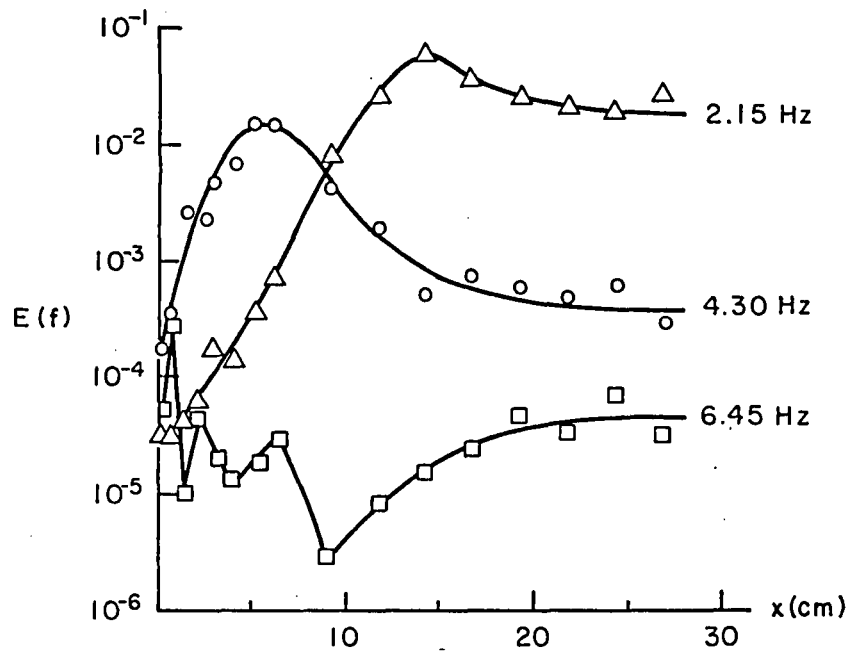

LIU: FIG. 4

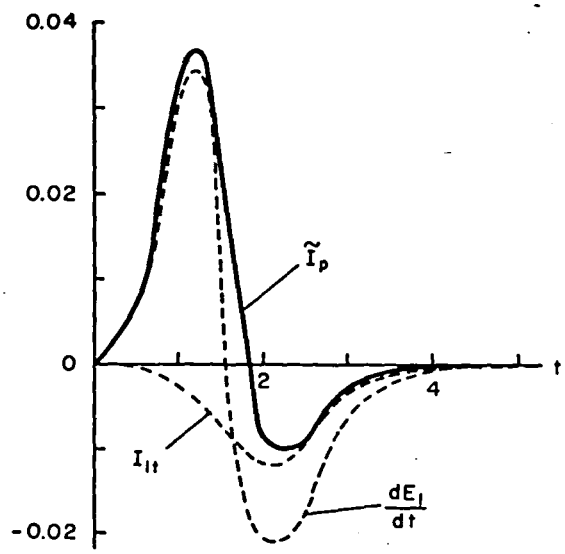

FIG. 5

← FIG. 5

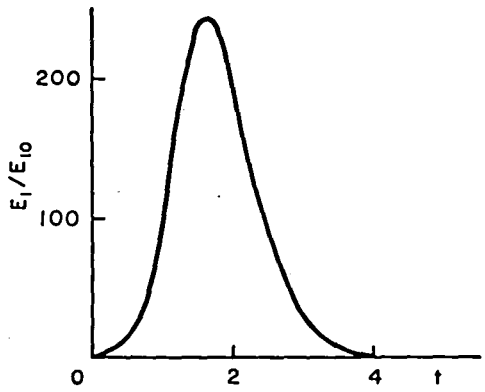

FIG. 6

← FIG. 6

LIU

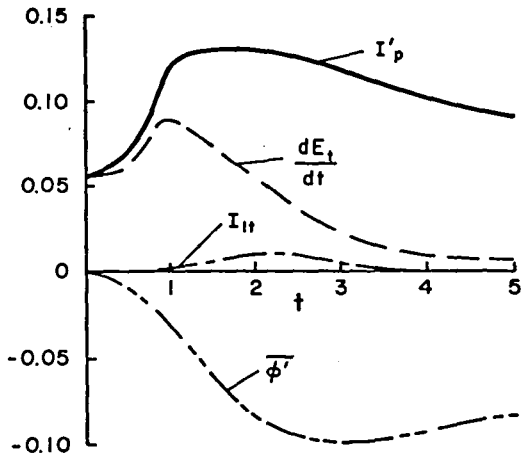

FIG. 7

← FIG. 7

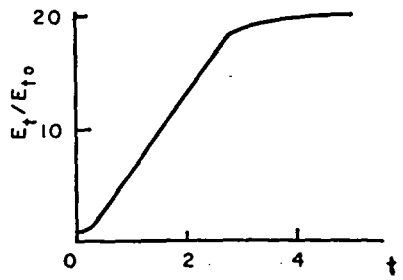

FIG. 8

← FIG. 8

Liu

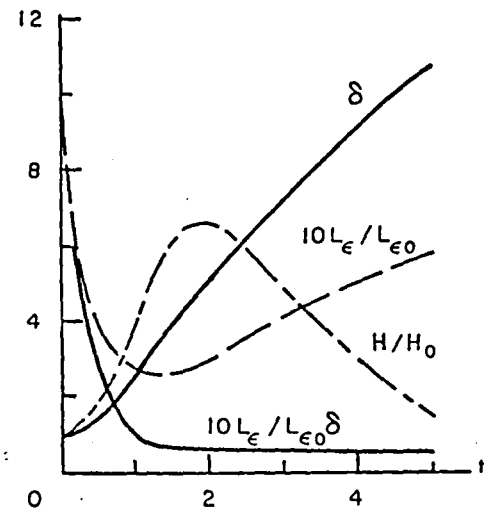

FIG. 9

LIU: FIG. 9

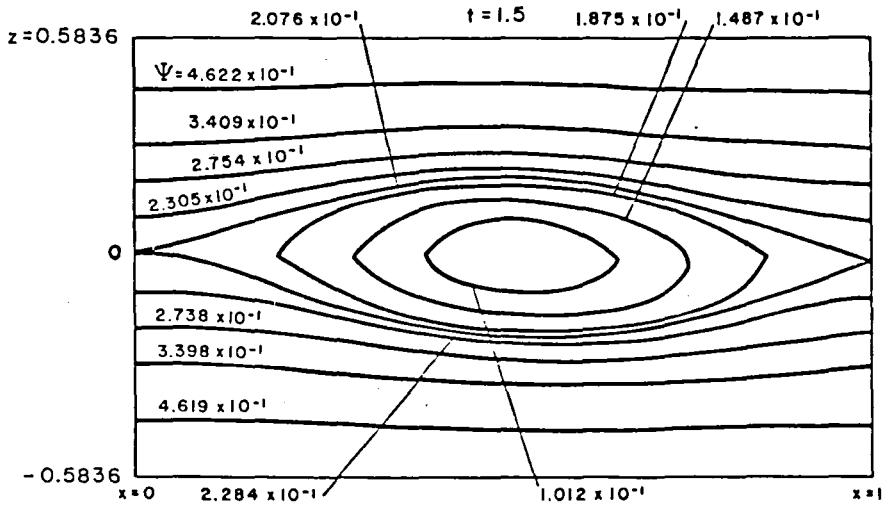

FIG. 10

LIU: FIG. 10

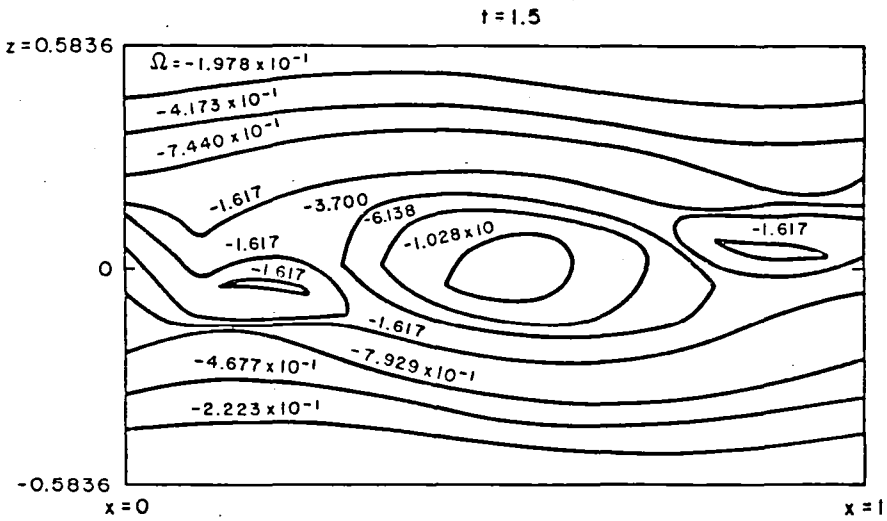

FIG. 11

LIU: FIG. 11

FIG.12b

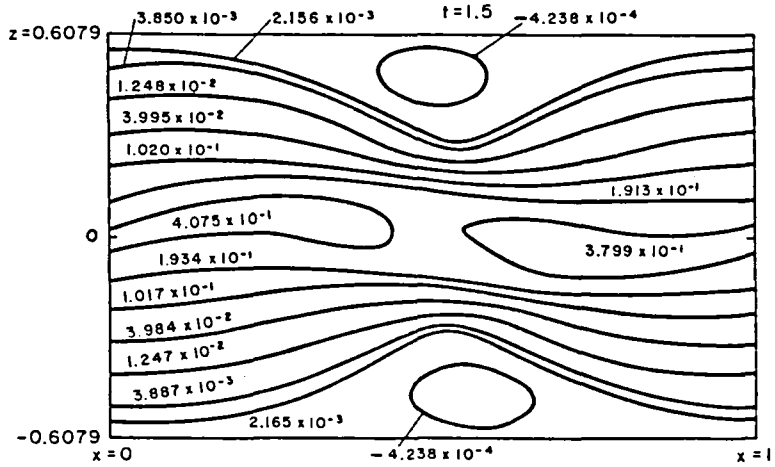

← FIG. 12(b)

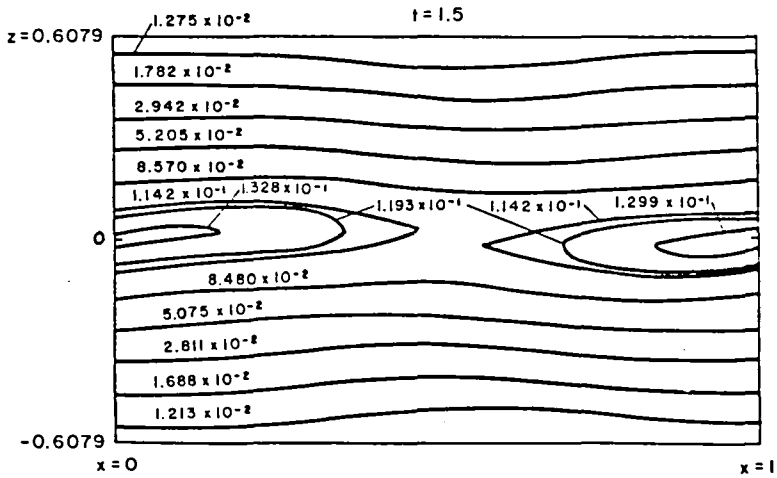

← FIG. 12(a)

FIG. 12a ↑

LIU

FIG. 13a

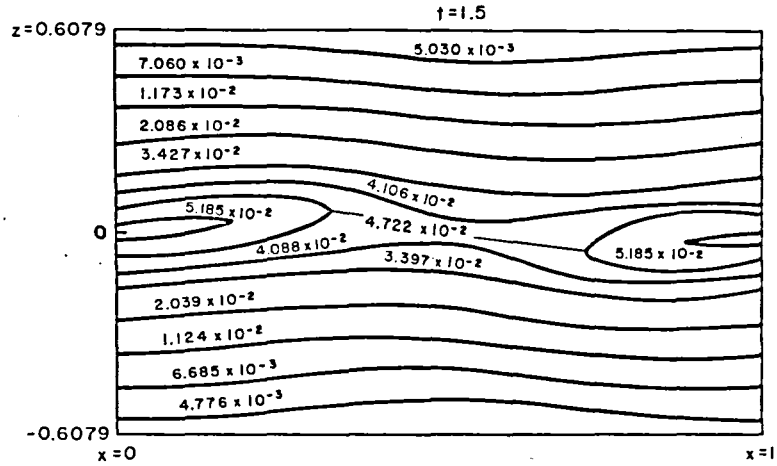

← FIG. 13(a)

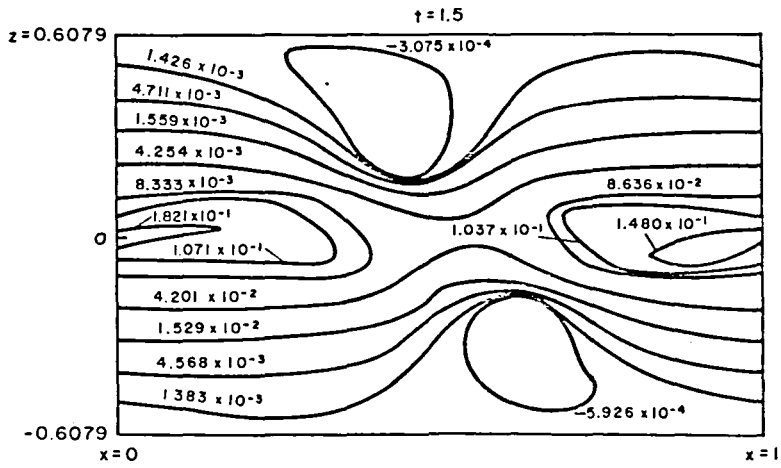

← FIG. 13(b)

FIG. 13b

LIU

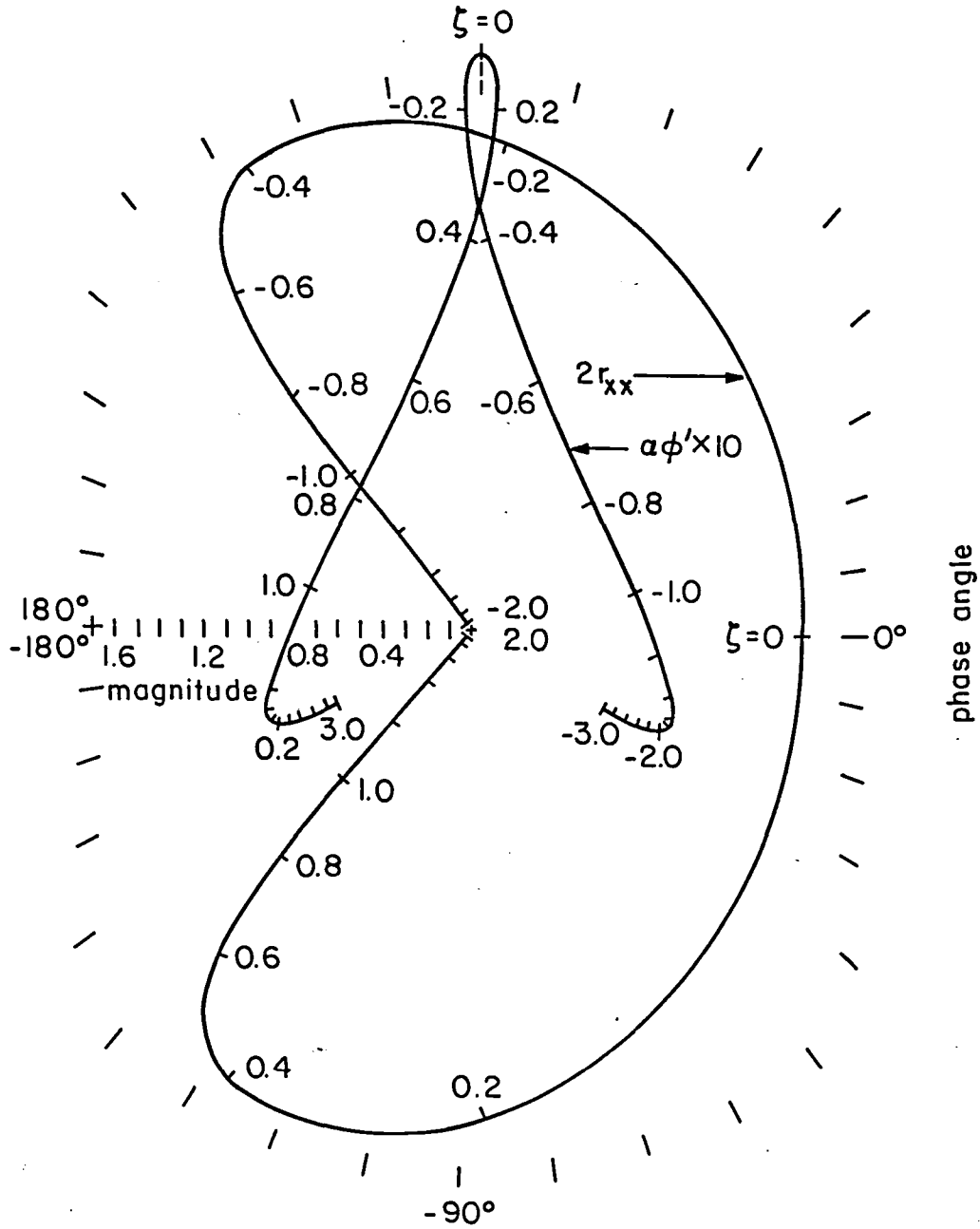
ζ=0
0.2
-0.2
-0.4
0.4
-0.6
0.6
-0.8
0.8
-1.0
1.0
2r_xx
aφ'×10
180°
-180°
1.6
1.2
0.8
0.4
magnitude
-2.0
2.0
3.0
-3.0
ζ=0
-0°
phase angle
-90°

Liu : FIG. 14.a

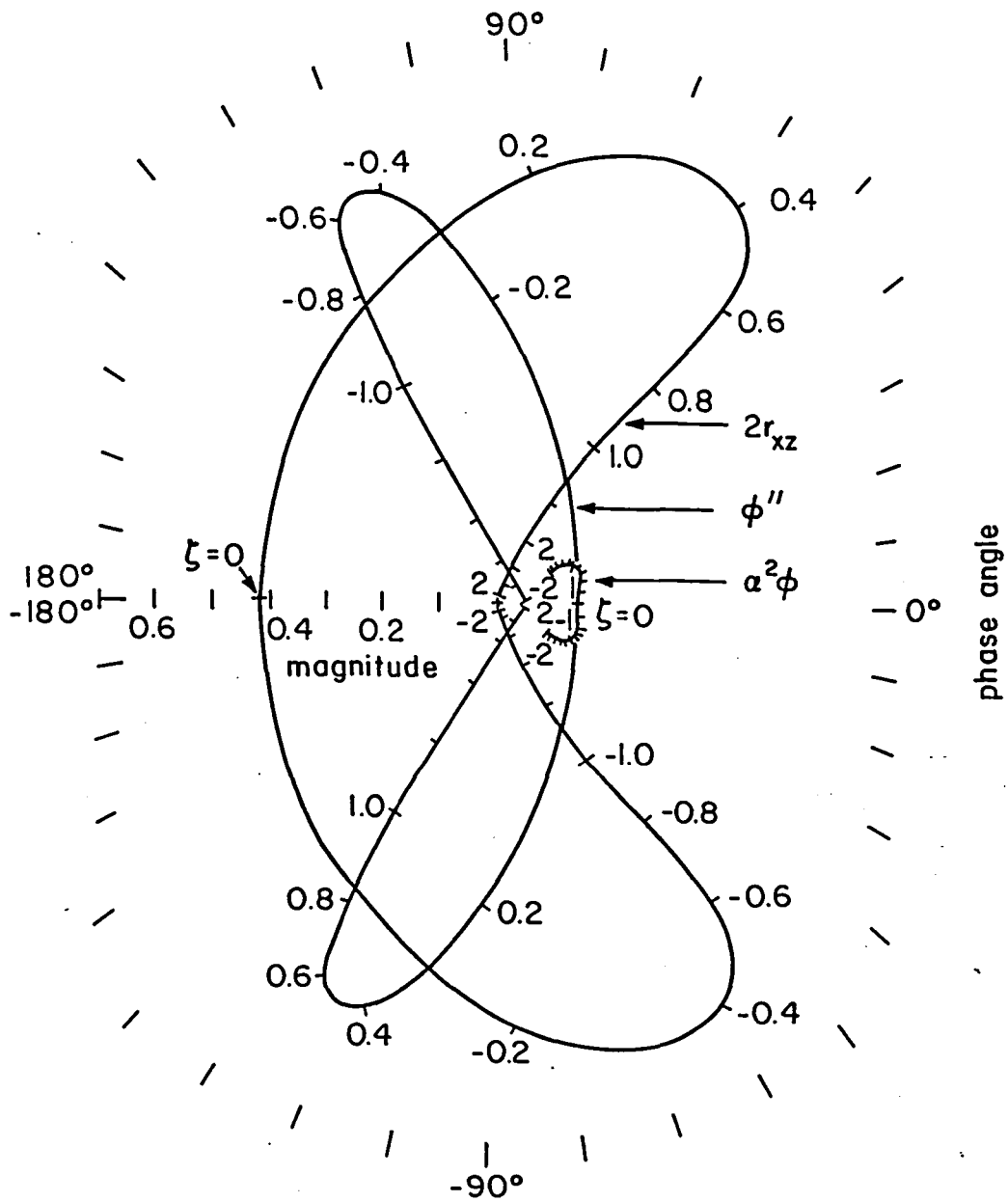
90°
-0.4
0.2
-0.6
0.4
-0.8
-0.2
0.6
-1.0
0.8
$2r_{xz}$
1.0
ϕ''
$\alpha^2\phi$
$\zeta=0$
180°
-180°
0.6
0.4
0.2
magnitude
$\zeta=0$
0°
phase angle
-1.0
1.0
-0.8
0.8
0.2
-0.6
0.6
0.4
-0.4
-0.2
-90°

LIU: FIG. 14b

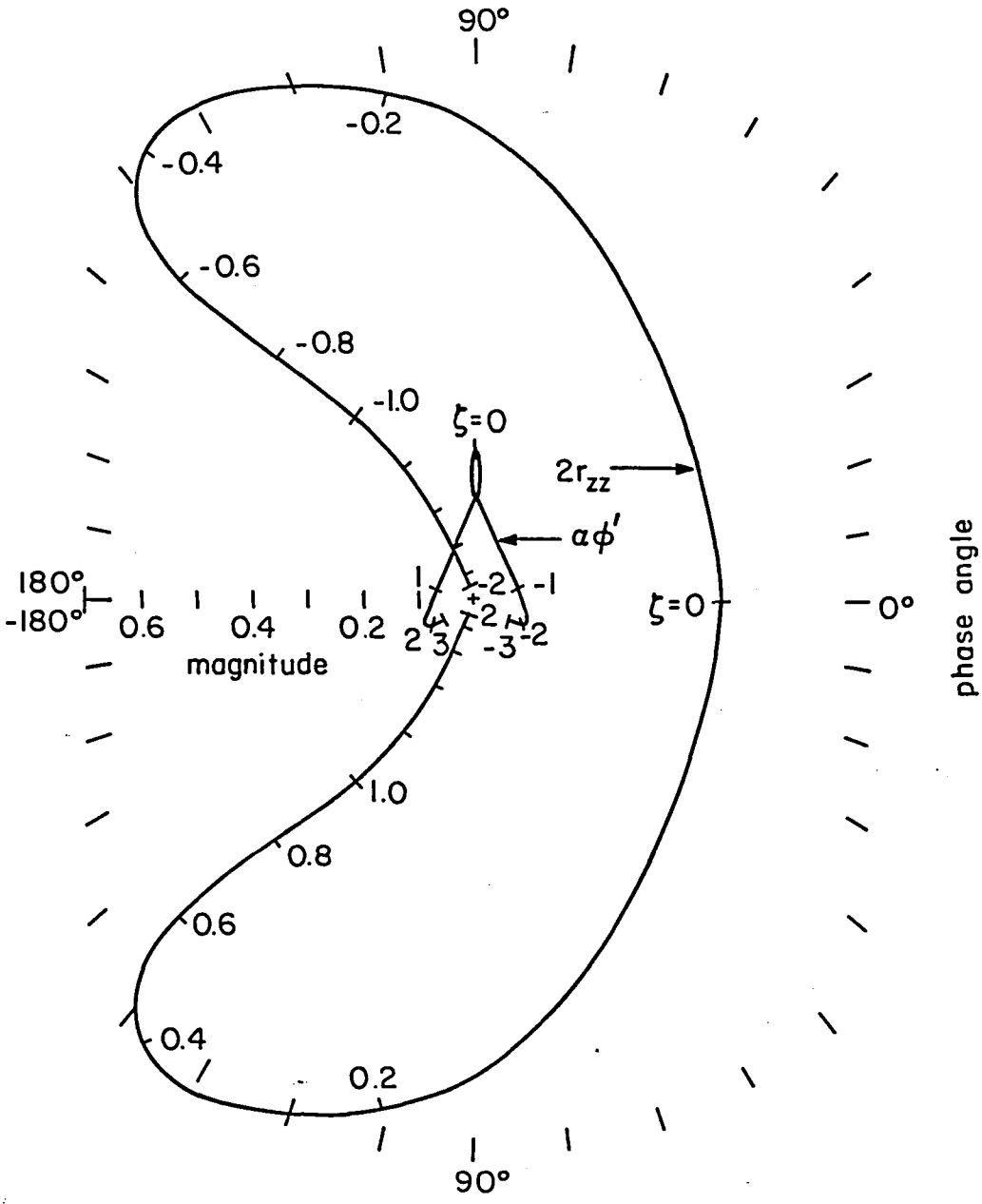
90°
-0.2
-0.4
-0.6
-0.8
-1.0
ζ=0
2r_zz
aφ'
180°
-180°
0.6
0.4
0.2
magnitude
-2
-1
2
3
-3
-2
ζ=0
0°
phase angle
1.0
0.8
0.6
0.4
0.2
90°

LIU: FIG. 14c

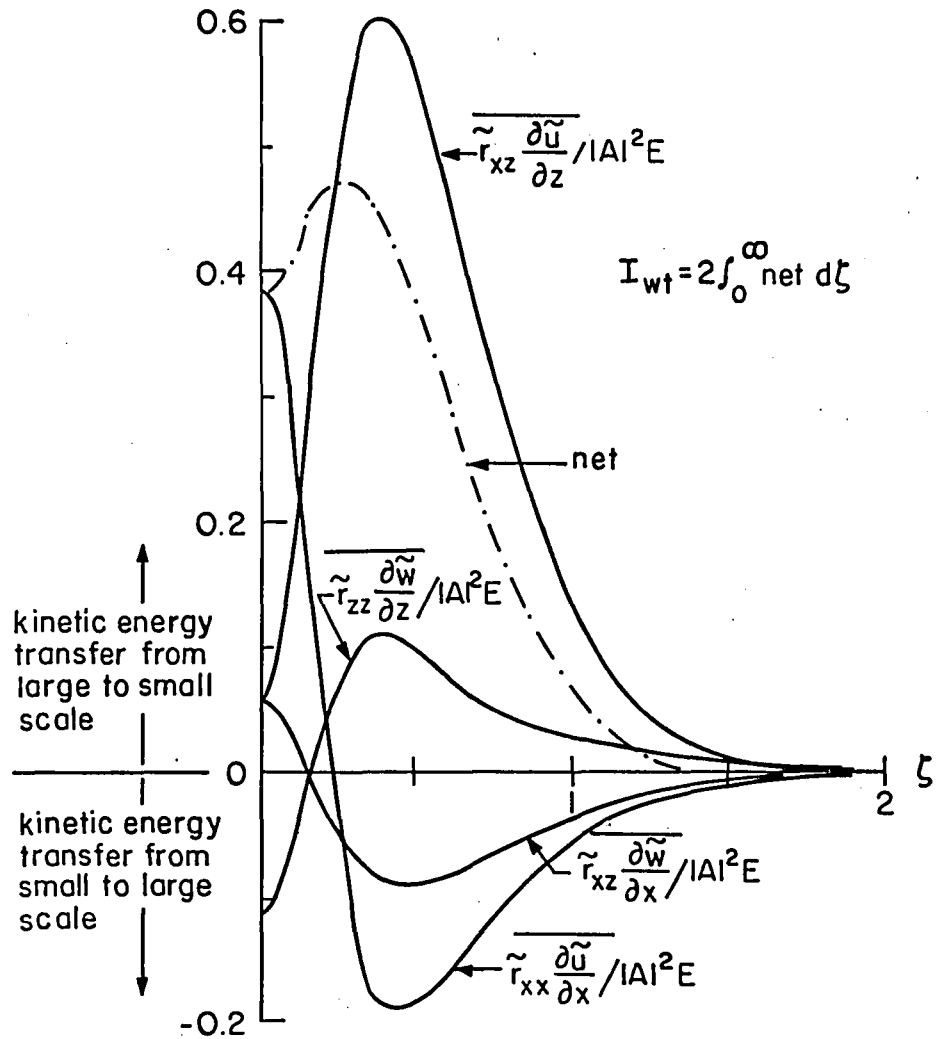
0.6
0.4
0.2
0
-0.2
2
ζ
$\overline{\tilde{r}_{xz}\frac{\partial\tilde{u}}{\partial z}}/|A|^2E$
$I_{wt}=2\int_0^\infty \text{net}\, d\zeta$
net
$\overline{\tilde{r}_{zz}\frac{\partial\tilde{w}}{\partial z}}/|A|^2E$
kinetic energy transfer from large to small scale
kinetic energy transfer from small to large scale
$\overline{\tilde{r}_{xz}\frac{\partial\tilde{w}}{\partial x}}/|A|^2E$
$\overline{\tilde{r}_{xx}\frac{\partial\tilde{u}}{\partial x}}/|A|^2E$

LIU: FIG. 15

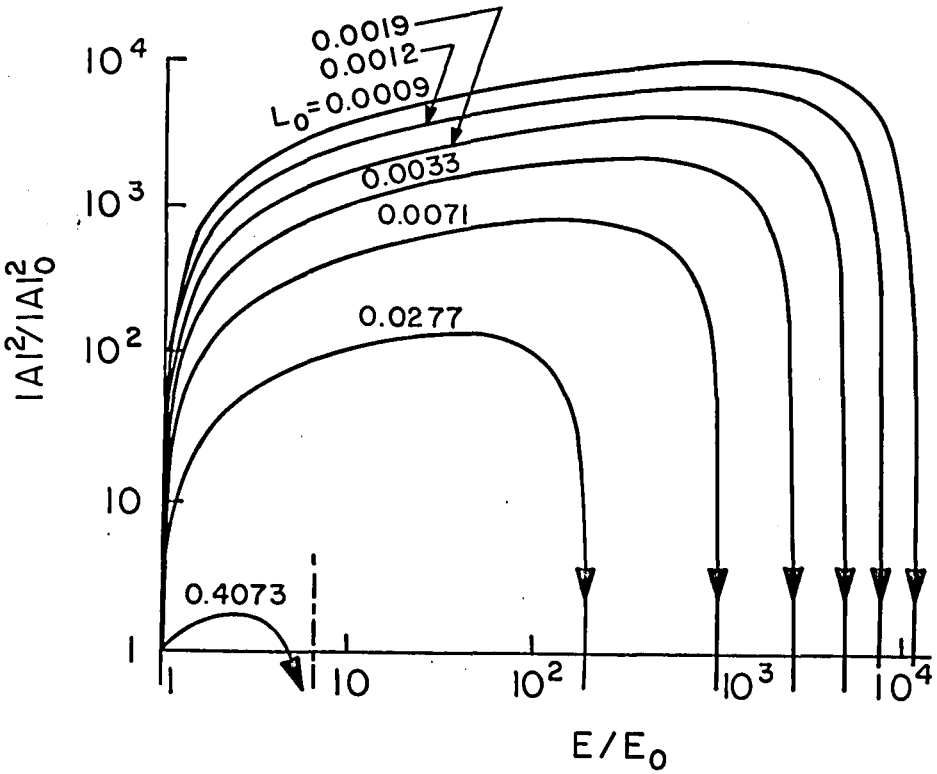
0.0019
0.0012
L_0=0.0009
0.0033
0.0071
0.0277
0.4073
10^4
10^3
10^2
10
1
$|A|^2/|A|_0^2$
1
10
10^2
10^3
10^4
E/E_0

LIU: FIG. 16

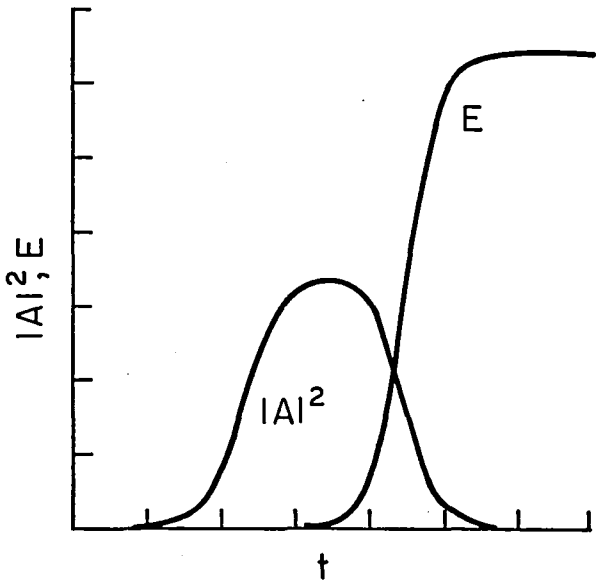

LIU: FIG. 17

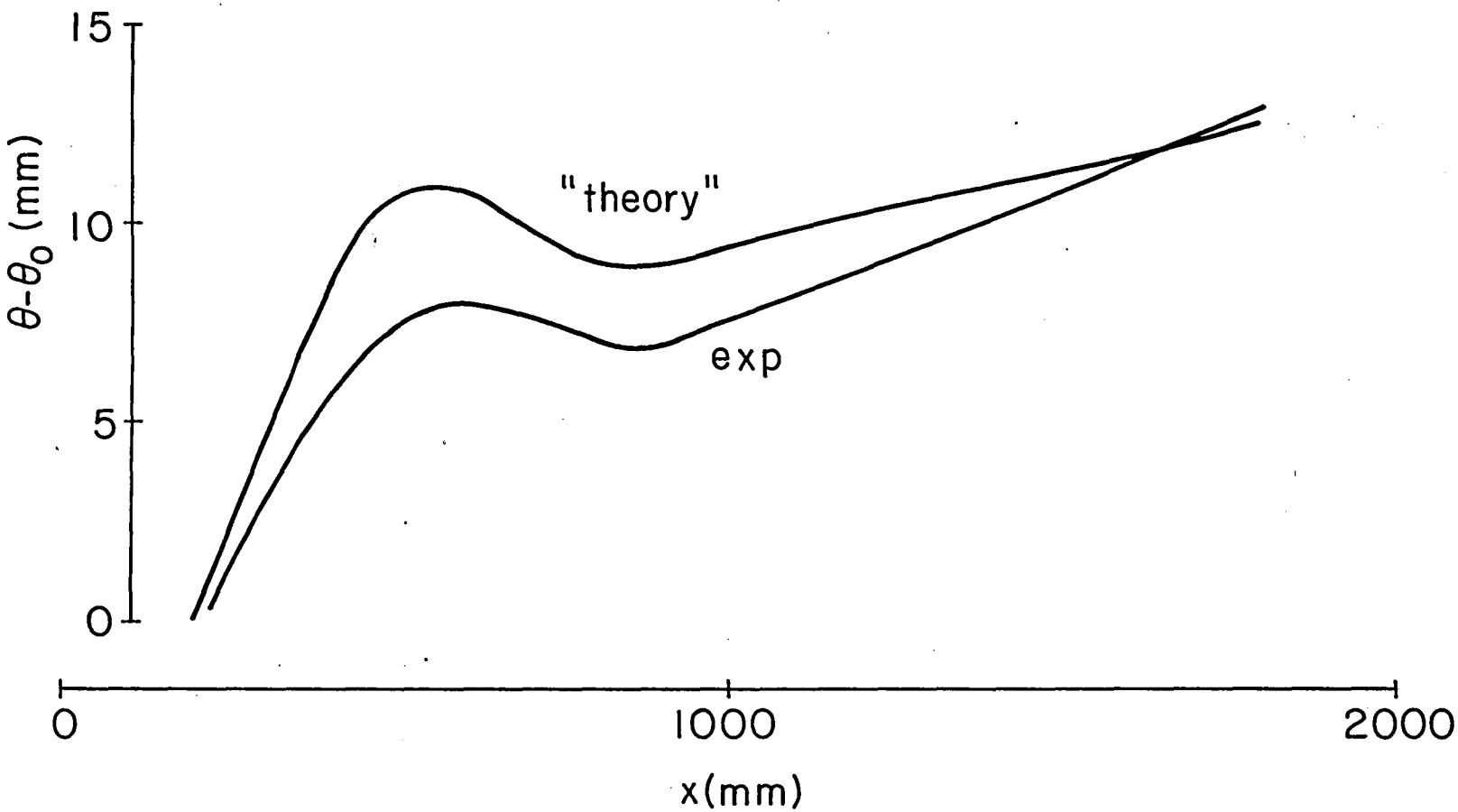

LIU : FIG. 18

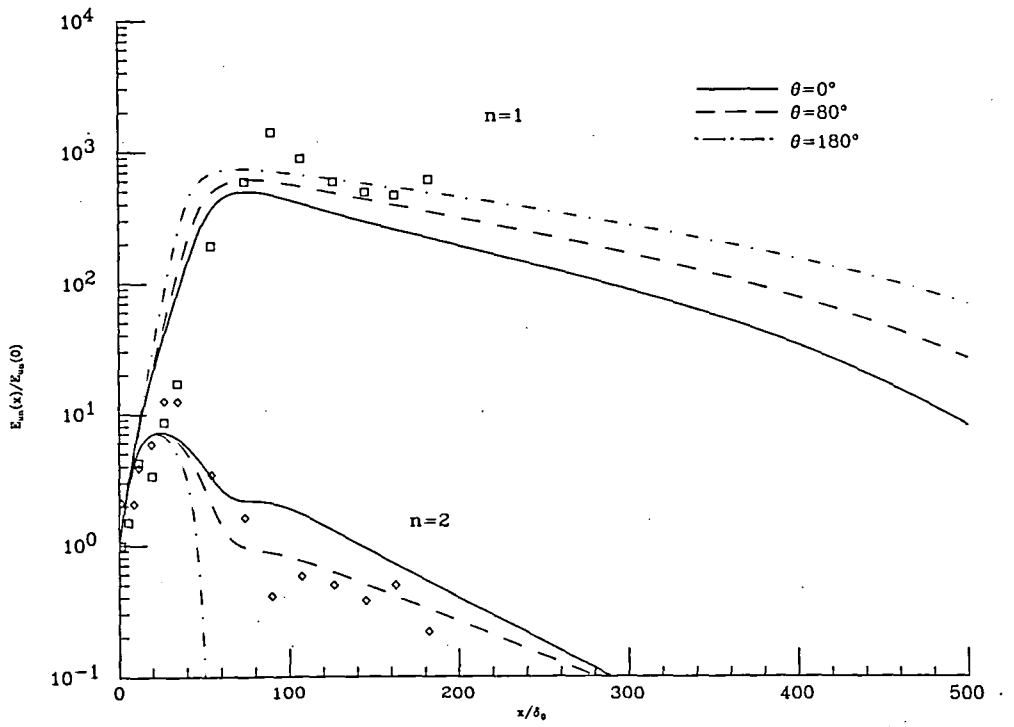

FIG. 19

LIU: FIG. 19

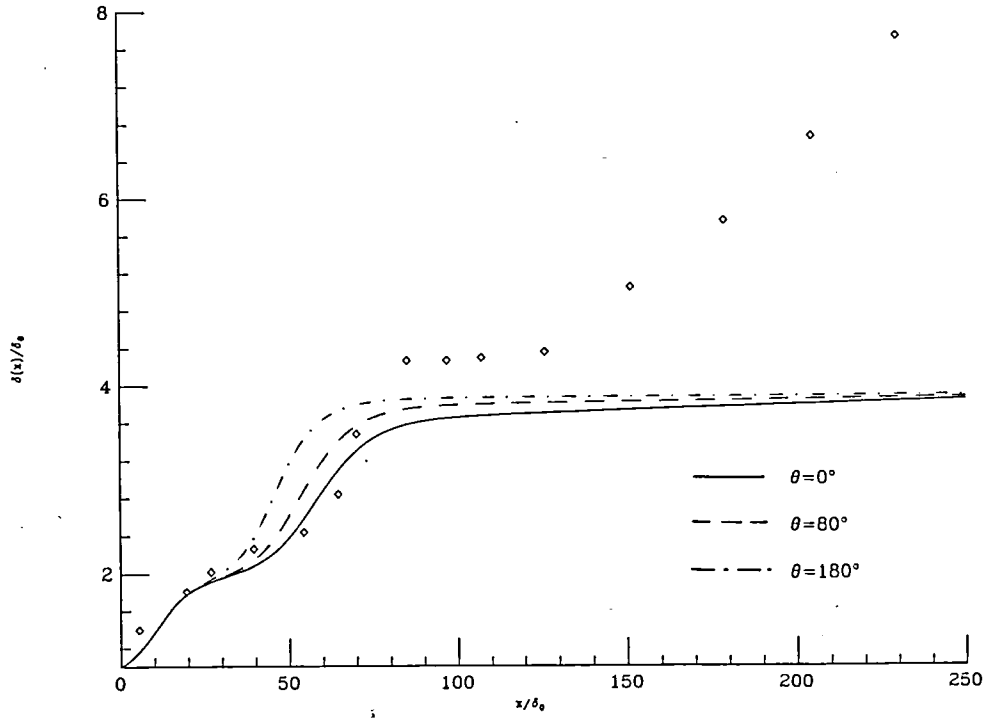

FIG. 20

LIU: FIG. 20

21a

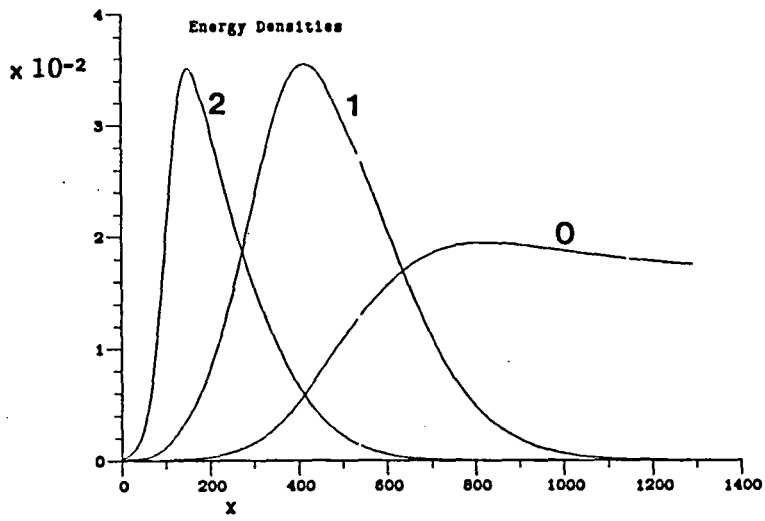

21b

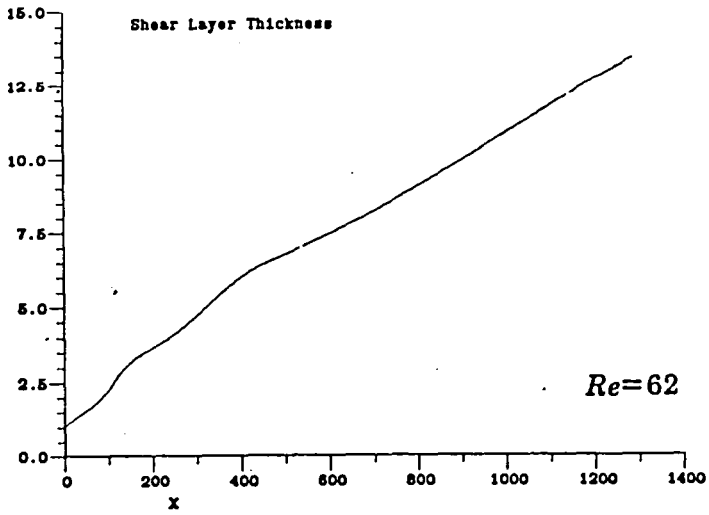

Liu Figs 21 a, b

22a

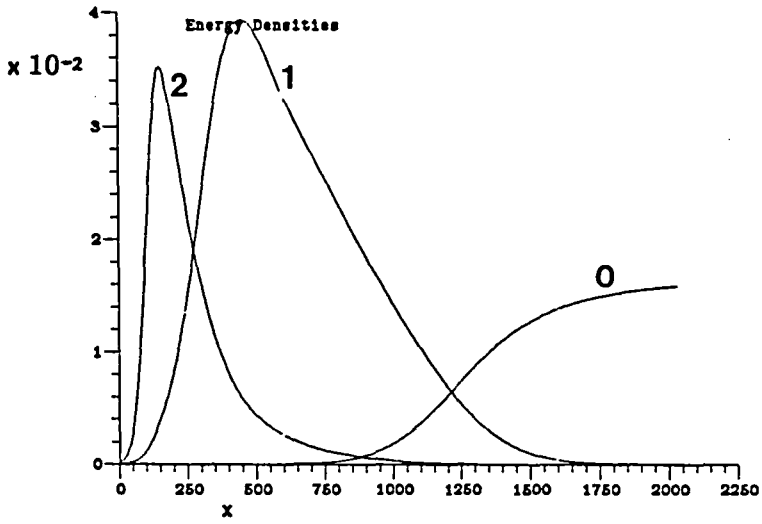

22b

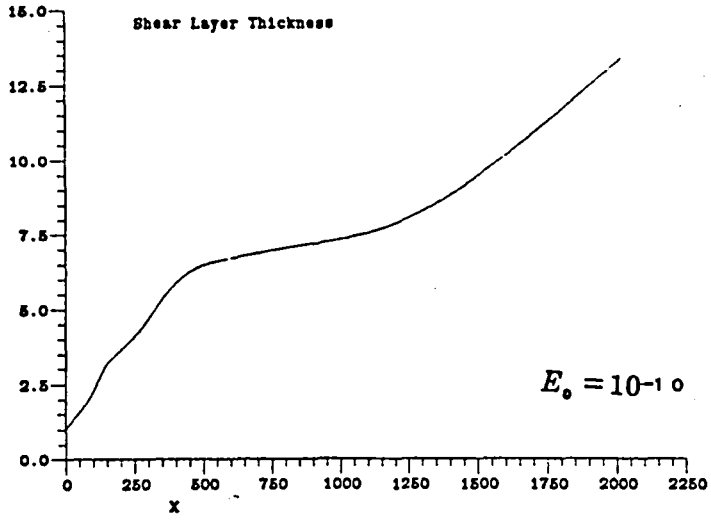

Liu : Fig. 22 a, b

23a

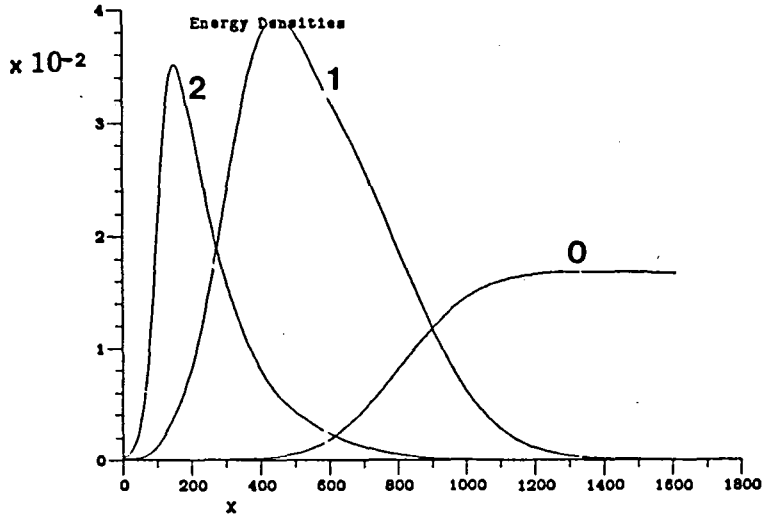

23b

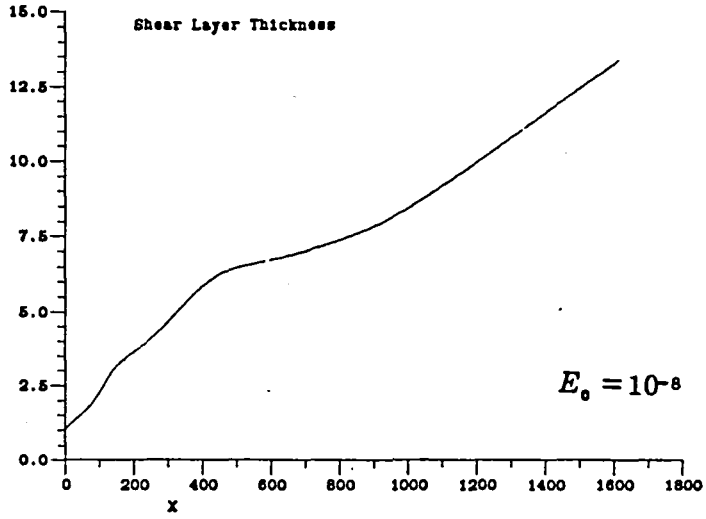

LIU: Fig 23 a, b

24a

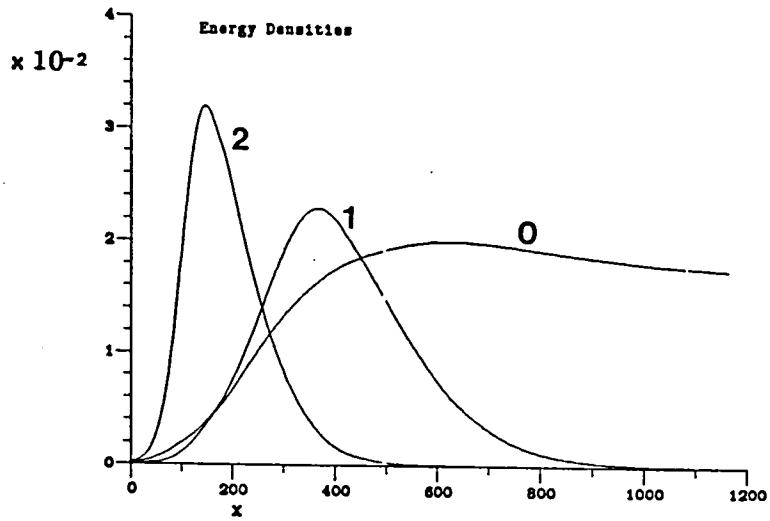

24b

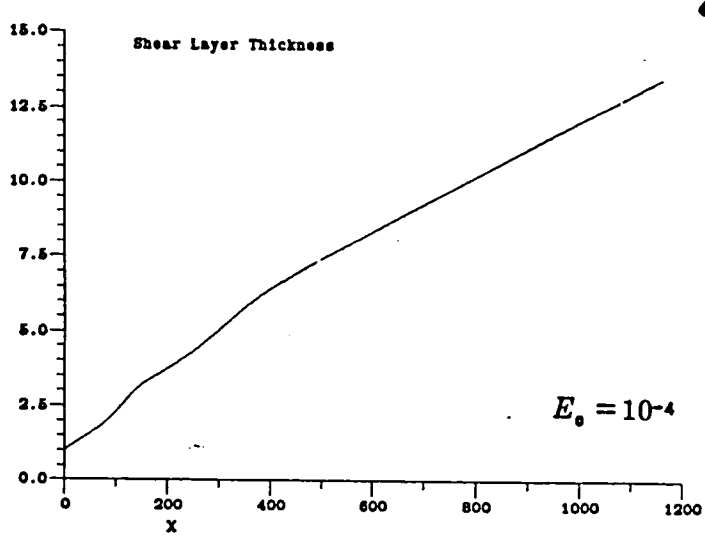

Liu: Fig. 24a, b

25a

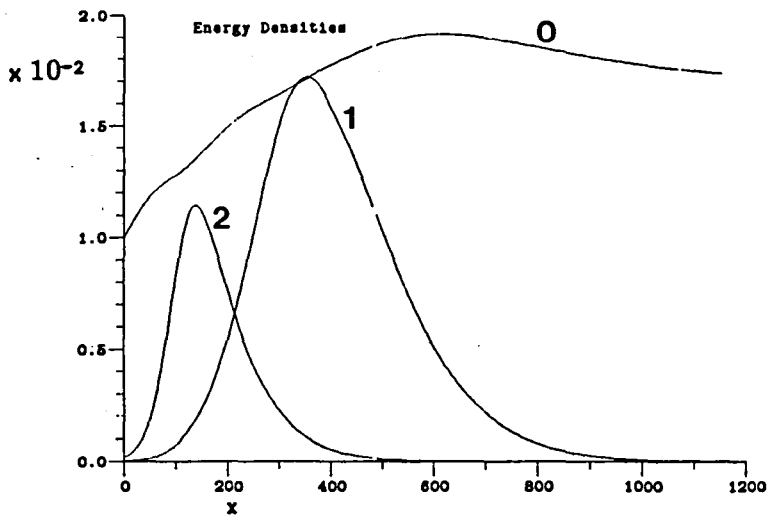

25b

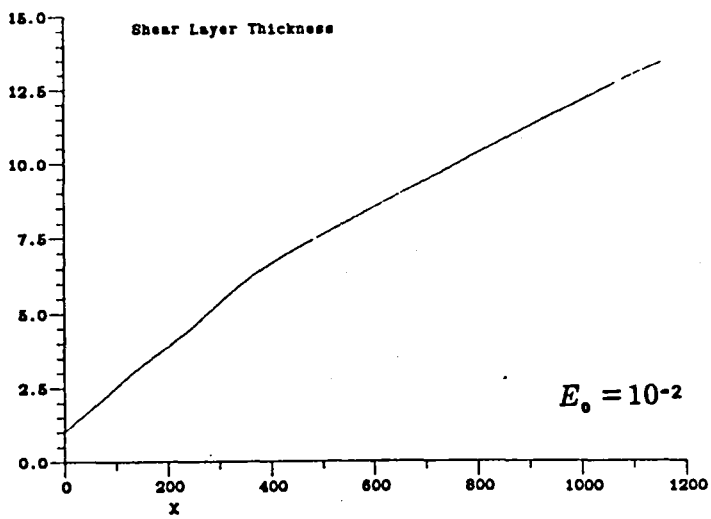

LIU: Fig. 25a,b

26a

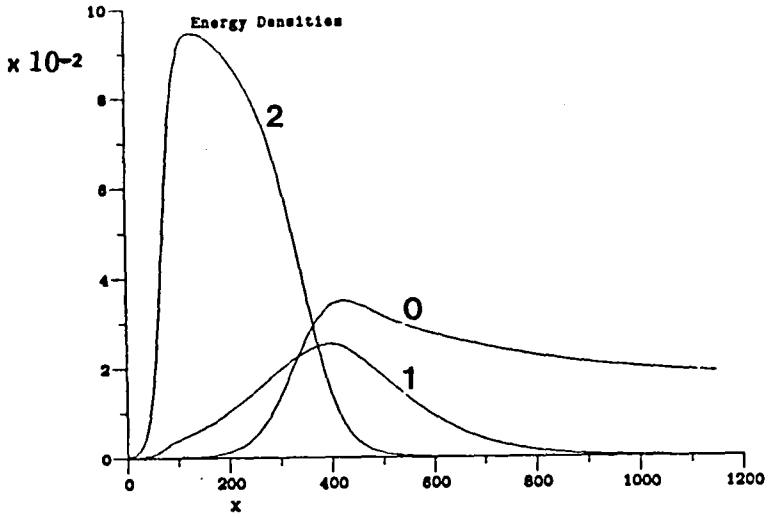

26b

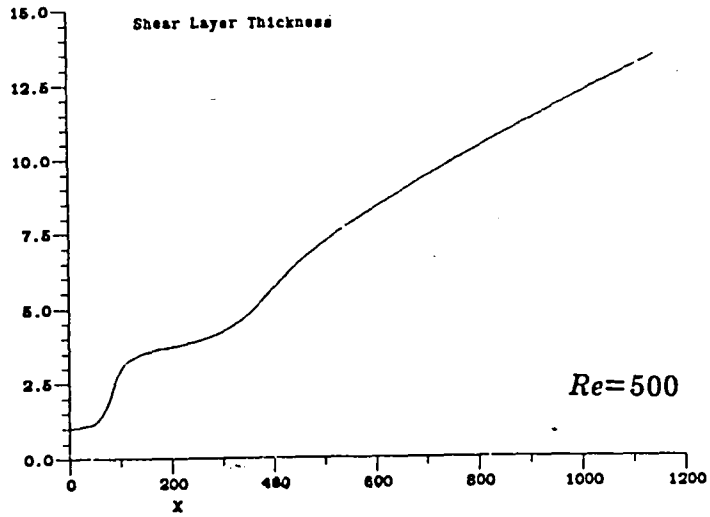

FIG. 26 a, b

27a

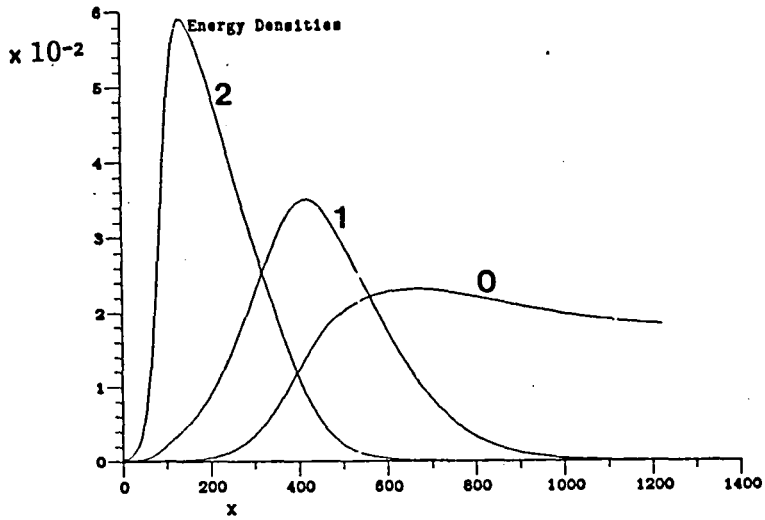

27b

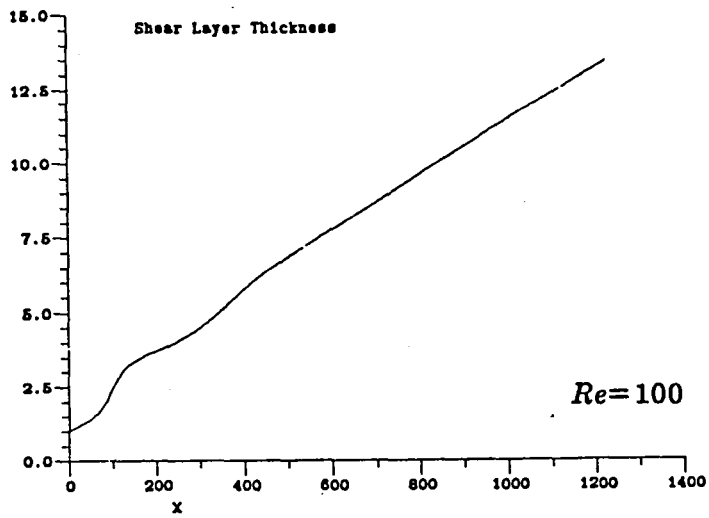

LIU: Fig. 27a, b

28a

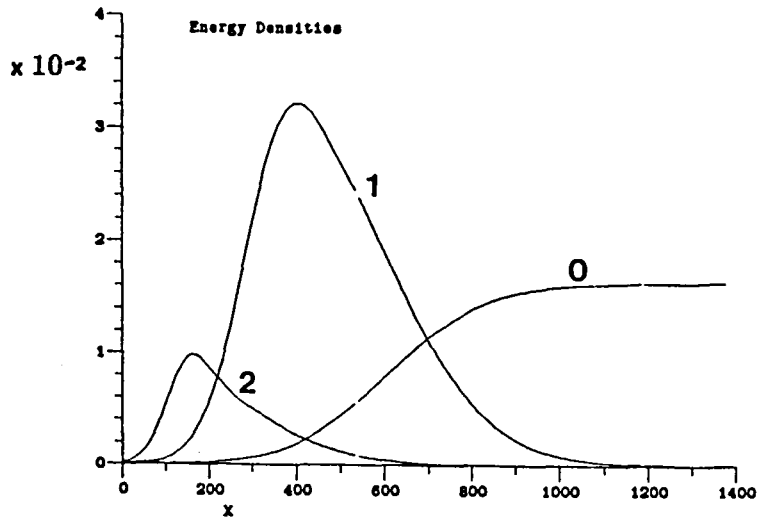

28b

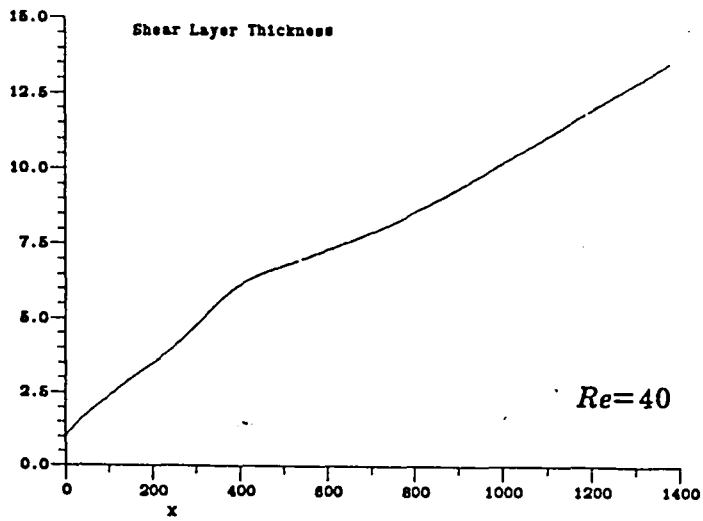

Liu: Fig. 28 a, b

29a

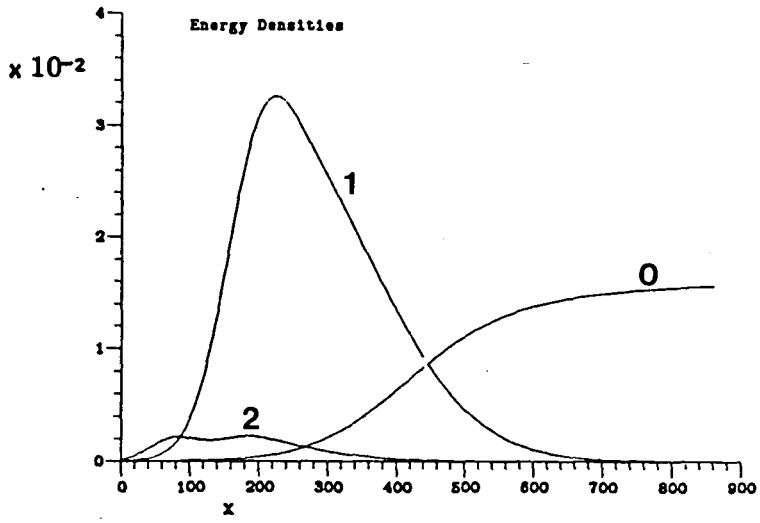

29b

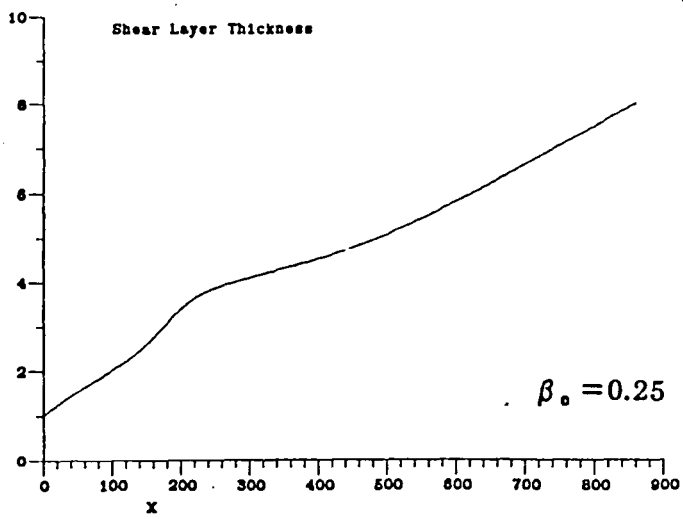

LIU: Fig. 29 a, b

30a

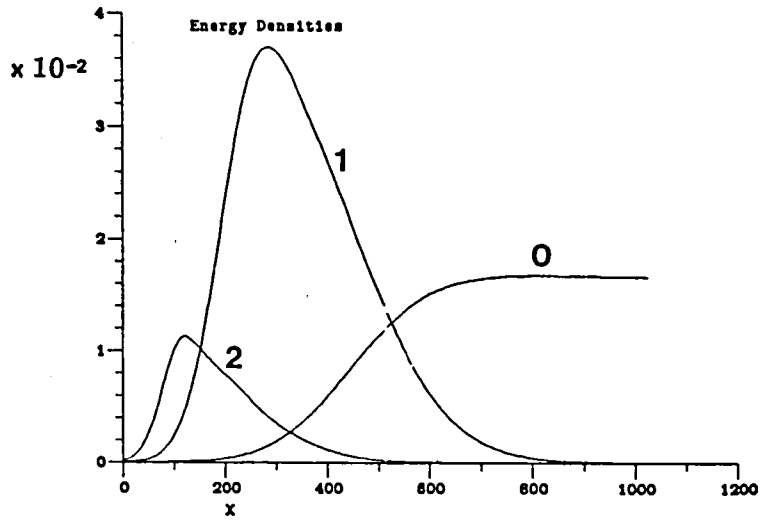

30b

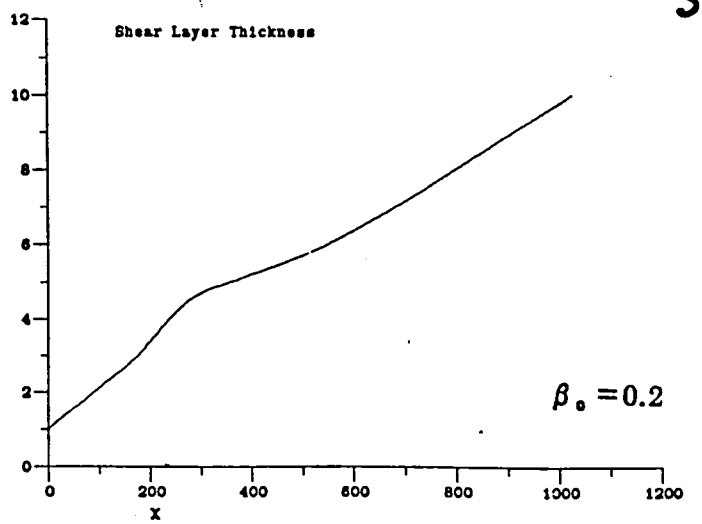

LIU: FIG. 30 a,b

31a

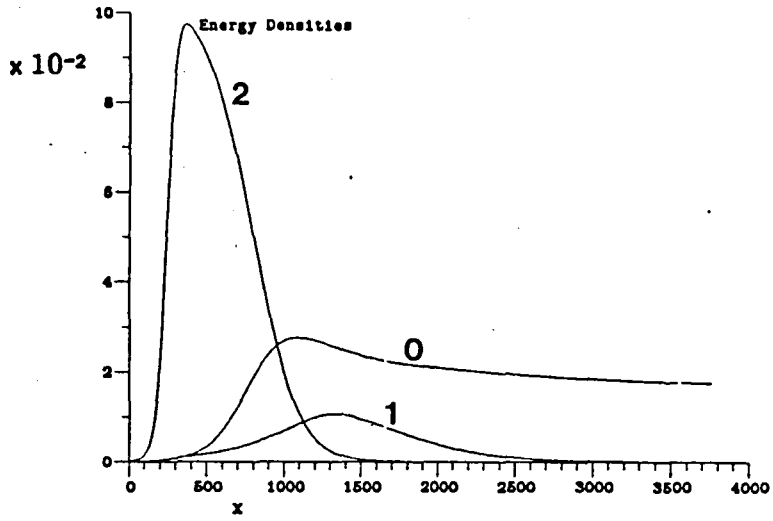

31b

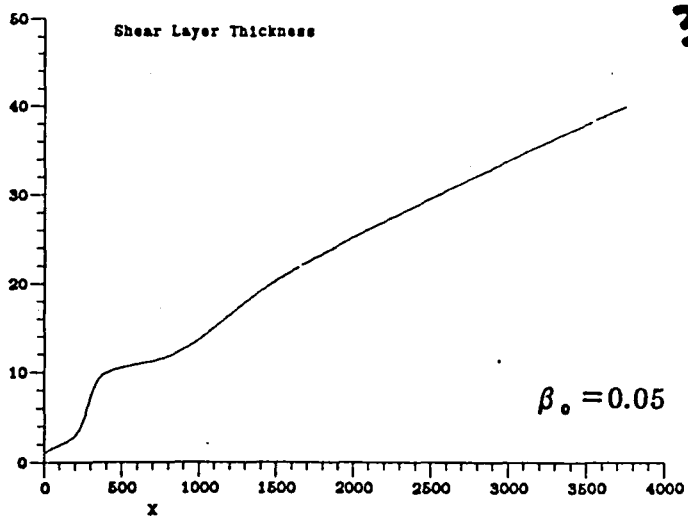

Liu: Fig 31 a,b

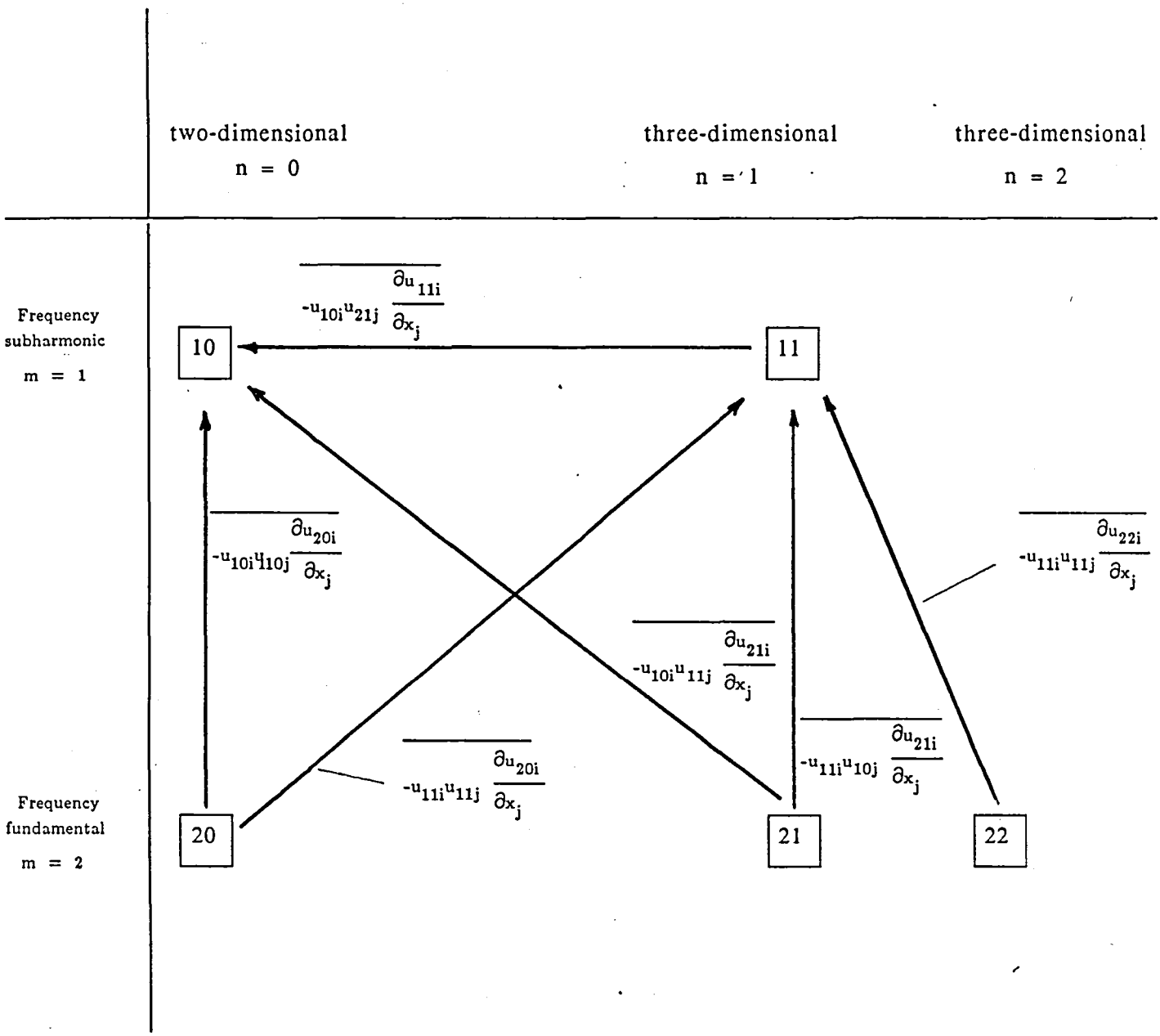
two-dimensional
n = 0
three-dimensional
n = 1
three-dimensional
n = 2
Frequency
subharmonic
m = 1
Frequency
fundamental
m = 2
$-\overline{u_{10i}u_{21j}\frac{\partial u_{11i}}{\partial x_j}}$
$-\overline{u_{10i}u_{10j}\frac{\partial u_{20i}}{\partial x_j}}$
$-\overline{u_{11i}u_{11j}\frac{\partial u_{20i}}{\partial x_j}}$
$-\overline{u_{10i}u_{11j}\frac{\partial u_{21i}}{\partial x_j}}$
$-\overline{u_{11i}u_{10j}\frac{\partial u_{21i}}{\partial x_j}}$
$-\overline{u_{11i}u_{11j}\frac{\partial u_{22i}}{\partial x_j}}$
10
11
20
21
22

LIU: FIG. 32

End of Document